NON-INTRUSIVE EFFICIENCY ESTIMATION OF INDUCTION MACHINES

by

Barbara Linda Herndler

A thesis submitted to the Department of Electrical Engineering, University of Cape Town, in fulfilment of the requirements for the degree of

MSc Electrical Engineering

University of Cape Town

October 2010

DECLARATION

This dissertation is submitted to the Department of Electrical Engineering, University of Cape Town, in complete fulfilment of the requirements for the degree of Master of Science in Electrical Engineering. It has not been submitted before for any degree or examination at this or any other university. I know the meaning of plagiarism and declare that all the work in the document, save for that which is properly acknowledged, is my own.

Signed: _____ Date: _____

To Mom and Dad

Thank you for your endless love and support. Your encouragement and belief in me has been motivating and inspirational. Know that I look up to you as a friend and a mentor.

ACKNOWLEDGEMENTS

My sincere thanks and gratitude extends to my supervisor, Dr P. Barendse for all his encouragement an inspiration. His patients and sincerity has made him a highly admirable mentor to me. I also thank my co-supervisor, Dr M.A Kahn, for all his words of guidance and support throughout this thesis.

To Mr C. Wozniak and Mr P. Titus, your continuous and valued support in the Machines Laboratory is indispensible

I would like to thank the administration staff of the Electrical Engineering Department at the University of Cape Town for their outstanding kindness and goodwill. This includes Mrs K. van Wyk, Mrs N. Moodley and Mrs M. Joubert.

To Mrs A Kahn, I am indebted to you for taking the time to read over my thesis.

I am also grateful for the support received from my friends and colleagues in the AMES research group. To Mr A. Van Wyk, I thank you for your willingness to provide assistance, despite having your own stresses. Your practical knowledge in the labs has been truly invaluable. To Mr W.J Gitonga, you have brought much light and laughter even during the difficult times-your positive attitude towards life and its challenges is truly inspirational. To Mr and Mrs Jagau, you have shown nothing but compassion and acceptance towards me. I am grateful to have spent the past year getting to know you. To Mr E. Anyang, I thank you for your generosity and support. Your selfless actions have showed me that I could always count on you. To Dr. R. Okou, you were always there when I needed advice. Your honesty and integrity is admirable to those who are privileged to work with you. To Mr H. Lu and Mr. J de LeBat, I thank you for your assistance and time spent in the laboratory. Your continuous support and enthusiasm is very encouraging.

To my beloved friends who have stood by me during the time I have spent at UCT, I am honoured and privileged to have met you. To Miss D Babu, you have been the best friend anyone could ask for. You have never stopped believing in me and my capabilities and your honesty and humbleness is both enduring and commendable. To Miss C. Hofmeyer, I thank you for your continuous support and encouragement; you too have been my pillar of strength during the darkest times. To Mr. G Apsey, I am grateful to have a friend of such a high calibre. You are a true gentleman who can bring laughter and joy to those around you. To Mr D Clough, thank you for being supportive, your kind and gentle mannerism to others is admirable. To Mr R. Pott, thank you for being the friend that you are. We have shared many wonderful moments together. You are a truly remarkable gentleman. To Mr. T. Edimu, thank you for your cheerful disposition, you have a brought much light by helping me get perspective when times were tough. To Mr W. Sikwete, I thank you for being there when I need help. Your kind and gentle nature is wonderful. To Mr. M. Truyens, I thank you for continuously being there for me. You have brought much joy into my life and without you this would not be possible. Your words of motivation and inspiration have allowed me to get through many of the challenges I had to face. You are an amazing person and I am honoured to have you in my life.

Lastly, I would like to thank the EEDSM Hub bursary for their financial assistance. I thank you for providing me with the opportunity to continue my studies.

SYNOPSIS

Background

Determining the efficiency of an in-service motor poses a challenging task. Many of the testing standards require the motor to be decoupled from its load, or require the use of highly specialised equipment which, unlike under laboratory conditions, is often unavailable. In order to assess the efficiency of an induction machine, it is subjected to numerous testing procedures established by recognised international testing standards. These procedures are considered to be time consuming, manually intensive and disruptive to the machine's operation. Thus, these tests cannot be implemented practically under industrial applications. Additionally, the efficiency of the machine quoted after the conduction of these laboratory tests often does not reflect the motor's efficiency under operating conditions. As an example, during laboratory testing, the supply conditions are not polluted with degrees of harmonic distortion and unbalances as in the case out in industry, which further affects the motor's efficiency.

Aims and objectives

This thesis aims to address the aforementioned concerns by implementing a non-intrusive efficiency estimation technique that is applicable to induction motors in industry.

Approach/Methodology

Many non-intrusive efficiency estimation techniques, with varying degrees of accuracy and intrusion, have been developed. The air gap torque method was identified as the most accurate of these methods; however it is considered to be highly intrusive due to the measurements of stator resistance, rotor speed and no load losses. The non-intrusive air gap torque (NAGT) method measures only the motor terminal quantities and combines various estimation techniques to determine these parameters in a non-intrusive manner.

The stator winding resistance (R_s) is estimated by employing a DC signal injection based topology. The rotor speed estimation is determined by incorporating a vibration spectrum analysis technique. The no load loss components are estimated empirically as a percentage of rated input power. The stray load losses are determined according to an assigned allowance relative to its size as defined by the IEC Std 34-2-1.

Based on the aforementioned estimation techniques, efficiency tests are conducted on three motors with ratings of 7.5kW, 11kW and 15kW. Each of these motors are four-pole, 380/400V, 50Hz and are totally enclosed fan cooled (TEFC) squirrel cage induction motors. Additionally, the machines are connected in a delta configuration. Efficiency tests according to the IEC Std 34-2-1 segregation of losses and direct methods are also performed and serve as the premise for which the results attained from the NAGT method can be compared. Additionally, the performance of the NAGT method during unbalanced supply voltage conditions is also considered.

An error analysis is conducted to quantify the effects of instrumentation errors in parameter measurements on the efficiency value of the motor. To achieve this, the worst case error estimation (WCEE) and realistic error estimation (REE) techniques are applied

Results

The stator resistance estimation results indicate an over estimate in comparison to the expected resistance values. Additionally, the percentage error between these values is not consistent over the entire loading range. The percentage errors for the 7.5kW, 11kW and 15kW are within 2.15%, 2.51% and 3.57% respectively.

For the case of the speed estimation technique, the results prove to be successful in comparison to the measured values. Accuracy levels within 0.16% are attainable for all three motors tested. The rotational frequency components, from which the speeds are obtained, are dominant and easily detectable over the entire load range making speed estimation highly dependable.

The estimated no load losses prove to be an under estimate for the 11kW and 15kW motors. In contrast, an over estimate is indicated for the 7.5kW motor. For the case of stray load loss estimation, the estimated values show a constant overestimate in SLLs over the load range in comparison with the values attained from the IEC Std 34-2-1. This is due to the estimated values being constant over the load range and not load dependant as reflected by the results obtained in the IEC Std 34-2-1. An improved method of SLL estimation indicates values which are load dependant and follows a similar trend as the IEC Std 34-2-1. This efficiency of the NAGT method showed an improvement when incorporating these SLLs.

The efficiency results using the NAGT method generally showed an underestimate in comparison to the IEC Std 34-2-1 and direct methods. In particular, the deviations in efficiencies at the lower loading points are larger than at the higher loading range. This discrepancy is attributed to the overestimation of stray load losses.

The effect of magnitude voltage unbalance reflects a decrease in efficiency with an increase in voltage unbalance. This is due to the increase in motor losses and hence increase in the motor's operating temperature. The efficiency results using the NAGT method consistently indicate lower values of efficiency for each of the unbalanced cases in comparison to the direct method hence further validating the method.

The error analysis indicates that the uncertainties due to instrumental errors are larger for the NAGT method in comparison to the values obtained for the IEC Std 34-2-1. The effects of introducing stricter tolerances in instrumentation accuracies show an improvement in errors associated with the NAGT method. Additionally, the uncertainties according to the WCEE and REE technique show a variation according to the loading condition of the machine.

Conclusions

This thesis presents a means of determining the efficiency of an induction machine, non-intrusively, by using the NAGT method. The NAGT method combines various non-intrusive methods to estimate various parameters that are traditionally measured in a highly intrusive manner. The stator winding resistance is estimated non-intrusively by injecting DC components into the stator windings of the machine and can achieve accuracies of within 3.57%. The rotor speed estimation using vibration spectrum analysis presents an effective and reliable technique that can estimate the rotor speed (within 0.16%) without degrading at low load conditions. The estimation of no load and stray load losses is achieved using empirical values related to the size of the motor. In general, the estimation of these losses is an overestimate and its effect is to reduce the estimated efficiency values. Therefore, the efficiency values obtained using the NAGT method are lower than the values attained using the IEC Std 34-2-1 and direct methods. Additionally, the NAGT method can effectively be used to estimate the efficiency of an induction machine during unbalanced supply conditions. The measurement uncertainty due to instrumental errors is associated with the accuracy of the instrument, the influence of the measured parameters, the methodology of the efficiency test and the load of the machine. The uncertainty of the NAGT method is higher in comparison to the uncertainties associated with the IEC Std 34-2-1 and direct methods.

Recommendations

Improvements to the NAGT method can be made by considering the estimated parameters individually. The rotor speed estimation technique can be improved by incorporating a peak detection algorithm, such that the rotor speed can be detected online. Improved methods of SLL estimation should be incorporated so that the SLLs are load dependant and more reflective of the values attained in the IEC Std 34-2-1. The NAGT method acquires parameters such as voltages and currents of which are used in many condition monitoring techniques. Therefore, the NAGT method can be implemented in conjunction with these techniques in order to develop a multipurpose device.

TABLE OF CONTENTS

LIST OF FIGURES

LIST OF TABLES

LIST OF SYMBOLS

$\widetilde{A}$	Estimated value
A_t	True value
d	distance
f_r	Rotational frequency
f_s	Fundamental supply frequency
F	Force
g	9.796 m/s^2 is the gravitational force for Cape Town
I'_{rp} , I'_{rn},	Positive and negative referred rotor current
$I_{a,dc}$	DC current in phase A
i_a,i_b, i_c	Instantaneous line currents
I_d, I_q	Current in direct and quadrature reference frame
i^s_{dr}, i^s_{qr}	Rotor current along the direct and quadrature axis in the stationary reference frame
i^s_{ds},i^s_{qs}	Stator current along the direct and quadrature axis in the stationary reference frame
I_{offset}	Offset current
I	Rated line current
I_s	Stator current
I_r	Rotor current
I_s	Stator current
I_x	Influence coefficient
L_m	Magnetising inductance
m	Mass
k_1	234.5 for 100% IACS conductivity copper
k_θ	Temperature correction factor
n_r	Rotor speed (rpm)
n_s	Synchronous speed (rpm)
P_1	Input power

P_2	Rated output power
P_{Core}	Core loss
$P_{Cu,rotor}$	Rotor copper loss
$P_{Cu,stator}$	Stator copper loss
$P_{Electrical}$	Electrical power
P_{FW}	Friction and windage loss
P_{Input}	Input power
$P_{Mechanical}$	Mechanical power
P_{NLL}	No load power
P_{Output}	Output power
P_{SLL}	Stray load loss
p	Number of poles
P	Pole pairs
P_{ag}	Air gap power
r	Phase resistance
R_{ext}	External resistor
R'_{rn} , R'_{rp}	Positive and negative referred rotor resistance
R_{ab}, $R_{bc,}R_{ca}$	Stator winding line to line resistance
R_{as}, R_{bs}, R_{cs}	Stator winding phase resistance
R_{cable}	Cable resistance
R_{LL}	Line to Line Resistance
R_r	Rotor resistance
R_s	Stator winding resistance
s	Slip
T_{ag}	Air gap torque
T_{em}	Electromagnetic torque
$T_{Mechanical}$	Mechanical torque
T_{shaft}	Shaft Torque in N.m
V_a, V_b,V_c	Phase voltages
V_{ab},V_{bc},V_{ca}	Three phase line voltage

V_{avg}	Average voltage
V_{dc}	DC voltage
v_{dqs}	Stator voltage along direct and quadrature axis
V_n	Negative sequence voltage
V_{offset}	Offset voltage
V_{Ref}	Reference voltage
V_{th}	Threshold voltage
X_m	Magnetizing reactance
V_p	Positive sequence voltage
X_s	Stator winding reactance
η	Efficiency
θ_c	Inlet coolant temperature
θ_w	Winding temperature
λ_{dqs}	Total flux linkage vector
ψ_a,ψ_b,ψ_c	Flux linkage of phase a, b and c
ω_r	Rotor speed (rad/s)
ω_{sync}	Synchronous speed (rad/s)
ζ	Absolute measurement error
ζ_h	Human error
ζ_i	Instrumental error
ζ_m	Methodological error
$\varepsilon_{Relative}$	Relative error
Π	System parameter
φ	Power factor angle

NOMENCLATURE

ANN	Artificial neural network
AS/NZ	Australia and New Zealand Standards
BOV	Balanced over voltages
BUV	Balanced under voltage
CSA	Canadian Standards Association
ESKOM	Electricity Supply Commission
FFT	Fast Fourier Transform
IEC	International Electromechanical Commission
IEEE	Institute of Electrical and Electronics Engineers
JEC	Japanese Electrotechnical Commisison
LVUR	Line Voltage Unbalance Ratio
MEE	Maximum error estimation
MEM	Maximum entropy method
MMF	Magneto-motive force
MOSFET	Metal-Oxide Semiconductor Field Effect Transistor
MRAS	Mutual model reference adaptive system
NAGT	Non-intrusive Air Gap Torque
NEMA	National Electric Manufactures Association
Op-amp	Operational amplifier
ORNL	Oak Ridge National Laboratory
PVUR	Phase Voltage Unbalance Ratio
PWM	Pulse width modulation
REE	Realistic error estimation
RMS	Root mean square
SANS	South African National Standards
SLL	Stray load loss
THD	Total harmonic distortion
UBOV	Unbalanced over voltage
UBUV	Unbalanced under voltage
VUF	Voltage unbalance factor
WCEE	Worst case error estimation

CHAPTER ONE

INTRODUCTION

This thesis aims to investigate, develop and implement a non-intrusive efficiency estimation technique that can be applied to induction machines that are installed in industry. The effects of supply unbalances on the efficiency estimation technique will also be investigated. The results obtained will be compared with the IEC Std 34-2-1.

1.1 Background

It is well known that induction motors dominate the field of electromechanical conversion. The endeavour to conserve energy is ever increasing and research is currently being conducted to investigate possible methods to improve machine efficiency. Not only is this applicable in the global market, but it is also highly topical in a South African context. There is no accurate means of measuring the efficiency of the motor while it is operating in industry. Adopted strategies are most commonly done under laboratory conditions with the use of expensive torque transducers. Therefore, there is a need to determine the efficiency and loading of motors in industrial applications. Preferably, this should be conducted in a non-intrusive manner so that the operation of the machine is not affected and the down time minimized. Not only does this reduce the financial implications associated with down time but also helps in prolonging the life span of the machine.

Determining the efficiency of a motor on the jobsite poses as a challenging task since many of the testing standards require the motor to be decoupled from its load, or require the use of highly specialised equipment, of which is often unavailable unlike under laboratory conditions. The need for efficiency estimation becomes prominent when feasibility studies of replacement or repair procedures are conducted. Once the motor has been repaired or rewound, the need to quantify the effects of these procedures on the motor's efficiency may arise. Additionally, it may be necessary to determine whether the motor is operating within the efficiency range specified by the manufacturer such that its maximum capability can be achieved.

1.2 Problem Statement

In order to assess the efficiency of an induction machine, the machine is subjected to numerous testing procedures which have been established by recognised testing standards. These tests require the use of expensive equipment and that the machine is decoupled from its load. These procedures are considered to be time consuming, manually

intensive and disruptive to the machine's operation. Thus, these tests cannot be implemented practically under industrial applications. Additionally, the efficiency of the machine quoted after the conduction of these laboratory tests often does not reflect the motors capability under operating conditions. During laboratory testing, the supply conditions are not polluted with degrees of harmonic distortion and unbalance of which has an effect on the motor's efficiency. This does not realistically reflect the conditions met in industry applications and thus the motor does not deliver at the efficiency levels as specified by the manufacturer.

Many non-intrusive efficiency estimation techniques, with varying degrees of accuracy and intrusion, have been developed. Some of these methods require information from the motors nameplate. This becomes problematic when machine's nameplate data is no longer visible or if the machine has been rewound.

Therefore, there is a need to address the above issues by implementing a non-intrusive efficiency estimation technique that is applicable to any induction motor under any load condition.

1.3 Key Questions

The research presented in this thesis focuses on the investigation and implementation of a non-intrusive efficiency estimation method for induction machines

In this regard, several research questions have been formulated:

- Can the efficiency of induction machines be estimated non-intrusively by measuring the instantaneous line voltages and currents?
- What is the impact of individual parameter estimation on the overall motor efficiency?
- Does the estimation method perform under all load conditions?
- Is the estimation method applicable to a range of motor sizes?
- How does the method perform under unbalanced supply conditions?

- Can we adopt these techniques in the relevant industrial applications suitable in a South African context?

1.4 Aims and Objectives

The aims and objectives of the thesis are to:

- Provide a relevant literature review on efficiency testing of induction motors
- Investigate and select an appropriate non-intrusive efficiency estimation technique
- Develop and implement the technique experimentally on an induction machine.
- Provide the relevant analysis and discussion of the experimental results obtained
- Investigate the impact of voltage unbalance on the proposed technique
- Conduct the associated error analysis and asses its impact on motor efficiency
- Draw conclusions based on the analysis of the experimental results
- Make recommendations on future work to be conducted

1.5 Scope and Limitations

The experiments and simulations conducted in this thesis are limited to efficiency estimation of induction machines and does not include (although may be applicable to) other motor types.

All the motors tested in this thesis include the 7.5kW, 11kW and 15kW motors available in the Machines Laboratory at the University of Cape Town (UCT). All motors are line connected, are 380V/400V, 50 Hz, 4 pole machines connected in a delta configuration.

The performances of the techniques implemented are limited to steady state conditions.

The investigation of the impact of voltage unbalance is restricted to magnitude voltage unbalances in accordance to the NEMA definition.

1.6 Outline of Thesis

The remainder of this thesis is structured as follows:

Chapter two introduces the basic structure and operation of an induction machine and provides a definition of motor efficiency. The various factors affecting the efficiency of a machine are also presented. In particular, a background to voltage unbalance conditions is provided in order to provide a foundation so that the performance of efficiency estimation under unbalanced conditions can be addressed. Furthermore, a discussion of existing international motor efficiency testing standards and their differences are identified.

Chapter three provides an overview of existing efficiency estimation techniques available in literature. A detailed comparison between these techniques based on their relevant testing and measurement requirements are presented. Furthermore, this chapter presents an estimation technique which allows for motor efficiency to be determined non-intrusively by measuring the instantaneous line voltages and currents. The technique is elaborated in Chapter six where the non-intrusive air gap torque method is developed.

Chapter four offers a literature review of different stator winding resistance estimation techniques. Furthermore, the advantages and disadvantages the estimation methods are presented.

Chapter five contains an overview of rotor speed estimation techniques. The advantages and disadvantages, in terms of accuracy and intrusion, of these methods are also indicated.

Chapter six shows the development of the non-intrusive air gap torque method for efficiency determination of induction machines. The chapter provides motivation in terms of the need and relevance of non-intrusive efficiency estimation in a South African context. Furthermore, a detailed theory development of the candidate topologies of stator resistance and rotor speed estimation techniques chosen for this thesis is provided.

Chapter seven contains a description of the experimental setup and methodology of the laboratory experiments conducted. The chapter describes the design and implementation of the circuitry required for stator resistance and rotor speed estimation. The motor testing procedure is extended to a range of motor sizes, namely 7.5kw, 11kW and 15kW. This allows for the investigation as to whether the motor efficiency estimation technique is applicable to a wide range of motor sizes.

Chapter eight presents the results and analysis of the experiments conducted. The performance of the various estimation techniques adopted and their impact on the overall motor efficiency is investigated. The performance of the developed non-intrusive air gap torque method is compared to the results obtained from the IEC Std 34-2-1 and direct methods. In doing so, the performance of non-intrusive air gap torque method can be compared across a wide range of load conditions. Lastly, performance of the non-intrusive air gap torque method during unbalanced supply conditions is presented.

Chapter nine offers an error analysis of the experimental results. The focus of this chapter is aimed at the effects of instrumentation errors on the acquired motor efficiencies.

Chapter ten provides the concluding remarks based on the analysis conducted in chapters eight and nine. This chapter also acknowledges the proposed recommendations for future work.

CHAPTER TWO

EFFICIENCY OF INDUCTION MACHINES

This chapter introduces the basic structure and operation of an induction machine. A definition of motor efficiency in terms of the direct and indirect method is provided. The various factors affecting the efficiency of a machine are outlined and possible solutions to avoid the negative impacts of these factors are offered. Furthermore, a discussion of existing international motor efficiency testing standards provides a foundation for the comparison of the IEEE Std 112 and IEC Std 34-2-1. The differences in terms of power quality, instrumentation tolerances and testing methodologies are subsequently identified.

2.1 Introduction

Induction machines have provided industry with the ability to convert energy from electrical to mechanical form. With the reputation for being the workhorses of industry, due to their robust nature, induction machines have become the most popular choice of motor. These machines provide the driving force to various equipments such as conveyors, fans and pumps and are necessary for numerous processes in production and manufacturing plants. Induction machines, therefore, play a vital role in industry and subsequently maintaining the economic status of a country. Every effort should be made to preserve the machine at their optimal capabilities in order to obtain the desired maximum output with minimum input.

2.1.1 The Basic Structure of an Induction Machine

The basic structure of the induction machine consists of a stationary stator, an air gap and rotating rotor. The stator forms the magnetic core of the machine and is composed of laminations made from high-grade sheet steel [1] which are stacked together to form the metal frame. This part of the machine is stationary during operation, hence the name stator. The laminations consist of numerous slots around its inner perimeter in which the phase windings of the machine are inserted.

For the case of a three-phase machine, the stator windings are evenly distributed at 120 electrical degrees around the stator core and are connected to the three-phase supply. Distributed winding configurations, as opposed to concentrated winding configurations, allow for a more efficient use of iron and have the benefit of obtaining a high quality magneto-motive force (mmf) waveform [1]. The machine can then be configured accordingly to form a star or delta connection depending on the application of the machine.

A uniform air gap separates the stator from the rotating rotor and is designed to be as small as possible. This allows for a minimised path of reluctance and provides for maximum flux densities to be established within the core of the machine.

The rotor iron core is constructed in a cylindrical form with integrated slots into which the rotor windings can be inserted. The induction motor can be configured to produce two main types, namely the wound and squirrel-cage type. The squirrel cage design is constructed by shorting the end windings with aluminium or copper end rings. This construction is considered to be simpler, more rigid and more cost effective [1]. Figure 2.1 shows the basic structure of an induction machine.

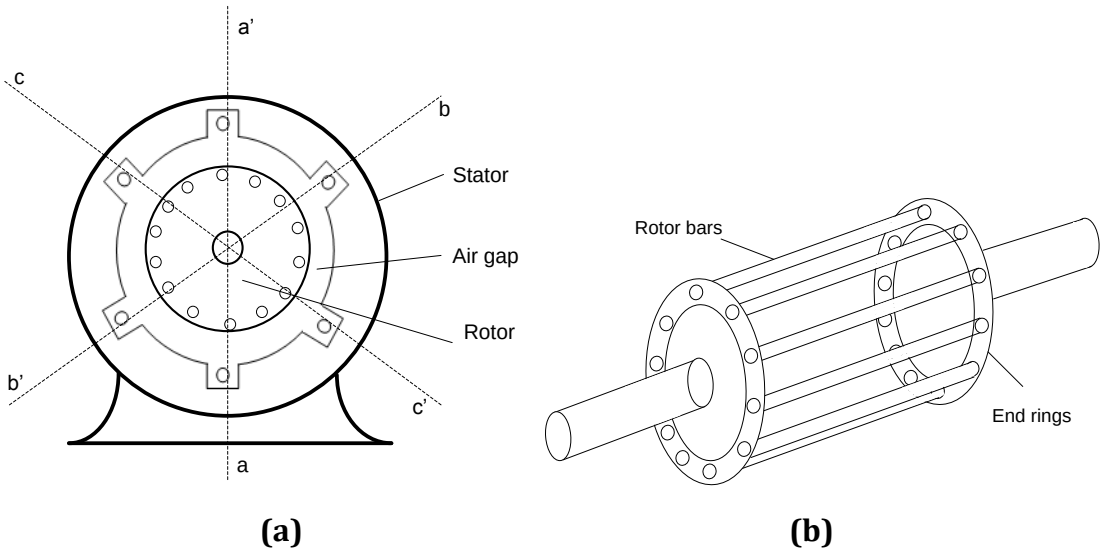

Figure 2.1: Construction of (a) the stator and (b) squirrel cage rotor [1]

2.1.2 Principles of Operation

The stator windings of the induction machine are connected to a supply from which an alternating current is supplied to the stator windings. Current flowing in the stator windings creates a sinusoidal mmf which is cantered along the axis of the windings [1]. Space vectors along the phase axes of the machine can represent this mmf, with its magnitude dependant on the instantaneous value of the current flowing through the phase

coil [1]. The resultant mmf (the vector sum of all three coils) produces a rotating magnetic field in the air gap of the machine and rotates at synchronous speed, n_s (rpm), where

$$n_s = \frac{120 f_s}{p} \tag{2.1}$$

Where:

f_s is the fundamental supply frequency

p is the number of poles

Figure 2.2 below indicates how the rotating mmf is generated and shows that the resulting mmf amplitude (F) remains constant as the phasor rotates with time.

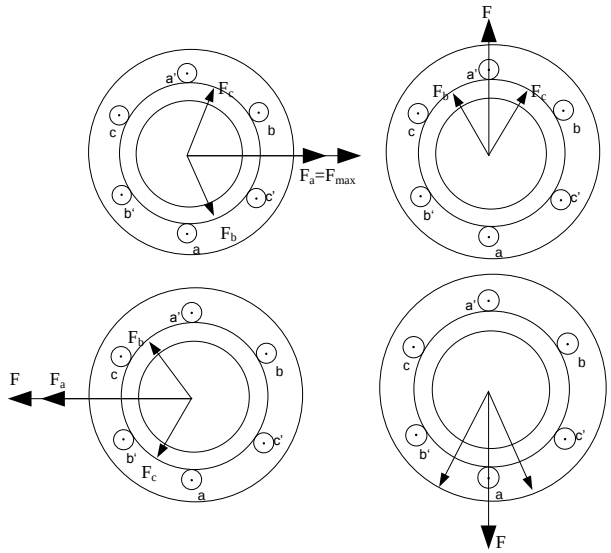

Figure 2.2: Diagram showing the rotating magnetic fields [1]

By the principle of Faraday's law, the rotating magnet field induces a voltage across the rotor bars, which results in the flow of rotor currents. These rotor currents, like that of the stator currents, produce a rotating magnetic field within the air gap. The two rotating magnetic fields, from both the stator and rotor, will attempt to arrange themselves so that the opposite magnetic polarities align with respect to each other. The interaction between these two magnetic fields causes the rotor to turn and consequently produces the motor

torque when coupled with a load. The difference in synchronous speed (n_s) and rotor speed (n_r) is known as the slip [1]and is defined by

$$s = \frac{n_s - n_r}{n_s} \tag{2.2}$$

Depending on the machine design and operating parameters, the machine prediction of performance characteristics ensures the motor adequately matches its application. When the machine is coupled to a load, a mechanical torque and power is developed. In order to achieve the maximum output power, the maximum efficiency of the machine should be achieved and maintained. The subsequent sections will describe motor efficiency and the factors affecting it in more detail.

2.2 Definition of Efficiency

Efficiency of an induction motor represents the effectiveness of the machine in converting electrical power at its input to the mechanical power at its shaft (or output) [2]. The efficiency of a machine can be calculated using the direct method as shown in equation 2.3

$$\eta = \frac{P_{Mechanical}}{P_{Electrical}} = \frac{P_{Output}}{P_{Input}} \tag{2.3}$$

In other words, the efficiency is described as the ratio of mechanical output power to electrical input power.

An ideal motor would represent 100% efficiency; however, in reality a motor's efficiency is succumbed to the effects of losses, which is mostly dissipated as heat. When these losses are accounted for, the efficiency of the machine can be calculated indirectly according to equation 2.4 [3], [4] , [5]

$$\eta = \frac{P_{Mechanical}}{P_{Mechanical} + \sum Losses} = \frac{P_{Electrical} - \sum Losses}{P_{Electrical}} \tag{2.4}$$

The sum of these losses associated with the machine is the difference between the input (electrical) and the output (mechanical). The sum of the five losses of a typical induction motor can be expressed according to equation 2.5,

$$\begin{aligned}\Sigma\text{Losses} &= P_{\text{Input}} - P_{\text{Output}} \\ &= P_{\text{Cu,stator}} + P_{\text{Cu,rotor}} + P_{\text{Core}} + P_{\text{FW}} + P_{\text{SLL}}\end{aligned} \tag{2.5}$$

Where:

$P_{\text{Cu,stator}}$ is the stator copper loss

$P_{\text{Cu,rotor}}$ is the rotor copper loss

P_{Core} is the core loss

P_{FW} is the friction and windage loss

P_{SLL} is the stray load loss

The origin and effects of these losses on the motor efficiency will further be described in the next section.

2.3 Factors Affecting Motor Efficiency

Many factors can affect the efficiency of a machine. These factors should be closely monitored and maintained within suitable levels such that the efficiency of the machine is represented realistically.

2.3.1 Induction Motor Losses

The losses associated with an induction machine are the main determining factors when calculating the efficiency of a machine. Thus, it is vital that they are taken into account as accurately as possible. The losses of a machine can be broadly categorised into load dependant losses and load independent losses [6]. These losses are dependent on both the size and speed of the motor.

Table 2.1 shows the type of losses and loss distribution for a typical 4-pole induction machine [3], [6].

Table 2.1 Types of loss and losses distribution in an induction machine

Type of loss	% of total loss	Load dependent/ independent
Stator Losses	25-40	Dependent
Rotor Losses	15-25	Dependent
Core Losses	15-20	Independent
Stray Load Losses	10-15	Dependent
Friction and Windage	5-15	Independent

As the above losses are accounted for, the power flowing through the machine decreases and consequently reduces the overall efficiency of the machine. Figure 2.3 shows the power flow through a typical machine in motor mode indicating losses developed under typical operating conditions.

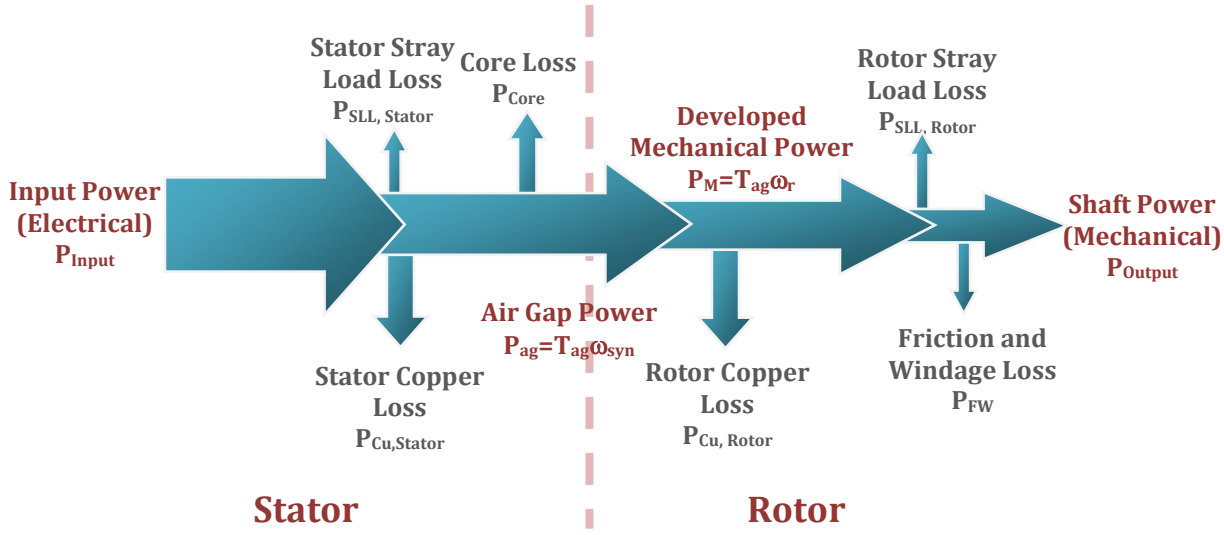

Figure 2.3: Power flow through a typical induction motor [7]

As depicted, in order to obtain a maximum output shaft power, it is necessary to reduce the amount of losses dissipated during the power flow process. The following subsections will describe each loss component, and how they can be reduced

- **Stator Winding Resistance Losses**

Stator winding resistance losses are the copper losses associated with the stator windings of the electric machine [3], [8]. The stator losses are dependent on the value of resistance (which is a function of conductor material, length, and cross-sectional area) and the amount of current flowing in the stator winding. The stator resistance loss per phase can be calculated by

$$P_{Cu,stator} = I_s^2 R_s \tag{2.6}$$

Where:
I_s is the stator current
R_s is the stator resistance

Stator winding resistance losses can be reduced by increasing the volume of copper wire in the stator, through improved stator slot design and/or by using thinner insulation [3].

- **Rotor Winding Resistance Losses**

Rotor winding resistance losses are the copper losses in the rotor conductive bars. The rotor resistance losses, per phase, is calculated according to

$$P_{Cu,rotor} = I_r^2 R_r \tag{2.7}$$

Where:
I_r is the rotor current
R_r is the rotor resistance

These losses can be reduced by increasing the size of the rotor conducting bars and end rings in order to increase the cross-sectional area and thereby decreasing the conductor resistance and its associated losses [3], [9].

- **Core Losses**

These losses constitute hysteresis and eddy current losses in the iron laminations of the machine. Hysteresis losses are attributes of the flux of the motor and supply frequency [4]. Hysteresis losses can be reduced by improving the permeability of the steel, extending the length of the core, or using thinner laminations [3], [9], [10]. Eddy-current losses results from rapid changes of flux density within the core. [1]. Theses losses can be reduced by making use of thinner laminations in the core [1] or by using a core material which has high resistivity [1].

- **Friction and Windage Losses**

These losses are due to the sources of friction and air movement in the motor and are considered to be appreciable in large high speed or totally enclosed fan-cooled motors, [3], [9], [10]. These losses are considered to be constant from no load to full load and hence are not load dependent. No load losses are obtained under no load conditions by performing a no load test. These losses can be reduced by lowering the friction between the bearings and improving the fan design to allow for better air flow [3], [9].

- **Stray Load Losses**

Stray load losses are considered to be the most misunderstood area of losses due to their complexity to measure and quantify [4]. These losses cannot be measured directly and constitute all the losses not included above. Stray load losses are expressed as follows [4]

$$P_{SLL} = P_{Input} - (P_{Output} + P_{Cu,Stator} + P_{Cu,Rotor} + P_{Core} + P_{FW}) \quad (2.8)$$

The causes of stray load losses are a result of the following:

- Fundamental and high frequency losses in the structure of the machine
- Space harmonics associated with the stator and rotor and leakage flux associated with the end windings [4]
- Losses due to the active iron and other metal parts other than conductors [11]

- Eddy-current losses in stator (primary) or rotor (secondary) winding conductors caused by current dependent flux pulsation [11]

2.3.2 Power Supply Quality

The quality of the input power is another aspect which affects the performance of a motor. The voltage and frequency of the supply are required to be within specified tolerances for the motor to perform adequately [6]. Traditionally the nameplate efficiency is defined under perfectly sinusoidal and balanced supply conditions, which can be obtained under laboratory conditions. The rated nameplate efficiency values, therefore, may not be obtainable under more realistic non-perfect conditions which are characteristic of industry supply [10].

The supply quality suffers, with varying degrees of severity, from various defects such as voltage variation, unbalances and harmonics. Figure 2.4 shows an overview of the type of polluted conditions associated with a voltage supply.

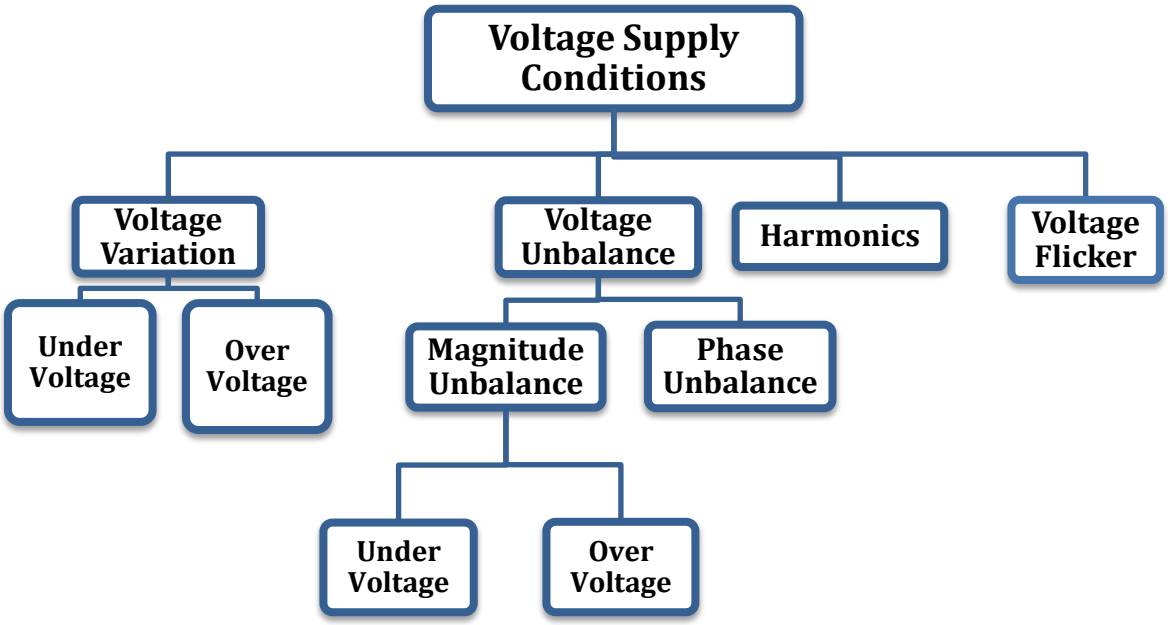

Figure 2.4: Overview of polluted voltage supply conditions

From the above diagram, one can see that there are numerous ways in which a voltage supply can be polluted. These effects are often reflected in the mains supply in varying degrees and combinations. The following sections will describe each defect in more detail.

- **Voltage Variation**

Voltage variation is the variation of voltage magnitudes [12]. Under this condition, the supply remains balanced, yet can be described as under-voltage or over-voltage relative to the rated voltage. Balanced under-voltage (BUV) describes the case where all three-phase voltages are equally lower in magnitude than the rated value [12]. Alternatively, balanced over-voltages (BOV) occurs in the case where all three phases are equally higher in magnitude than the rated value [12]. Figure 2.5 shows an example of over-voltage and under-voltage conditions.

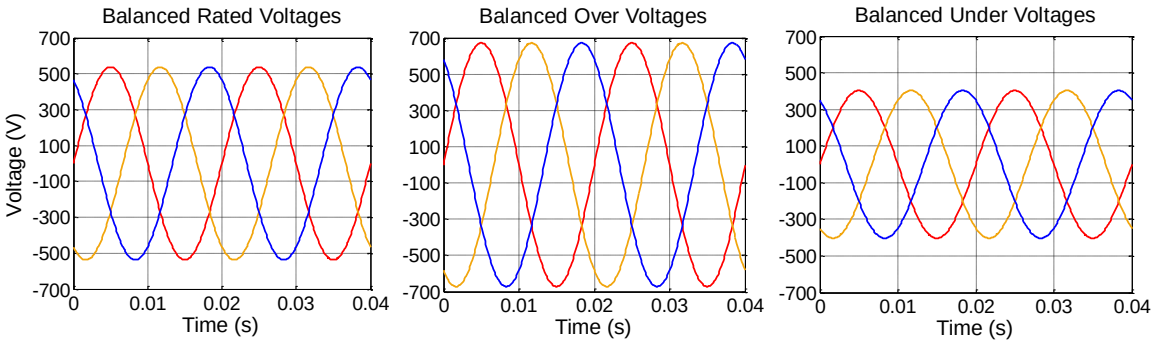

Figure 2.5: Example of voltage variation

It should be noted that this 25% deviation of rated voltage indicated in each case is not realistically expected but is depicted here merely for demonstration purposes.

- **Voltage Unbalance**

Voltage unbalance describes the non-equality of voltage magnitudes and/or phase angles between all three phases at any given point in time [12]. The magnitude balance and unbalance can be further categorised in terms of over-voltage and under-voltage conditions. Unbalanced under-voltage (UBUV) describes the condition where each of the phases are not equal in magnitude and that the resulting positive sequence voltage is less

than rated [12]. In contrast unbalanced over-voltage (UBOV) is the case where each of the phases are not equal in magnitude and that the resulting positive sequence voltage is higher than rated [12]. Figure 2.6 shows an example of voltage magnitude and phase unbalances. Again, the cases shown here are extreme cases and are merely for demonstration purposes.

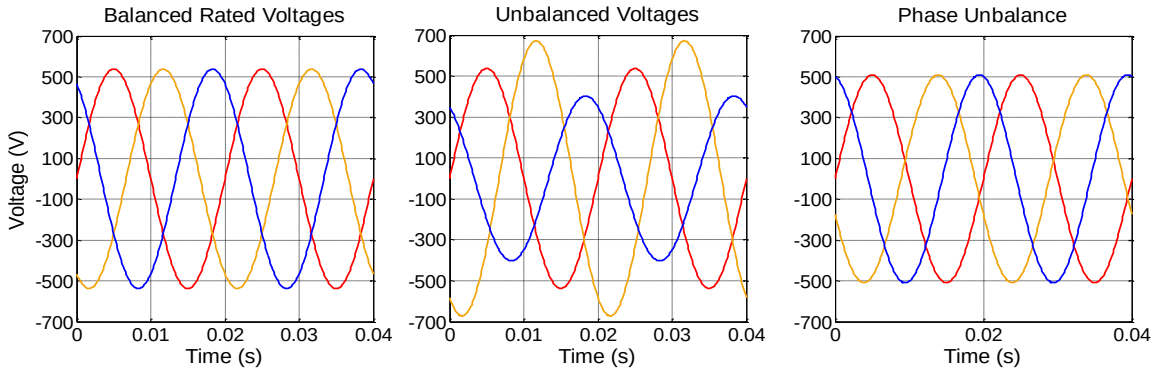

Figure 2.6: Example of voltage magnitude and phase unbalance

Voltage unbalance can be defined using the Line Voltage Unbalance Ratio (LVUR) [13]. In this case, only the voltage magnitudes are accounted for and the phase angles are neglected, making it a quick and simple method to calculate the percentage unbalance. This definition has been adopted by National Electric Manufactures Association (NEMA) and is described by [13], [14], [15]

$$\text{LVUR}(\%) = \frac{\text{Max}\left[\text{V}_{ab} - \text{V}_{avg}, \text{V}_{bc} - \text{V}_{avg}, \text{V}_{ca} - \text{V}_{avg}\right]}{\text{V}_{avg}} \times 100 \qquad (2.9)$$

Where:

$$\text{V}_{avg} = \frac{\text{V}_{ab} + \text{V}_{bc} + \text{V}_{ca}}{3} \qquad (2.10)$$

Alternatively, the Phase Voltage Unbalance Ratio (PVUR) can be used, where the phase voltages are used instead of the line voltages. This definition has been adopted by the Institute of Electrical and Electronics Engineers (IEEE). [13], [14], [15]

$$\text{PVUR}(\%) = \frac{\text{Max}\,[V_a - V_{avg}, V_b - V_{avg}, V_c - V_{avg}]}{V_{avg}} \times 100 \qquad (2.11)$$

Where:

$$V_{avg} = \frac{V_a + V_b + V_c}{3} \qquad (2.12)$$

On the other hand, the International Electrotechnical Commission (IEC) or 'true' definition of voltage unbalance is defined by acquiring the ratio of negative sequence voltage to positive sequence voltage. This is also known as the percentage voltage unbalance factor [12], [13], and is calculated by

$$\text{VUF}\ (\%) = \frac{V_n}{V_p} \times 100 \qquad (2.13)$$

The positive and negative sequence voltage components are obtained by resolving three-phase unbalanced line voltages into two balanced symmetrical components [13], [15]. These are calculated according to

$$V_p = \frac{V_{ab} + aV_{bc} + a^2V_{ca}}{3} \qquad (2.14)$$

$$V_n = \frac{V_{ab} + a^2V_{bc} + aV_{ca}}{3} \qquad (2.15)$$

Where

$a = 1\angle 120°$

$a^2 = 1\angle 240°$

Considerations of voltage unbalance often lead to induction motor analysis using an appropriate set of balanced positive and negative sequence equivalent circuits. The positive sequence equivalent circuit is considered to represent the normal operating condition of the machine. The negative sequence equivalent circuit can be considered to represent the effects of the unbalanced condition and sets up a reverse rotating field such

that the negative sequence slip is 2-s. Figure 2.7 shows the equivalent set of positive and negative sequence circuits of an induction machine.

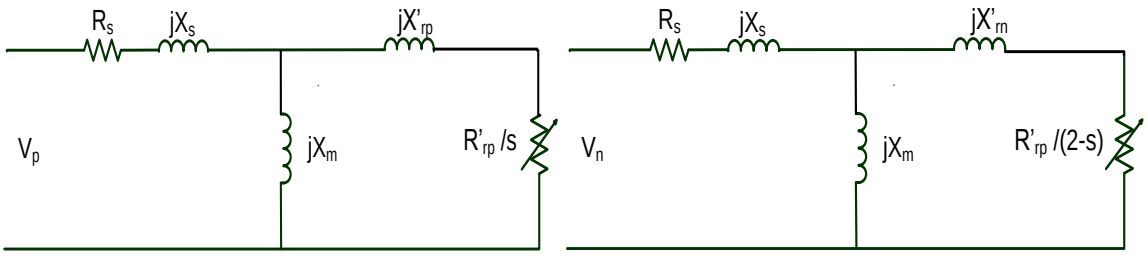

Figure 2.7: Sequence equivalent circuits for an induction machine [15]

Based on Figure 2.7, the negative and positive currents can be obtained by observing that they are a function of their sequence voltages, the machine parameters and the motor slip.

The effect of voltage unbalance (i.e. the negative sequence component) on the power and torque of the machine is to produce less than expected output conditions. When accounting for the positive and negative sequence components, the mechanical power and torque is calculated by [13], [15]

$$P_{Mechanical} = I_{rp}'^2 \, R'_{rp} \frac{1-s}{s} - I_{rn}'^2 R'_{rn} \left(\frac{1-s}{2-s}\right) \tag{2.16}$$

$$T_{Mechanical} = I_{rp}'^2 R'_{rp} \left(\frac{1}{s\omega_{sync}}\right) - I_{rn}'^2 R'_{rn} \left(\frac{1}{(2-s)\omega_{sync}}\right) \tag{2.17}$$

The above equations show that the negative sequence rotor currents cause a decrease in the output power and hence the overall output torque of the machine. Therefore, the overall effect of this decreased power has a direct effect of decreasing the motor's efficiency.

Since the resultant torque is reduced, the motor will be forced to operate at higher slip values if it is required to meet the expected full load torque demand [14]. This causes an

increase in rotor current and loss in the form of heat dissipation and thus further decreasing the efficiency [13], [16]. The increase in thermal stress due to the negative sequence current will lead to a reduction in the lifespan of the machine and the motor will thus succumb to the necessity to operate the machine under derated conditions [15].

When operating at lower than rated voltages the motor will compensate by drawing more current in order to produce the required torque [16]. This enhances the contribution to the I^2R_s losses already associated with the machine. It was shown in [12] that an increase in UBUV conditions causes the rotor current to increase which consequently contributes to the increase in overall motor losses, hence decrease in motor efficiency.

In contrast running the machine at over-voltage causes an increase in the magnetizing current within the core of the machine [16]. The possibility of saturation becomes evident and a decrease in efficiency will occur. Not only does the magnetizing current have an effect on the motor's efficiency, but it will also affect the motor's overall power factor [16]. The stator and core losses will increase and cause further decrease in the motor's efficiency [16].

Based on the above it is important that operators of electric machines endeavour to operate the machines under the best allowable conditions as close to rated voltages as possible.

- **Harmonics**

Induction motors driven by variable frequency drives are subjected to a degree of harmonic content, which appear at the motor terminals [6]. The time harmonic currents produce rotating fields within the air gap of the machine. These rotating fields rotate at a higher speed than fields produced by the fundamental current and consequently produce parasitic torques in the machine. Space harmonics are a consequence of non-sinusoidal mmf within the air gap. Thus, the air gap flux contains the fundamental and harmonic

components of flux [1]. These space harmonics contribute to parasitic torques in the machine.

2.3.3 Loading and Load factor

On average, industrial motors operate at approximately 60% of rated load [7], [17]. As seen on a typical efficiency curve, the efficiency does not vary drastically above 60% loading and it is a common fallacy that a motor's maximum efficiency occurs at maximum load [16]. In fact, the maximum efficiency is seen to occur between 50% and 80% loading, depending on the size and design of the machine [6], [18]. Below the 50% loading point, the efficiency is seen to decrease dramatically [19]. Since motor efficiency is specified at rated load, the actual efficiency obtained when operated at other than rated load can no longer be obtained from the motor's nameplate. Based on theoretical analysis, the authors of [18] showed that the maximum efficiency occurs when the sum of the load independent losses equates to the sum of the load dependant losses described by [18]

$$P_{Core} + P_{FW} = P_{Cu,Stator} + P_{Cu,Rotor} + P_{SLL} \tag{2.18}$$

Figure 2.8 shows a typical efficiency curve with a plot of load dependant and independent losses. The plot clearly shows that this maximum efficiency occurs when the variable and fixed losses are equal.

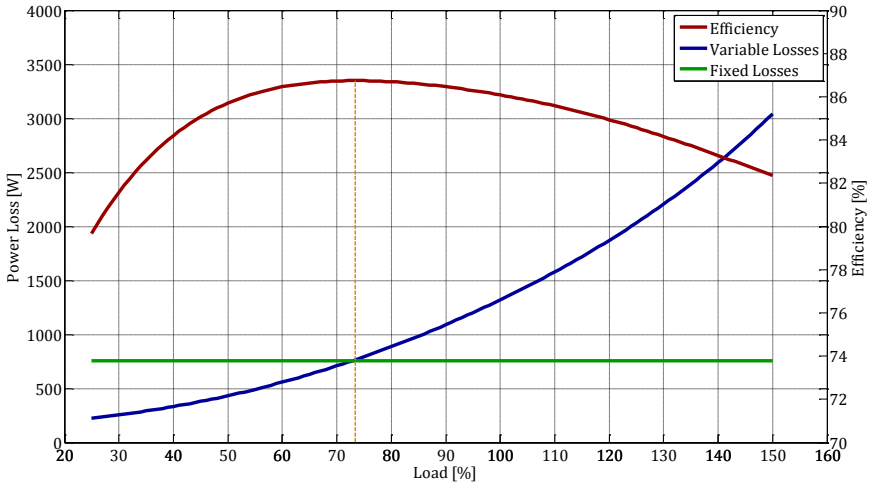

Figure 2.8: Efficiency curve showing maximum efficiency [18]

It is possible to modify the point of maximum efficiency by redefining the point of intersection. This can be achieved by either decreasing the load dependent losses or increasing the load independent losses [18].

- **Under- Loaded Conditions**

One of the most common factors contributing to lower than expected motor efficiency is attributed to under-loading [10]. An under-loaded motor is characterized by a significant efficiency drop at low values of load, as seen on a typical efficiency load curve. The effects of under-loaded conditions are often seen as a consequence of under utilization of the equipment. This often occurs in cases where a motor rating is selected on the basis that it may be required to perform under full load capacity of which occurs on the rare occasion such as peak conditions, resulting in under-loaded operations for most of its operating lifespan [10]. Another reason contributing to under loaded conditions is the choice of an oversized motor required for the application. This often occurs when the user desires that the output power be maintained at the desired level, despite abnormally low input voltages [10]. Therefore, when a motor is run under reduced load conditions it has the following advantages [18].

a) Accommodates load fluctuations and voltage imbalance
b) Contains the capacity for a safety margin, when meeting the requirements, when the mechanical load is uncertain.
c) Provide the ability for increasing future loads

Although maximum efficiency occurs below rated load, it is important that the correct loading factor be selected such that the compromise between maximum load and efficiency is achieved. Process demands require that maximum process output is obtained for as long as possible in order for industry to be profitable. Therefore, engineers should be aware of this and should select the most appropriate motor required for the application.

- **Over-Loaded Conditions**

Over-loaded motors contribute negatively to the efficiency of a motor since the increase in losses cause the machine to increase in temperature. Thus, this decreases the overall motor efficiency and decreases the life span of the machine.

Considerations of under-loading and over-loading of motors have provided engineers with an area of investigation and operators should ensure that the correct loading be sustained such that the motor operates at an acceptable efficiency level and that the loading conditions is not harmful to the machine. This should be achieved by not compromising the need to maintain the turnout required by industry.

2.3.4 Condition Monitoring and Maintenance

Condition monitoring and diagnostics are very important and can provide improvement when it comes to reliability, availability and maintainability of a system [17]. Machine misalignment, physical looseness and other imbalances can have an impact on the machines efficiency as well as its lifespan. Improper lubrication can cause increased friction resulting in increased losses. Unwanted vibrations may exist if the machine is not properly mounted or correctly aligned, which also decreases the efficiency. The effects of

neglecting regular maintenance of motors lead to an increase in losses, unnecessary breakdown and eventually malfunction. Sufficient lubrication and ensuring that ventilation ducts remain unblocked assist in ensuring that losses remain at a minimum. The installation of fans or other cooling methods will assist in the dissipation of excess heat and reduction of excessive losses and thus improving the efficiency.

Not only is this good practice in ensuring optimal efficiency of the motor, it will also prolong the life span of the machine. The running time of an induction machine often has a direct effect on the efficiency of the machine. Longer running times are associated with lower efficiencies. This is expected since worn out machines, due to age, often contain more losses. However, if sufficient maintenance procedures are practiced, the effects of motor aging will not drastically contribute to the deterioration of motor performance [10].

2.3.5 Effects of Motor Repair and Rewind

In industry, it is common practice to rewind damaged motors [10]. The objective is to return the motor to its original state. However, this is a challenging procedure which often results in a drop in efficiency [10]. Therefore, the decision to repair a machine should also account for the type of procedures adopted by a rewind company. Rewinding procedures have been known to reflect changes in winding and slot design, the choice of winding material, insulation performance and operating temperature [10]. These factors are characterised by changes in loss contribution emitted by the machine [10], [18], [20]. Due to the impacts of motor rewind on the type of losses associated with the machine, the overall efficiency is also affected. A case study performed in [18] and [21] showed an overall decrease in efficiency after a set of motors had been rewound. It should be noted that in special cases, when the motor is rewound under controlled conditions, an increase in motor efficiency can be achieved.

2.4 International Motor Efficiency Testing Standards

Several standards for testing the efficiency of electrical machines exist worldwide. Each of these standards contains their own testing procedures and requirements. Table 2.2 shows an outline of existing motor efficiency testing standards that exist globally.

Table 2.2 Global motor efficiency testing standards

Standard	Description	Year
IEEE Std 112	Standard Test Procedure for Polyphase Induction Motors and Generators	2004
IEC 60034-2-1 Part 2	Standard methods for determining losses and efficiency from tests (excluding machines for traction vehicles)	2007
SANS 60034 Part 2-1	Methods for determining losses and efficiency of rotating electrical machinery from tests (excluding machines for traction vehicles)'	2008
JEC-2137	Japanese Electrotechnical Commisison	2000
AS/NZ 1359.5	Three-phase cage induction motors -High efficiency and minimum energy performance standards requirements	2004
CSA 390	Energy Efficiency Test methods for Three-Phase Induction	1999

2.4.1 Overview of Existing Standards

A great deal of research is continuously being conducted to identify and compare motor efficiency testing standards. The following reviews highlight the main perspectives that have already been established.

a) P G Cummings et al, (1981) [8]

The authors provided a basic overview of the basic efficiency estimation methods. They proceeded to provide a detailed description of the tests methods involved in the IEEE Std 112 (1977), IEC Std 34-2 and JEC Std 37 in order to compare them. The authors

concluded that the IEEE 112 method is the most rigorous method when it comes to determining efficiency.

b) B Renier et al, (1999) [4]

The aim of this paper was to compare the similarities and differences between IEEE Std 112 and IEC Std 34. The paper stated that the three most important standards that exist are the IEEE Std 112 (1996), the IEC Std 34-2 and the JEC Std 37, since other national standards are seen to be harmonized with either one of them. The authors identified that the main difference between the standard is the way in which the stray load loss is determined. The author conducted efficiency tests and concluded that the IEC Std 34 and JEC Std 37 provide over estimations of efficiency compared to that of the IEEE Std 112. This is due to the fact the IEC Std 34 estimates a fixed value of stray load loss (0.5% of rated input power) while the JEC Std 37 completely neglects them.

c) A.T. de Almeida et al, (2002) [11]

The authors state that the two main methods that exist globally are the IEEE Std 112 and the IEC Std 34-2. Since the IEC Std 34-2 was under review due to inaccuracies in stray load loss determination, the authors also compared the proposed IEC 61972 methodology. The team then conducted experiments comparing the IEEE Std 112 and IEC Std 34-2. The authors concluded that the IEC Std 34-2 was not an accurate method for efficiency determination due to the estimation of stray load losses. It was then stated that the new IEC Std 61972 standard would assist in improving the standard in terms of motor efficiency testing.

d) A. Boglietti et al, (2004) [5]

The most important international standards declared by the authors are the IEEE Std 112, the IEC Std 34-2 and the JEC Std 37. The aim of the study was to compare the measurement procedures and experimental results obtained for the determination of efficiency. The authors concluded that the IEEE Std 112 is the most suitable standard for stray load loss measurements and efficiency determination.

e) W. Cao, (2009) [22]

The author constructively compares the differences between the IEEE Std 112 and the new IEC Std 34-2-1. The paper investigates factors such as instrumentation accuracies and methodologies established by the two standards. Upon the conduction of laboratory test outlined by the standard, the author concluded that the efficiency values obtained by the new IEC Std 34-2-1 are similar to its IEEE Std 112 counterpart.

In summary, the three most important standards that exist globally are the IEEE Std 112 [23], the IEC Std 34-2 (-1) [24] and the JEC Std 37 standards, while other existing standards resemble either the IEEE Std 112 or the IEC Std 34-2. The main difference between various testing standards is evident in the way in which the losses are determined, in particular the stray load losses. Due to the different strategies associated with the testing procedures, the efficiencies obtained for a given motor may differ significantly. Comparison of standards IEEE Std 112 and IEC Std 34-2-1 is discussed further below.

2.4.2 A Detailed Comparison between the IEEE Std 112 and IEC Std 34-2-1

For the purpose of this thesis only the IEEE Std 112 and IEC Std 34-2-1 will be reviewed since these methods are well established. The IEC Std 34-2-1 was adopted in South Africa in 2008 as the SANS 34-2-1 [25] and therefore is applicable in a South African context. The following section will outline some of the similarities and differences between the two standards.

- **Supply Conditions**

During laboratory testing, it is imperative that supply conditions are maintained within tolerances as stated by the standards. Table 2.3 outlines the required tolerances set by the IEEE Std 112 and IEC Std 34-2-1 standards.

Table 2.3 Required tolerances for supply conditions

Parameter [%]	IEEE Std 112 (2004)	IEC Std 34-2-1 (2007)
Maximum THD	5	5
Maximum Voltage Unbalance	0.5	0.5
Frequency Deviation	±0.1	±0.3

The tolerances of the supply conditions are identical for each of the standards with the exception of the supply frequency deviation. This reduces the level of discrepancies when comparing efficiency results obtained from testing.

- **Instrumentation Accuracies**

The accuracy of the instrumentation used in efficiency testing is an important aspect to consider when testing the efficiency value of a machine. Table 2.4 shows the respective requirements of full-scale instrumentation accuracies for each of the standards.

Table 2.4 Required instrumentation accuracy

Parameter [%]	IEEE Std 112 (2004)	IEC Std 34-2-1 (2007)
Instrument Transformer	±0.3	±0.3
Power	±0.2	±0.2
Voltage	±0.2	±0.2
Current	±0.2	±0.2
Torque	±0.2	±0.2
Speed (rpm)	±1	±1
Frequency	±0.1	±0.1
Resistance	±0.2	±0.2
Temperature (˚C)	±1	±1

As shown above, the new IEC Std 34-2-1 defines the same instrument accuracies as the IEEE Std 112. This is an improvement to the old IEC Std 34-2 [22] whose accuracy range is greater.

- **Test Procedures**

Based on the definition of efficiency (direct or indirect), the test procedures may differ within each of the standards. For comparison purposes, reference is made to the method with separation of losses (indirect method) since it is widely used [22]. Table 2.5 shows the required test procedures for each of the standards.

Table 2.5 Required test procedures

Parameter	IEEE Std 112 (2004)	IEC Std 34-2-1 (2007)
Cold Resistance and Temperature	✓	✘
Temperature Test at Rated Load	✓	✓
Rated Resistance and Temperature	✓	✓
Load Test	✓	✓
No Load Test	✓	✓
Stabilization of No Load Losses	✓	Optional

As shown above, the two standards are similar, except for the requirement of the initial cold resistance temperature. The IEEE Std 112 uses these measurements as a reference to which resistances can be corrected according to the recorded temperature during testing. The IEC Std 34-2-1 does not require the cold resistance and temperature measurement but alternatively uses the temperatures and resistances obtained during a load test. The techniques for stator winding correction for temperature will be further discussed in the subsequent section.

- **Loss Determination**

As mentioned before the main differences between established international standards are the way in which the losses are accounted for. Table 2.6 shows the specific requirements of each standard in order to determine each of the losses associated with the machine [22], [23], [24].

Table 2.6 Requirements for loss determination

Parameter	IEEE 112 (2004)	IEC 34-2-1 (2007)
Temperature correction of resistances	✓	✓
Installed temperature sensor	✓	✘ (optional)
Segregation of losses	✓	✓
Core loss with voltage drop compensation	✘	✓
Stray load loss using linear regression (correlation factor)	✓ (0.9)	✓ (0.95)
Torque meter correction	✓	✘
Dynamometer correction	✘	✓
Output power correction	✓	✓

As shown, there are numerous discrepancies in the procedures required for loss determination. A more detailed description of these differences is provided below.

a) Stator winding resistances and temperature correction

The IEEE Std 112 requires that the stator winding cold resistance be measured prior to the performance of any heat run test. The cold winding resistance measurement is then used as a basis when applying temperature correction. The cold winding resistance is then used to calculate the resistance of the winding at any load, provided that the temperature is measured at each load. Equation 2.19 shows how the temperature correction is catered for [23]

$$R_2 = \frac{R_1(t_2 + k_1)}{t_1 + k_1} \tag{2.19}$$

Where:

R_1 is the known value of winding resistance, in ohms, at temperature t_1

T_1 is the temperature, in °C, of winding when resistance R_{a1} was measured,
T_2 is the temperature, in °C, to which the resistance is to be corrected
R_2 is the winding resistance, in ohms, corrected to the temperature t_2
k_1 is 234.5 for 100% IACS conductivity copper

The IEC Std 34-2-1 does not require that internal temperature sensors be installed. Instead, the standard requires that the winding resistance be measured before the highest load and after the lowest loading point. The resistance for rated and higher loads shall be the value obtained before the highest load reading, while the resistance for less than rated load shall be determined by linear extrapolation using the two readings taken before the test for the highest load and after the lowest reading for 25% load [24]. This method has the advantage that it does not require internal temperature sensors to be installed and thereby the test can be applied to a wider range of motors (ie those without thermocouples) [22]

However, in the case of installed thermocouple, the IEC Std 34-2-1 follows a similar procedure in obtaining resistance values to that of the IEEE Std 112.

b) Core loss voltage compensation

The IEEE Std 112 and IEC Std 34-2-1 follow similar procedures when it comes to the determining the friction and windage loss independently from the core losses during the no load test. The IEEE Std 112 determines the core loss at each test voltage by subtracting the friction and windage loss and stator losses from the input power. A plot of voltage versus core loss is then obtained to find the value of core loss at any voltage value [23]. Ideally, the core loss obtained is constant and independent of the load.

The IEC Std 34-2-1, on the other hand, obtains the core losses by accounting for the stator resistive voltage drop at each loading point. A curve of voltage verses core loss power ($P_{core}= P_{Input}-P_{FW}$) is then plotted. The core losses at any loading point is then obtained from the curve at voltage U_r using equation 2.20 which accounts for the stator resistance voltage drop.

$$U_r = \sqrt{\left(V - \frac{\sqrt{3}}{2} \times I \times R_{LL} \times \cos\varphi\right)^2 + \left(\frac{\sqrt{3}}{2} \times I \times R_{LL} \times \sin\varphi\right)^2} \qquad (2.20)$$

Where :

V is the rated line voltage (V)

I is the rated line current (A)

R_{LL} is the line to line resistance (Ω)

φ is the power factor angle

The IEC Std 34-2-1 reflects a more precise value of core loss than the IEEE 112 due to the resistive voltage compensation [14].

c) Stray load losses

In the case of the IEEE Std 112, the stray load losses at different loads are obtained by subtracting the output power and all the losses accounted for from the input power, as shown in equation 2.8. In order to correct these values and reduce the influence of measurement error [4], the stray load losses are smoothed, using linear regression techniques, by expressing the stray load loss as

$$P_{SLL} = AT_{Shaft}^2 + B \qquad (2.21)$$

Where:

A is the slope

T_{Shaft} is the shaft torque in N.m

B is the intercept with the zero torque line

A correlation factor is used to determine whether the results are satisfactory. A good measurement is seen to have a correlation of higher than 0.9. [23]. The corrected value of stray load loss used for efficiency calculations is then obtained by shifting the line to pass through the origin and calculated as

$$P_{SLL.corrected} = AT_{Shaft}^2 \quad (2.22)$$

Traditionally the IEC Std 34-2 computed the stray-load loss by quantifying them to a fixed value of 0.5% of the full load power [14]. The new IEC Std 34-2-1 has revised this method due to its questionable accuracy. The new method follows the same procedure as the IEEE Std 112 when calculating the stray-load loss, however requires a higher correlation factor of 0.95 in order for the results to be useable.

In situations where it is not feasible to determine the stray load loss directly, it is possible to estimate the value of stray load loss. According to the IEEE Std 112, the stray load loss can also be estimated relative to the size of the machine. Table 2.7 shows the assumed values of stray load loss at rated load as a percentage of rated output power [23].

Table 2.7 Assumed values for stray load loss in IEEE Std 112 [23]

Machine rating	Stray-load loss percent of rated output power
0-90 kW	1.8%
91-375 kW	1.5%
376-1850 kW	1.2%
>1851 kW	0.9%

For other than rated load conditions, the stray load loss can be assumed to be proportional to the square of the rotor current and can be calculated at any desired load using [23]

$$P_{SLL} = P_{SLL,Rated} \times \left(\frac{I_{Rotor}}{I_{Rotor,Rated}}\right)^2 \quad (2.23)$$

The rotor current can be obtained according to

$$I_{Rotor} = \sqrt{I_{Stator}^2 - I_{No\ load}^2} \quad (2.24)$$

In the case of the IEC Std 34-2-1, the stray-load losses can be estimated by relating a fixed amount from a predefined curve based on the power rating of the machine [24]. The curve can be seen in Figure 2.9 and the governing equations for the graph are shown in Table 2.8 where P_1 is the input power and P_2 is the rated output power. The relevant equations defining the above curve are shown in Table 2.8.

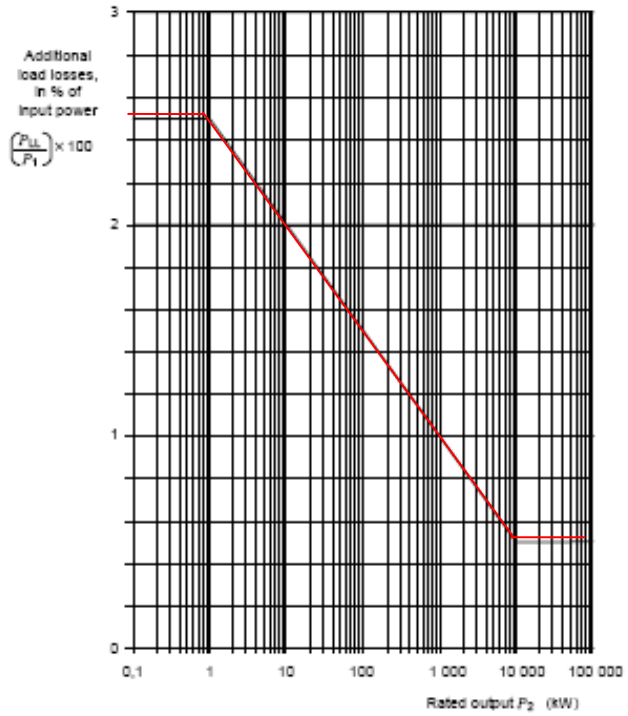

Figure 2.9: Assigned allowance for additional load loss [24]

Table 2.8 Equations of stray load loss for the IEC Std 34 2-1

Machine rating	Equation
P_2<1 kW	$P_{SLL}=P_1 \times 0.025$
1kW <P_2<10 000kW	$P_{SLL}=P_1 \times [0.025-0.005\log_{10}(P_2/1kW)$
P_2>10 000 kW	$P_{SLL} = P_1 \times 0.005$

Based on the above, the difference between the IEEE Std 112 and the IEC Std 34-2-1 is that the former estimates the stray load loss as a function of output power, while the latter estimates the stray load loss as a function of the input power.

2.5 Concluding Remarks

This chapter has provided an introduction to induction machines and its efficiency. The basic structure of the induction machine and its principles of operations were provided. Furthermore, a definition of motor efficiency using the direct and indirect method was outlined and the differences between the techniques were established. The various factors affecting the resulting efficiency were described in detail. Measures to reduce the implications of the factors in order to improve efficiency values were mentioned. Investigation of international efficiency testing standards were identified and showed that the most important standards are the IEEE Std 112, IEC Std 34-2 and JEC Std 37. Moreover a comparison between the IEEE Std 112 and IEC Std 34-2-1 in terms of supply tolerances, instrumentation errors and methodologies were performed. It was concluded that the IEEE Std 112 and IEC Std 34-2-1 are comparable and therefore efficiencies obtained by either method will be in close proximity to each other. In South Africa, the IEC Std 34-2-1 was adopted as the SANS 60034-2-1 in 2008. Therefore, this standard has been approved and is currently established in the motor testing industry. Therefore, the IEC Std 60034-2-1/SANS 60034-2-1 standard shall provide a baseline for comparison of efficiency values for the remainder of this thesis.

CHAPTER THREE

OVERVIEW OF EFFICIENCY ESTIMATION TECHNIQUES

This chapter provides an overview of existing efficiency estimation techniques. Each of these techniques is critically reviewed in terms of accuracy and level of intrusion. Furthermore, a comparison is made between each of the techniques in terms of tests and measurements required in order to obtain the overall efficiency of a machine. Motivation for the Non-Intrusive Air Gap Torque Method as a candidate for industrial application is also provided.

3.1 Introduction

Over the years there has been much research and development of various techniques and procedures that allow for the efficiency of induction machines to be estimated. These methods differ from accuracy, levels of intrusiveness, costs, labour intensity and overall complexity. The following sections will provide an overview of the various existing efficiency estimation methods.

3.2 The Nameplate Method

The name plate method, as the name describes, makes use of the information on the machine's nameplate in order to estimate the efficiency of the motor and assumes that the efficiency of the motor is constant and equal to the nameplate value [26]. The main advantage of this method is that it is considered to be the least intrusive of all the efficiency estimation methods [26] since it merely requires access to the motor's nameplate. Figure 3.1 shows an example of a typical name plate of an induction machine.

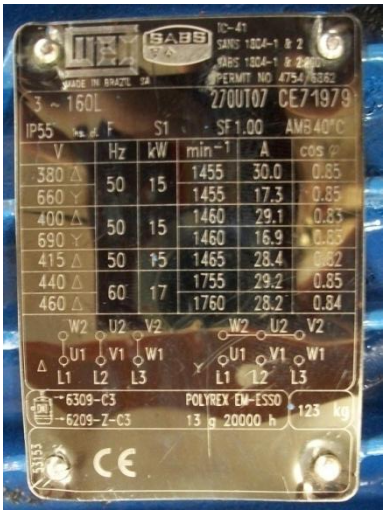

Figure 3.1: Example of a typical nameplate on an induction machine

Despite the low intrusiveness, there are three main areas of concern which put the method at a disadvantage when it comes to accuracy. These include 1) discrepancies in the adopted testing standards when nameplating the efficiency, 2) the nameplate data is no longer

applicable to rewound motors and 3), the effect of supply conditions on actual operating efficiency does not reflect the condition in which the motor was stamped [26].

3.3 The Slip Method

The slip method makes use of the motor speed measurement and is considered to be a simple method to implement. The simplest version of this method exploits the fact that the percentage of load is presumed to be proportional to the ratio of the measured slip to the full-load slip. Alternatively, the input power can easily be measured and the ratio of measured slip to rated slip is multiplied by the ratio of powers as described by [17], [26].

$$\eta = \frac{s}{s_{rated}} \times \frac{P_{Output,rated}}{P_{Input}} \tag{3.1}$$

The method has a relatively low intrusion level if the speed is measured using an optical tachometer and the input power is measured non-intrusively [26]. Although this method provides an improvement to the nameplate method, it is not considered to be accurate. Since NEMA allows the motor speed to deviate by 20% of nameplate speed, the resulting efficiency value will also deflect by 20% and thus propose inaccurate efficiency values [26]. Another error associated with this method is that the slip ratio represents the percentage of load when in fact efficiency is not equal to the percentage of loading [17]. The authors of [17] explored modifications to the standard slip methods, namely *The Ontario Hydro Modified Slip Method* and, *The Upper Bound Slip Method.*

3.4 The Current Method

The current method makes use of current measurements and nameplate values to estimate efficiency. It presumes that the percentage of load is closely proportional to the percentage of the ratio of measured current to full load current [17], [26], and that the efficiency can be described by

$$\eta = \frac{I}{I_{Rated}} \times \frac{P_{Output,rated}}{P_{Input}} \tag{3.2}$$

This method does provide an improved accuracy when compared to the slip method, however, it is still dependant on nameplate values. It should also be noted that the current-load curve is slightly non-linear in reality [17] and this makes the proportionality concept somewhat distorted. The main advantage of the current method is its ease in implementation and the use of clamp on current probes provides this method with a low level of intrusion [17].

An adaptation to the standard current method calculates the efficiency by taking into account the no load current and is calculated according to [17]

$$\eta = \frac{2I - I_{No\ load}}{2I_{Rated} - I_{No\ load}} \times \frac{P_{Outout,rated}}{P_{Input}} \tag{3.3}$$

This technique is, however, highly intrusive since the no load current is required, requiring the motor to be decoupled from its load in order to conduct a no load test. In [26] it is suggested that the average of the two approaches in equation 3.2 and 3.3 be calculated in order to obtain a more accurate result. In addition, NEMA states the current should not vary by more than 10% of the nameplate current [17]. This, as with the slip method, causes a deviation of the acquired efficiency value, making this method unreliable when a high level of accuracy is desired.

3.5 The Equivalent Circuit Method

The equivalent circuit model can be used to calculate the efficiency of an induction machine. The IEEE Std 112 F/F1 are the standard equivalent circuit methods. Method F is considered as too intrusive and not very user friendly due to its requirement for a no load, impedance and reverse rotation test [23]. Method F1 is similar to method F, except that it

does not require a reverse rotation test and that the stray load losses are determined by assumed values relating to the size of the machine as shown in section 2.4.2.

The Ontario Hydro Simplified Method F1 provides an alternative by eliminating the need for variable voltage. The method further incorporates the magnetising branch elements to be connected in series instead of the original parallel connection to allow for simplification purposes [17]. An additional resistance is added to the rotor circuit and accounts for the stray load losses which is mostly dependent on the rotor current. This method still requires a no load test and full load test at rated voltage [17].

The Nameplate Equivalent Circuit Method (ORMEL96) makes use of nameplate data and the value of resistance to determine the equivalent circuit of a machine. A parasitic resistance is inserted into the rotor equivalent circuit to account for the stray load loss [17]. Researchers from the Oak Ridge National Laboratory (ORNL) have developed a set of algorithms to determine the equivalent circuit parameters from the nameplate data [27]. The accuracy of this method is, therefore, determined by the accuracy of the nameplate data. Issues relating to the accuracy of the nameplate data were discussed in section 3.2.

Other modified methods include the *Rockwell Motor Efficiency Wizard Method*, the *Locked Rotor Method*, and the *Standstill Frequency Response Method*, [17]. These methods are still considered to be highly intrusive.

3.6 The Segregated Loss Method

The segregated loss method is considered to be the most straight forward method of efficiency estimation [17]. The method makes use of estimating the magnitudes of each loss component contributing to the power loss of the motor. The method further sums these loss components and subtracts the total from the input power to achieve an estimated output power.

The IEEE Standard 112 Method E/E1 is the standard segregated loss method. In order to determine the relevant losses, the method requires a variable load and variable voltage power supply. Also, it requires that a no load test be performed to obtain the constant losses. In order to account of the stray-load losses, the method uses the assumptions based on the percentage of rated output power according to the size of the machine. Once all the data is obtained from the above tests, the method uses a set of algorithms to calculate the individual loss components. Due to the nature of the tests required for this method, it is considered as intrusive and too disruptive for industrial applications hence only applicable to laboratory testing [17], [26].

The Ontario Hydro Modified Method extends the standard method by assuming the combined windage, friction and copper losses to be 3.5-4.2% of the rated input power, [17]. This technique allows for an alternative to performing the tedious task of no load testing. The stray load losses are estimated as with method E1. Further simplification is achieved by assuming a value of 0.8 for rated power factor and stator resistance estimation by using the motor current to predict temperature rise [17]. Thus, the only other required parameters are the input power and rotor speed. This method can be used as an in-service efficiency estimator due to its low intrusive and high accuracy attributes.

3.7 Torque Methods

The torque methods are considered to be the most direct of all the efficiency determination methods. The two main torque methods consist of the Air Gap Torque method and the Shaft Torque method. These are outlined below.

3.7.1 The Air Gap Torque Method

The air gap torque method makes use of the product of air gap torque and rotor speed as the air gap mechanical power to calculate the efficiency [26]. The air gap torque is calculated by using instantaneous measurements of the line voltage and current waveforms to obtain a set of integral equations as shown by [7], [17], [26].

$$T_{ag} = \frac{p}{2\sqrt{3}}[(i_a - i_b)\int V_{ca} - R_s(i_c - i_a)dt - (i_c - i_a)\int V_{ab} - R_s(i_a - i_a)dt \quad (3.4)$$

Where:

p is the number of poles

i_a, i_b, i_c are the line currents

V_{ab}, V_{ca} are the line voltages

R_s is the stator resistance.

The efficiency is calculated by observing that the air gap power equates to the product of the air gap torque and speed. After the subtraction of the friction and windage and the stray load losses, the output power is obtained. The efficiency is therefore calculated by [17], [26]

$$\eta = \frac{T_{ag} \times \omega_r - P_{FW} - P_{SLL}}{P_{Input}} \quad (3.5)$$

It was noted that there is a discrepancy in the efficiency equation when using the air gap torque method. The authors of [7], [17], [26], and [28], do not explicitly account for the core loss and calculate the efficiency using equation 3.5. In publications [27], [29] and [30], the core loss is accounted for after the air gap torque is acquired as shown in equation 3.6. This will be further discussed in subsequent sections.

$$\eta = \frac{T_{ag} \times \omega_r - P_{FW} - P_{Core} - P_{SLL}}{P_{Input}} \quad (3.6)$$

A notable feature of the air gap torque method is that it takes into account the negative rotating torque that occurs due to supply unbalances. This is of great significance since the voltage supply in industry is always polluted [17]. The air gap torque method uses the air gap torque power as its initial point for loss subtraction. This resultant air gap torque has already accounted for both the negative and positive sequence torques because it

recognizes the sign difference between them [27]. A more detailed investigation of the effects for unbalanced conditions is provided in [27].

The air gap torque method is considered to be accurate, [17], [26]; however, its pitfall lies in its need to conduct a no load test to determine the no load losses. Also, stator resistance and speed measurements make this method undesirable for field applications.

The Non-intrusive Air Gap Torque method (NAGT) is an adaptation to the original air gap torque method. Since the major disadvantage of the air gap torque method is its high level of intrusion, the authors of [7] have designed an online non-intrusive way to estimate efficiency. The stator resistance is estimated using a DC injection method, the rotor speed is obtained from current spectral analysis associated with rotor slot harmonics and the losses are accounted for using empirical values.

3.7.2 The Shaft Torque Method

The shaft torque method measures the shaft torque and speed directly in order to determine the output shaft power [17] The shaft torque method is the most straightforward method but is highly intrusive due to the need for direct access to the shaft [17], [26] and the need to couple the machine to a dynamometer. According to IEEE Std 112 method B, methods using dynamometers should not be implemented in field conditions [23]. The use of costly torque sensors also makes this method undesirable for field applications [17].

3.8 Alternative Methods

There are many other methods that exist regarding the estimation of motor efficiency. These methods will not be discussed in detail but are listed in this thesis for the purpose of completeness.

- Genetic Algorithms
- Statistical Methods
- Dedicated Instruments

3.9 Comparison of Efficiency Estimation Techniques

The efficiency estimation techniques discussed in the former sections, each has its own set of advantages and disadvantages. In general the main areas of concern are the level of intrusion (determined by the type and measurements of testing) and the accuracy. A comparision of these factors for each type of estimation technique is outlined below.

3.9.1 Accuracy Vs Intrusion

As discussed in the former sections, there is a trade-off between the level of accuracy and the amount of intrusion that each of the methods offer. As shown in Figure 3.2 the level of intrusion increases as the level of accuracy increases.

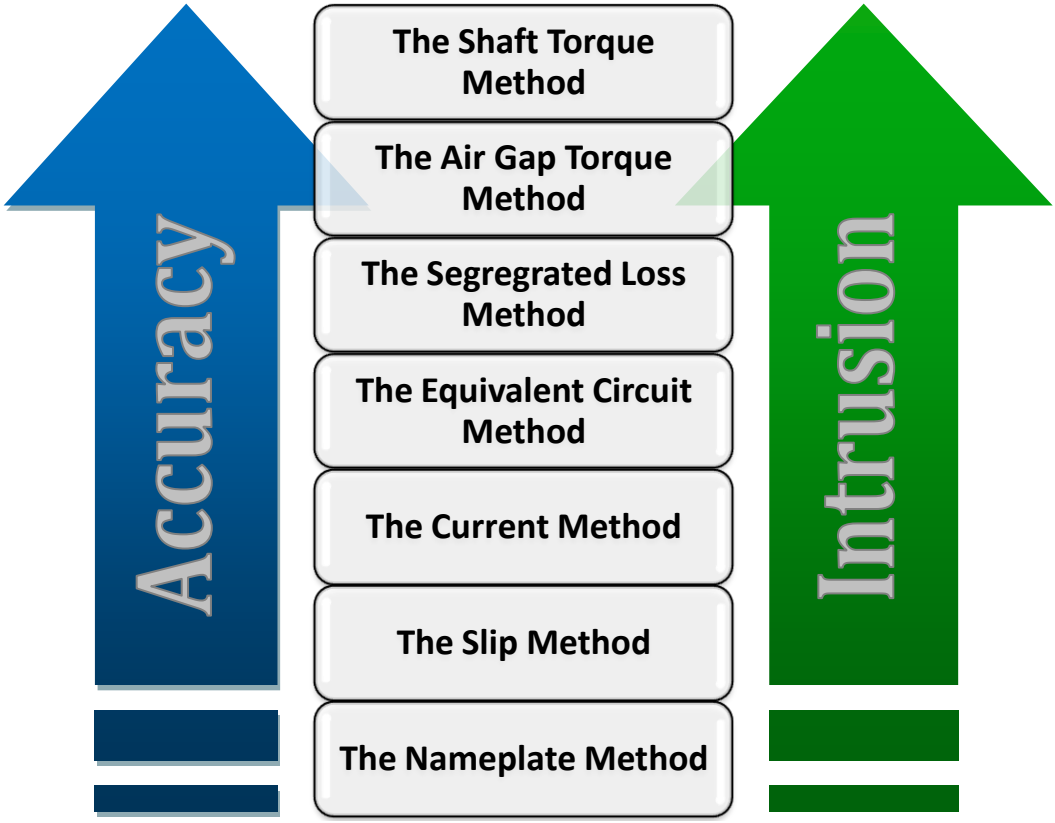

Figure 3.2: Comparison of accuracy and intrusion of efficiency estimation methods

The intrusion levels are dictated by the type of tests and data measurements required to acquire the motor's efficiency. The tests required by each of the above methods are outlined in the next section.

3.9.2 Required Tests and Measurements

The required measurements for the efficiency estimation techniques determine the level of intrusion and how tedious the method will be. The accuracy of the equipment used to obtain these measurements will also have a direct impact on the accuracy of the method and therefore it is imperative that test equipment meets the required accuracy levels. Based on the preceding sections, Table 3.1 depicts the required tests and data measurements necessary for each efficiency estimation method [17].

Table 3.1 Required tests and measurements for various efficiency estimation techniques

Method	No load test	Rated load test	Variable supply	Stator resistance	Speed	Torque	Nameplate data
Standard Nameplate Method	✗	✗	✗	✗	✗	✗	✓
Standard Slip Method	✗	✗	✗	✗	✓	✗	✓
Ontario Hydro Modified Slip Method	✗	✗	✗	✗	✓	✗	✓
Upper Bound Slip Method	✗	✗	✗	✓	✓	✗	✓
Standard Current Method	✗	✗	✗	✗	✗	✗	✓
Adapted Current Method	✓	✗	✗	✗	✗	✗	✓
Equivalent Circuit Method- IEEE 112 F1	✓	✗	✓	✓	✓	✗	✗
Ontario Hydro Simplified Method F1	✓	✓	✗	✓	✓	✗	✗
Segregated Loss Method- IEEE 112 E1	✓	✓	✓	✓	✓	✗	✗
The Ontario Hydro Modified Method E1	✗	✗	✗	✓	✓	✗	✗
Air Gap Torque Method	✓	✗	✗	✓	✓	✗	✗
Non Intrusive Air Gap Torque Method	✗ (Uses empirical values)	✗	✗	✗ (Estimated)	✗ (Estimated)	✗	✗
Shaft Torque Method	✗	✗	✗	✗	✓	✓	✗

3.10 Concluding Remarks

This chapter provided an overview of existing efficiency estimation techniques. The main attributes of each method were introduced and possible alternative modified methods were included. The comparison of each of these methods showed that there is a trade-off between accuracy and level of intrusion depending on the required test. In this regard, the nameplate method is considered the least accurate and intrusive, while the shaft torque method is the most accurate but contains a high level of intrusion. In the case of onsite implementations of these methods, the user should ensure that each of the advantages and disadvantages are considered before execution.

Based on the investigation of each of the techniques, the Non Intrusive Air Gap Torque Method provides a good trade-off between non-intrusiveness and accuracy in estimating the efficiency of motors while they are in operation. Due to the need to acquire parameters such as the stator resistance, speed, no load and stray load losses non-intrusively, the method still contains sources of inaccuracies. The remainder of this thesis will, therefore, investigate various methods for determining these parameters as accurately as possible, with the aim of estimating the efficiency of a machine under field conditions.

CHAPTER FOUR

OVERVIEW OF STATOR WINDING RESISTANCE ESTIMATION TECHNIQUES

This chapter provides an overview of existing stator winding resistance estimation techniques. The estimation techniques are categorised under model based estimation and signal based estimation methods. Furthermore the advantages and disadvantages of each of the estimation methods are discussed.

4.1 Introduction

The stator winding resistance of an induction machine is a highly sought after machine parameter since it is required in many motor efficiency estimation methods. In particular, the effects of resistance measurements have a great impact on the machine's operating characteristics. The accuracy of measuring this parameter is critically important when determining the stator winding losses and during thermal modelling applications where the stator resistance can be used to detect high temperatures.

The stator winding resistance of an induction machine is traditionally determined by performing an unpowered test. This primarily involves shutting down the machine and waiting until standstill before the resistance is measured using an ohmmeter or galvanometer. This procedure is often unacceptable in the field since it is highly intrusive. Also, the stator resistance is only measured at a particular temperature (usually under rated load conditions whereby it is obtained from a temperature test run). This is not a realistic determination since stator resistance is highly dependent on temperature. It is possible to perform temperature correction methods however; this relies on the installation of costly thermocouples.

Based on the above, researchers have investigated and developed various stator resistance estimation methods. These methods are predominantly used for the improvement of field orientated drives or in sensorless speed control applications where the shaft speed is desired at low speeds [31]. This is due to the requirement of stator resistance (R_s) in the induction motor model, upon which these methods are based. More recently, R_s estimation techniques have been developed in motor thermal monitoring and protection applications. High temperature readings of stator winding allow for the detection of insulation degradation and stator winding faults, both of which contribute negatively to the lifespan of the machine. This provides an alternative to expensive and intrusive thermocouple installations. There are two main approaches for R_s estimation, namely induction machine model-based R_s estimation and signal-based R_s estimation. These are discussed below.

4.2 Induction Model Based R_s Estimation

4.2.1 Field Orientated Controlled Drive Applications

Direct torque control of induction machines use the stator resistance in order to obtain the estimation of the stator flux developed within the machine. The variation of stator winding resistance will thus affect the value of stator flux, especially at low speeds, and thus needs to be estimated as accurately as possible.

A proportional-integral (PI) and fuzzy logic resistance estimation scheme was investigated in [32]. The estimation of R_s is based on the changes in the current vectors, since the stator current is affected by resistance changes [32]. The authors concluded that the fuzzy logic based resistance estimator was more robust and performed better than its PI counterpart, especially at low operating speeds.

In [33] an algorithm was developed to estimate the stator winding resistance using the stator voltages and currents. The application for the algorithm is aimed at on-line determination of leakage reactance and stator resistance of induction machines which are connected to a vector controlled drive. It was observed that a high level of accuracy for determining R_s is required since the stator flux is highly dependent on it. Also, the effects of temperature make it essential that the value of R_s be measured and updated during machine operation.

A mutual model reference adaptive system (MRAS) for field orientation control of induction machines was proposed in [34]. The method allows for the reference and adjustable model to be interchanged accordingly such that either the rotor speed or stator resistance can be determined. After being validated both by simulation and by experimentation, it was shown that the stator resistance of an induction machine can be usefully obtained with a rapid algorithm response time.

Another MRAS approach for the real time identification of induction motor stator and rotor resistance was explored in [35]. The proposed schemes were verified by simulations. The

authors concluded that the systems only provide satisfactory results in the case of persistent excitation. The need to conduct sensitivity analysis of these parameters and to verify the stator and rotor identifiers experimentally on the estimation techniques was identified.

4.2.2 Sensorless Speed Control Applications

Speed control of an induction machine requires the accurate estimation of the fluxes within the machine. This estimate is obtained from the motor's circuit parameters and therefore is dependent on the stator resistance.

In [36], the authors explored the effects of stator variations on motor speed control applications and developed a scheme to estimate R_s based on the induction motor model under steady state conditions. The method is based on evaluating the reactive power, obtaining the stator and rotor fluxes and calculating the developed torque in order to obtain R_s. An investigation into the sensitivity of R_s due to uncertainties in inductive parameters was also performed.

In [37], the authors attempted to adopt a two-time scale approach to the stator winding estimation process such that an adaptive online tuning algorithm can be implemented. The aim was to establish a reliable algorithm that can be applied to all loading conditions and operating speeds. A full order state observer of the stator resistance and its error estimation were developed. The two observers were analysed according to the assumption that each system contains two subsystems, of which accounts for its own dynamics, one being faster than the other. The authors concluded that an accurate and reliable estimation of R_s can be obtained.

An online stator and rotor resistance identification method without rotational transducers was investigated in [38]. The R_s identification algorithm is based on the power flow in the air gap. The method uses the values of the calculated load torque obtained from

measurable quantities of stator current, angular velocity and reactive power. Due to the need to determine the sign value of the load torque, the true value of R_s can only be obtained once the correct sign value is obtained. A DC flux injection procedure and filter design method (to avoid differentiation) was implemented. Experimental results proved that the technique can accurately estimate the value of R_s at any load when the machine is operating under steady state conditions.

4.2.3 Thermal Monitoring Applications

A fuzzy logic based stator resistance estimator is presented in [39]. The authors proposed a fuzzy logic algorithm that estimates the stator winding temperature based on the stator current and frequency. Based on the simulation and experimental performance of the logic estimator, the authors concluded that the stator winding resistance can be estimated accurately with excellent performance when calibrated with a thermistor network embedded in the machine.

In [40], the authors proposed a two-stage stator and rotor resistance estimation technique. The rotor resistance and flux linkages are estimated using MRAS techniques. The authors concluded that this method provides an accurate means of stator winding resistance estimation at high speeds provided that the accuracy of rotor resistance and rotor flux linkages is unquestionable. In particular the value of L_m largely affected the accuracy of R_s at high speeds.

4.2.4 Advantages and Disadvantages of Induction Model Based R_s Estimation

The induction model based R_s estimation techniques provide a non-invasive method to estimate the stator resistance. However, the pitfall of these methods is accuracy. According to the research done by the authors of [31], obtaining accurate measures of R_s at speeds other than low speeds deemed challenging. Although the observation has been considered empirically, the phenomenon has yet to be fully explained.

During high speed operations R_s is usually considered to be negligibly small when compared to the equivalent input impedance of the machine. Hence, as stated in [31], errors in terminal measurements drastically affect the accuracy of R_s as it will be highly sensitive to these errors. At low speed the method is appropriate although it depends on the determination of the other parameters.

Many of these estimation methods rely on the prior knowledge of parameters such as self, mutual and magnetizing inductance. Although these parameters can be determined from the nameplate data or obtained experimentally, there exist inherent errors. For instance, the nameplate data may no longer apply if the machine has been rewound. The conduction of necessary experiments in order to obtain these inductances makes the method highly intrusive. The accuracy of R_s is dependent on these parameters and therefore if they contain errors, the value of R_s will consequently also be inaccurate. Also, one could argue that if one needs to conduct experiments to obtain the inductance values, one might as well conduct experiments to obtain R_s with a somewhat more direct and less tedious approach.

It was also shown that the accuracy of R_s is sensitive to parameter variation. Thus, parameters are expected to be constant throughout operation if the R_s estimation technique is to be applied.

4.3 Signal Based R_s Estimation

Signal based R_s estimation techniques provide a more direct approach to R_s determination. In general these approaches often require additional circuitry or control operations in order to inject DC components into the stator windings of the machine.

In [41], the concept of DC bias injection in order to estimate R_s was introduced. The authors used an online approach by adding a DC bias to the reference signals, thereafter filtering the result to obtain the DC components. The value of R_s was then obtained via a regression model using a least squares algorithm.

In [42] the stator winding resistance was also estimated using a least squares minimization problem. The technique was applied to an AC drive connected system which contained an accessible neutral connection to which a central tap of a capacitor bank was connected [42]. The machine is supplied with a symmetrical three-phase voltage supply and a zero sequence component was simultaneously added. The stator winding resistance was obtained by applying a least squares algorithm to the data obtained during the addition of a zero sequence voltage.

In [43] a controlled DC bias signal injection circuit was developed to intermittently inject a DC signal into the stator winding of a motor. This was achieved by connecting a circuit, consisting of a power MOSFET connected in parallel with a resistor, between the source and terminals in one phase of the machine. By measuring the DC voltage and current, the value of R_s can be obtained. It was concluded that this technique provided an accurate means of R_s estimation of line connected machines.

In [44], the stator resistance is determined to allow for thermal monitoring of the stator winding of a machine. The estimation of R_s and R_r is based on the terminal measurement of voltage and currents and the equivalent circuit of the machine. The estimation process involves the injection of two signals of different voltage and frequency. After experimental validation the approach proved to be feasible. This method, however, is not applicable to line connected machines and thus contains a degree of limitation as a generic R_s estimation technique.

A superposition technique was used in [45] which incorporated a modified double-bridge circuit by switching in a DC supply into the stator windings. Tests involving an inverter supply with a six step control and pulse width modulation (PWM) were also investigated. Based on the experimental results, there exists a large degree of inaccuracies and thus did not prove satisfactory.

4.3.1 Advantages and Disadvantages of Signal Based Rs Estimation

The main advantage of signal based R_s estimation schemes is the accuracy level associated with the technique. Additionally, these methods are independent of motor parameters and are not affected by the inherent motor asymmetry. The use of zero sequence components is highly advantageous since it does not contribute to the generation of electromagnetic torque and therefore does not affect the operating conditions of the machine [42]. Unfortunately, this method requires an easily accessible neutral point to connect the capacitor. This requirement is not viable under plant conditions, especially for delta connected motors.

In most cases signal injection based methods do not require the prior knowledge of any other machine parameters. This contributes to the low level of intrusion contained by these methods. The only degree of intrusion that exists is found in the installation of the circuitry. This can be achieved during maintenance or scheduled downtime. Once the circuit has been installed the method can be considered as having a low level of intrusion [7].

DC injection circuits do however, contain some pitfalls. Due to the additional signal injection, a degree of unbalance within the machine is seen to exist. Also, the additional DC components contribute to levels of torque pulsations as a result of the interaction between the stator and rotor flux components [7], [43]. These torque pulsation may have a negative effect on the driven load if it exceeds the tolerable amount. Additional circuitry also contributes to increased power dissipation, which needs to be accounted for.

4.4 Concluding Remarks

This chapter summarized the existing stator winding resistance estimation techniques. These techniques were categorised into model based and signal estimation methods. The advantages and disadvantages associated with each of these categories were presented. In general, the model based estimation methods are dependent on the parameter of the machine and the accuracy of these methods is often compromised if these parameters are not accurately obtained. Signal based resistance estimation schemes, on the other hand, are considered to be more accurate, however their level of intrusion is jeopardized.

The signal based R_s estimation technique as proposed in [43] was selected as the candidate method for this thesis. This technique was chosen due to its application to line connected machines. Furthermore, the expected accuracy levels of this method are considered to be high relative to the other proposed methods. Additionally, the circuitry implementation is simple and the components readily available. Despite the intrusive nature of the installation process, it is only a once off procedure and thereafter the technique is considered to be non intrusive. This issues relating to negative effects of torque pulsations, power dissipation and unbalances will be addressed.

CHAPTER FIVE

OVERVIEW OF ROTOR SPEED ESTIMATION TECHNIQUES

This chapter provides an overview of different rotor speed estimation techniques. The majority of these techniques are based on various applications of model based methods or alternatively using analysis of electrical signal spectrums. In contrast, the use of mechanical signal spectrum techniques is also presented.

5.1 Introduction

The rotor speed of an induction machine is required in the efficiency determination of induction machines. Traditionally the use of shaft mounted speed encoders and highly advanced tachometers have proven to be costly and are highly intrusive to install. Also, in many cases access to the motor shaft is not feasible and thus hand-held optical tachometers cannot be used. Over the years, much research has been done to develop a technique for which the rotor speed can be estimated over a larger range of frequencies and load operating conditions. In most cases, sensorless speed estimation techniques have been developed to focus on field orientated control applications with inverter driven machines. Many of the techniques reviewed here use electrical signal spectrum techniques. However; the use of mechanical signals is also discussed. The following sections outline a few of the more common sensorless speed estimation technique.

5.2 Induction Motor Model Based Techniques

A model reference adaptive system (MRAS) for a speed sensor-less control of an induction machine is proposed in [46] and [47]. It was stated that estimating rotor speed using rotor flux becomes difficult at the low speed ranges. Also if the motor parameters are set incorrectly or are affected by variations such as temperature, incorrect speed values will be obtained. To overcome this, the authors of [46] developed a set of observers that identified the stator resistance simultaneously with the rotor speed.

In [47] a mutual MRAS based on two models allows for the models to be interchangeable in order to identify both the stator resistance and rotor speed for a field orientated control application. The authors of [47] noted that the stator leakage inductance also has an affect on the performance of speed identification. Based on the developed mutual MRAS system the need for integration and stator inductance was removed and allowed for a wider range of speed detection.

More recently, a comparison of the conventional and AI-based MRAS motor speed estimation techniques was presented in [48]. Based on simulation results the authors

verified and concluded that the AI-MRAS technique is more accurate and robust when incorporating simultaneous online stator resistance estimation than the conventional MRAS system

Another method to address the resistance variation issue is proposed in [49] which incorporates an algorithm in which the rotor resistance is estimated on-line using a least squares method obtained during a speed transient, while the stator resistance is estimated using the instantaneous reactive power. In [50] the authors devised a speed equation from an equivalent circuit by taking the dot and cross product of the rotor flux and current.

Model based speed estimation using the MRAS have proven to be successful speed estimators, however it is known to fail under low speed operations. The methods are known to be parameter dependent and are affected by parameter variation. Also, the machine's parameters are not always easily obtainable, especially in cases where the nameplate is not visible or the motor has been rewound. On the other hand, the method does not suffer from high intrusion levels and this is advantageous to its application.

5.3 Electrical Signal Spectrum Techniques

The speed of an induction machine can be determined by using the motors' input electrical quantities, namely voltages and currents. A few of these techniques are outlined in the subsequent sub-sections.

5.3.1 Rotor Slot and Eccentricity Fault Frequency Harmonics

Induction motors are constructed to contain slots on the stator and rotor core to allow for the insertion of windings. These slots are known to produce slot harmonics in the air gap flux which further induce slot harmonic voltages within the stator windings [51]. Based on the above, the authors of [51]and [52] employed an algorithm for speed detection of induction motors under variable frequency drive applications. The speed detection process utilizes the rotor slot harmonic voltage by employing sampling, subtraction, filtering and zero crossing techniques.

In [53] the authors focused on a similar approach to the existing rotor slot harmonic techniques mentioned above and incorporated Fast Fourier Transform (FFT) processing. However, the rotor slot harmonics are obtained from the induced currents instead of the induced voltages since it was observed that voltage degradation becomes prominent at low speed. The paper addresses the limitations of speed detection at low frequency and light load conditions by ensuring that a high frequency resolution for the FFT is used. The method requires measurements of only the stator current in order to predict, amongst many things, the rotor speed. The authors claimed an error of 15 rpm when comparing the developed technique with that of the measured speed using an opto-electrical sensor.
An overview of various spectral estimation techniques on rotor slot harmonics is presented in [54]. The authors verified and compared the techniques both by simulation and laboratory implementation. The authors concluded that a maximum entropy method (MEM) proved to be most successful especially at the higher ranges of operation speed whereas, the FFT approach is more suitable under low speed conditions where longer sets of data can easily be obtained. In [55] the authors also investigated numerous spectrum estimation techniques and outlined their advantages and disadvantages. The investigation was to establish which technique provided maximum accuracy with minimum sampling time. It was concluded that parametric spectrum methods provided the highest accuracy with minimum sampling time.

Rotor slot harmonic techniques provide an improvement on the MRAS type method since they are not affected by parameter variation and perform better at lower speed ranges. However, the pitfall lies in the algorithm's dependency on parameters and requires that the number of rotor slots be predetermined.

In [56], however, the authors developed an algorithm to detect the speed of an induction machine using the current harmonic spectrum. The algorithm incorporates the detection of the number of slot via an initialization procedure using eccentricity harmonics and merely requires the number of poles to be depicted by the user. The speed detection algorithm then employs various signal processing techniques in order to obtain the speed related frequency from one of the stator currents.

A speed estimation equation based on broken rotor bar fault detection was developed in [57]. The proposed algorithm utilizes the motor's stator current signal and applies an FFT to obtain the frequency spectrum. After searching for a harmonic component with the largest amplitude within a defined interval the speed can be obtained. However, the method requires that the number of rotor bars of the motor be known.

Despite the improvement suggested above, speed detection using rotor slot harmonics is a highly tedious task that involves high level signal processing and computation. One advantage is that these methods are generally non intrusive since they only require either voltage or current signals to be captured. This is easily obtainable at the motor's terminals or control centre.

5.3.2 Additional Carrier-Signal Injection

In [58] the rotor speed and position of an AC machine is detected by injecting a high frequency signal into the machine. The technique makes use of the rotor's magnetic saliency when a high frequency voltage signal is superimposed upon the fundamental input voltage.

Another high frequency signal injection method is proposed in [59]. The method employs the use of this high frequency carrier signal and their sideband frequencies (due to rotor eccentricities) to establish a frequency component that is related to the motor speed. In [60] a combination of signal injection and rotor slot harmonic detection technique is proposed. An additional carrier signal voltage is added to the excitation voltage. The carrier signal current which contains the spatial information is then analysed by obtaining the rotor slot harmonics.

The signal injection procedures discussed above are aimed at inverter driven induction machines. Thus, this injection of the carrier signal can be easily implemented without any

additional circuitry. In contrast, if the machine is line connected, additional signal injection circuitry is required. This can be a costly and highly intrusive procedure.

5.3.3 Neural Network Techniques

An artificial neural network (ANN) approach to obtain the motor speed from its dynamic equations is presented in [61]. It was explained that the effects of singularity produces a speed signal that contained a high degree of ripple. This was overcome by applying a portioned approached by separating the numerator and the denominator of the speed equation. This allows for the ANN algorithm to be 'trained' to recognise these values independently and calculate the speed accordingly.

More recently, in [62], a neural network approach was investigated in order to extract the rotor speed by applying a wavelet technique to the stator current of a motor. The authors adopted a 'training off-line estimating on-line' approach and incorporated a dynamic gradient learning algorithm. After implementation, the authors recorded an average error within ±5 rpm of the actual speed and indicated high precision in steady state operation and good dynamic tracking during transients.

5.3.4 Kalman Filters

A unique speed estimation using extended Kalman filters is proposed in [63]. The algorithm imports voltages and currents and calculates the output estimated speed via numerous state estimation processes. The authors produced a Matlab/Simulink model to implement the technique. Furthermore, optimising the extended Kalman filter was investigated using a genetic algorithm.

5.4 Mechanical Signal Spectrum Techniques

The analysis of the mechanical vibration spectrum is prominently used for fault detection purposes. Misalignment, bearing faults and motor eccentricities can be detected by observing the relevant frequency components of the vibration spectrum. In particular, the

mechanical imbalance of the rotating parts associated with the machine causes low frequency harmonics in the vibration signature spectrum. The largest harmonic in this low frequency range is primarily associated with the rotational frequency of the machine and hence can be translated into speed.

An overview of various rotor speed estimation techniques, including vibration analysis, is provided in [64]. The authors verified these methods experimentally on two induction machines. It was concluded that the performance of these techniques show a high degree of accuracy, with the vibration and flux signature analysis being the most favourable. In [65] a non-intrusive load and efficiency evaluation is presented. In particular, the paper discusses the use of vibration signature as a means to determine the rotor speed.

A speed estimation technique using piezo-electric sensors is proposed in [66]. The technique exploits the vibration harmonics due to electromechanical torque and radial force pulsations. The vibration signal is processed through various filters, a zero crossing detector and a moving average filter. The authors verified the technique experimentally and the results showed a correlation between the actual and estimated speed.

The main advantages associated with vibration signature spectrum is that, because a machine will always contain manufacturing imperfections, an inherent eccentricity will always be present ensuring that speed detection is guaranteed. The accuracy of the detection is therefore dependent on the instrumentation used and the signal processing methodologies used. Vibration analysis can be implemented on any induction machine; in particular those which are line-connected.

5.5 Concluding Remarks

This chapter investigated the various speed detection methods proposed in literature. Most of the speed detection schemes available are based on the electrical signal spectrum. Despite their non intrusiveness, these methods are often associated with high level signal processing. Additionally, the reliability of these methods was seen to degrade at the lower speed ranges. Mechanical signal spectrum techniques however, incorporate the motor's inevitable vibration as a means for rotor speed detection. These methods are non-intrusive, easy to implement and are accurate for the entire speed range.

Based on the above, the candidate method chosen for the estimation of rotor speed incorporates the use of the mechanical vibration spectrum. This method can be attributed to low intrusion levels in comparison to the other methods. Additionally the speed detection process can be easily implemented by simple signal processing FFT techniques. As shown in [64] the proposed technique shows a straightforward, reliable and accurate means of rotor speed estimation.

CHAPTER SIX

DEVELOPMENT OF THE NON-INTRUSIVE AIR GAP TORQUE METHOD

This chapter presents the development of the Non-Intrusive Air Gap Torque Method for efficiency estimation. Candidate methods for stator winding resistance and rotor speed estimation are presented. The derivation of the air gap torque equation is provided and discussions around its contribution to the efficiency estimation equation are given. Furthermore, the relevant empirical methods of no load and stray load loss estimation are discussed. Combining the aforementioned estimated components, the overall non-intrusive air gap torque efficiency estimation process is established.

6.1 Introduction

The development of the non intrusive air gap torque method (NAGT) incorporates the choice of various non-intrusive estimation techniques. This includes stator resistance, rotor speed, stray load loss and no load loss estimation. In order for these techniques to be implemented, it is necessary to develop the relevant theory in more detail so that their topologies can be combined to establish an overall efficiency estimation method. The following sections provide a detailed description of the chosen estimation techniques and indicate how the overall NAGT method is established.

6.2 Motivation for Non-Intrusive Efficiency Estimation

The main reason for efficiency determination lies in the ability to identify whether the machine is operating in such a way as to maximize production output with minimum input resources. The motor may be worn or out of date, thus analysis of the motor efficiency will assist in the decision to either replace or repair the existing motor [67]. Efficiency measurement provides industry with the ability to perform energy audits of its plants in order to assist with cost analysis [67], [68]. Another reason to be able to measure efficiency exists in the event of receiving a rewound machine [67].

Traditionally the efficiency of a motor is measured in a laboratory using advanced instrumentation that is accurate, precisely calibrated and the use of dynamometers. Under laboratory conditions, the efficiency is obtained under balanced, rated voltage and stable load. These tests are highly intrusive because they require a no load test, reduced voltage and unpowered stator resistance measurements [69]. These factors are often undesirable in the field environment due to cost and difficulty in implementation and thus they can only be conducted during plant outages or maintenance procedures.

The induction machine out in the field is subjected to many non-ideal conditions. For instance, the power supply could be polluted since it is not perfectly balanced or contains a certain degree of harmonics [26]. These factors affect the efficiency of the machine and thus it may not meet the ratings proposed by the manufacturers.

The need for in-service efficiency estimators has become mandatory in many industrial applications. The main requirement of these methods are to avoid the use of high cost equipment and to reduce the amount of intrusion while still maintaining a high level of accuracy [17].

6.3 The Air Gap Torque Equation for Efficiency Estimation

The development of the air gap torque method is required for the understanding of the relevant equations that need to be applied in order to use the NAGT method as a means for efficiency estimation. The derivations of these equations are outlined below.

6.3.1 The Air Gap Torque Equation

In the development of the air-gap torque equation, the following assumptions are made [28], [70],

- The three-phase leakage reactances are linear and identical
- The negative sequence winding spatial components (excluding the time harmonics) are negligible
- The instantaneous magnetic unbalances for three-phases are ignored
- The effects of the DC components of the flux linkages are neglected.

The air gap torque equation is derived in more detail in [70]. Based on these assumptions, the air gap torque equation can be expressed as

$$T_{ag} = \frac{p\sqrt{3}}{6}[i_a(\psi_c - \psi_b) + i_b(\psi_a - \psi_c) + i_c(\psi_b - \psi_a)] \qquad (6.1)$$

The term $i_a(\psi_c\text{-}\psi_b)$ represents the torque producing component of the phase a winding. The phase a current interacts with the air gap flux that is perpendicular to the magnetic axis of the winding. Similarly, the second and third term represent the torques produced by phase b and phase c respectively.

The air gap torque equation can also be viewed in terms of stator voltage equations.
The voltage developed in each of the three-phase windings can be expressed as follows [70].

$$v_a = \frac{d\psi_a}{dt} + ri_a \qquad v_b = \frac{d\psi_b}{dt} + ri_b \qquad v_c = \frac{d\psi_c}{dt} + ri_c \tag{6.2}$$

Where:

ψ_a, ψ_b, ψ_c are the flux linkage of phase a, b and c

i_a, i_b, i_c are the phase currents

r is the phase resistance

Solving for the flux linkages in terms of integrals, equation 6.2 can be expressed as the integral of the input voltage less the stator copper voltage drop.

$$\psi_a = \int (v_a - ri_a)dt \qquad \psi_b = \int (v_b - ri_b)dt \qquad \psi_c = \int (v_c - ri_c)dt \tag{6.3}$$

Equation 6.3 can then be substituted into the air gap torque equation in equation 6.1 and simplified to obtain the air gap torque equation in terms of three phase line voltages and currents as shown in equation 6.4.

$$T_{ag} = \frac{\sqrt{3}p}{6}\Big\{(i_a - i_b)\int [v_{ca} - R_s(i_c - i_a)] - (i_c - i_a)\int [v_{ab} - R_s(i_a - i_b)]\Big\} \tag{6.4}$$

Where:

p is the number of poles

i_a, i_b are the line currents

v_{ca}, v_{ab} are the line voltages

R_s is half the line to line resistance

When using the three leads of a wye or delta connected motor, the air gap torque equation can be further simplified by using only two line voltages and currents [7], [28], as shown in equation 6.5

$$T_{ag} = \frac{\sqrt{3}p}{6}\left\{(i_a - i_b)\int [v_{ca} + R_s(2i_a + i_b)] + (2i_a + i_b)\int [v_{ab} + R_s(i_a - i_b)]\right\} \quad (6.5)$$

The above equation is valid for both wye and delta connected motors. However, it should be noted that the R_s is defined according to the motor configuration as [28]

- R_s =phase resistance r for a wye connected motor
- R_s =r/3 for a delta connected motor

Alternatively, the T_{ag} equation can be derived using the space phasor components in the stationary reference frame, as was done in [7]. The stator voltage equations are then expressed as

$$v_{dqs} = R_s i_{dqs} + \frac{d\lambda_{dqs}}{dt} \quad (6.6)$$

Where λ_{dqs} is the total flux linkage vector

The air gap torque can then be expressed as the cross product between the flux linkage and currents

$$T_{ag} = \frac{P}{2}\left|\lambda_{dqs} \times i_{dqs}\right| \quad (6.7)$$

Equation 6.7 can be further expressed in the natural reference frame in terms of the two line currents and voltages as was shown in equation 6.5. For the purpose of analysis in this thesis, equation 6.5 will be used to obtain the air gap torque.

The numerical evaluation of the flux linkage integrals in the air gap torque equation can be computed using traditional integration methods. If the time increments between data points is sufficiently small, i.e. high sampling rate, a simple trapezoidal integration method can be used [7]. Other methods, such as Simpson's rule or Gauss's rule can also be used for higher accuracy.

Due to the initial value problem and drift associated with integration, an offset DC component in the flux linkage component is created. To rectify this, it is necessary to implement a filtering technique which obtains the moving average of the flux linkage terms. Obtaining the moving average for a number of cycles, it can be subtracted, thereby removing the DC offset in the air gap flux component [7].

6.3.2 The Input Power Equation

The input power can be determined from the instantaneous input voltages and currents. The input power can be expressed as the summation of the products of the instantaneous phase voltages and currents as shown in equation 6.8.

$$P_{input} = v_a i_a + v_b i_b + v_c i_c \tag{6.8}$$

When using only two leads of the three-phase motor, the two wattmeter method of measuring input power may be used, as shown in equation 6.9

$$P_{input} = -v_{ca}(i_a + i_b) - v_{ab} i_b \tag{6.9}$$

The average of the instantaneous power is used when determining the efficiency of the machine. This is to reduce the effect of the ripples associated with the energy stored in the windings [7], [28].

6.3.3 The Efficiency Equation

The output shaft power can be calculated from the product of the shaft speed and the shaft torque. In the case of the air gap torque method, the air gap torque is the starting point of subtraction. Thus the output shaft torque is the air gap torque less the mechanical and the rotor stray load loss. Therefore, the efficiency can be calculated as [7], [27],

$$\eta = \frac{P_{output}}{P_{input}} = \frac{T_{ag}\omega_r - P_{FW} - P_{SLL}}{P_{input}} \qquad (6.10)$$

As mentioned in Chapter 3, there is a discrepancy in the literature when calculating the efficiency using the air gap torque equation. In order to resolve the issue, the following discussions are made.

When observing the power flow through an induction machine (figure 2.3), the air gap power represents the power transferred across the airgap from the stator to the rotor of the machine. Thus, this transferred power can be seen as the power that remains after the stator winding losses and core losses have been accounted for. The air gap torque associated with this air gap power should, therefore, account for the stator winding copper loss and the core loss.

The air gap torque equation and its derivation show that the stator copper loss is accounted for (in the integral terms), however the core loss is not. It is evident that the derivations have either neglected the core loss component or alternatively lumped it together with the friction and windage loss.

Further investigation of this dilemma was conducted by simulating the air gap torque equation in MATLAB simulink (see Appendix). The case for ideal voltage and current waveforms for an 11kW motor under rated conditions was implemented. Simultaneously, the input power and the stator resistance loss component were calculated. Based on the simulation results, it appears that the air gap power ($P_{ag} = T_{ag} \times \omega_s$) closely resembles that of the input power less the stator copper loss.

It is evident that the air gap torque component does not account for core loss and therefore would need to be included in the final efficiency equation as shown in equation 6.11 [27], [29] and [30].

$$\eta = \frac{P_{output}}{P_{input}} = \frac{T_{ag}\omega_r - P_{FW} - P_{Core} - P_{SLL}}{P_{input}} \qquad (6.11)$$

As discussed in Chapter 3, the major disadvantage of the air gap torque method is that it requires measurements of stator resistance, rotor speed and no load losses. The following sections will describe how these parameters can be addressed in such a way that the overall method can be made to be non-intrusive, with a reasonably high degree of accuracy.

6.4 Stator Winding Resistance Estimation

The stator winding resistance estimation technique chosen for this thesis is based on the DC signal injection technique proposed in [43]. This technique was chosen based on its high accuracy and ease of implementation. Since this thesis focuses on line connected induction machines, additional circuitry is needed to inject the DC bias into the stator winding. The following sections describe the chosen DC bias injection topology in more detail.

6.4.1 Basic Circuit Topology

The basic structure of the topology makes use of an n-channel power MOSFET and an external resistor. The external resistor (R_{ext}) is connected across the drain and source of the MOSFET. These components are connected in parallel and are connected between the source and motor terminals of a single phase of the machine. Figure 6.1 shows the MOSFET and R_{ext} configuration when connected in line with a motor.

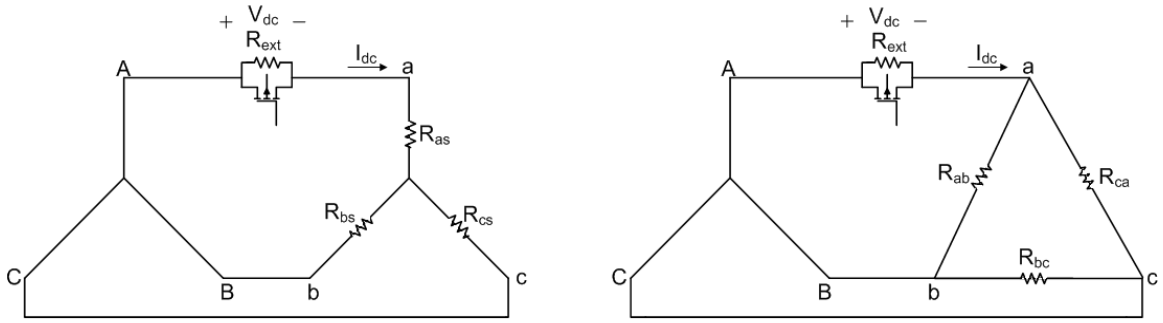

Figure 6.1: Steady state DC equivalent circuit for star and delta connections [43]

The MOSFET is a voltage controlled switching device. To turn the device 'on', the gate-source voltage is set to a value below the threshold, (V_{th}) and the stator current is passed through the induced channel. When the MOSFET is turned 'off', the stator current is passed through the $R_{ext.}$ The internal parasitic diode provides a path for the reverse current during this 'off' condition. This is shown more explicitly in Figure 6.2.

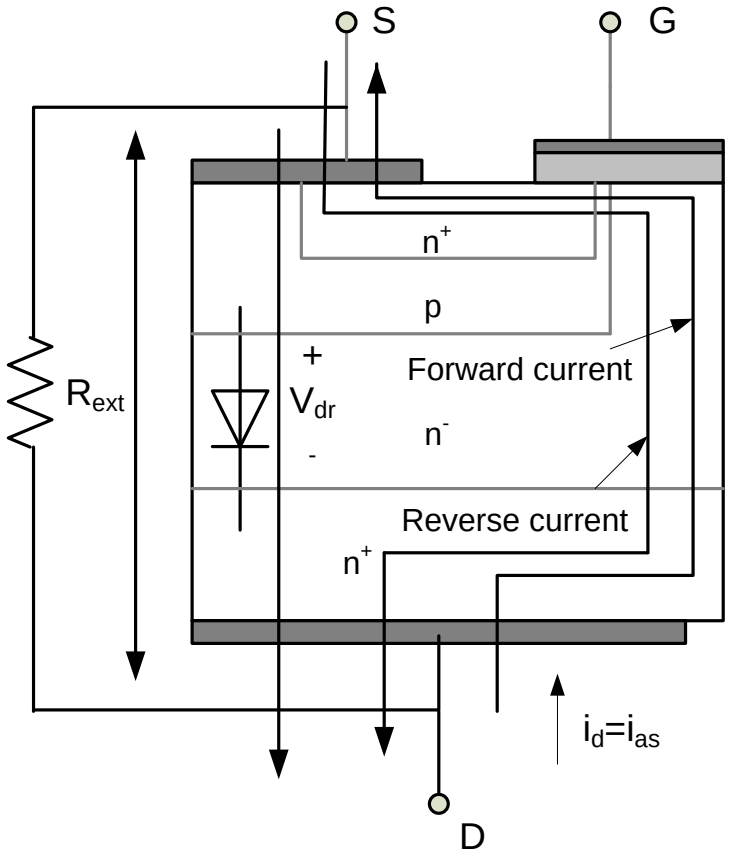

Figure 6.2: Forward and reverse current path through a MOSFET [43]

6.4.2 Circuit Operation for R_s Estimation

The basic principle of operation of the circuitry required for estimation R_s is to inject a DC bias. The DC bias is created by turning the MOSFET on during the positive half cycle of stator current ($i_a>0$), and off during the negative half cycle ($i_a<0$). As a result of this on-off switching, an asymmetrical resistance is created during each cycle (see Figure 6.3) and causes an asymmetrical voltage drop across the circuit. This results in a DC voltage component and consequently an injection of DC current into the motor windings.

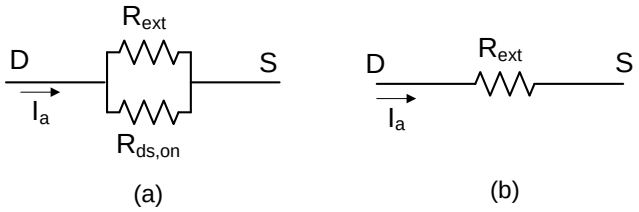

Figure 6.3: Equivalent circuit with MOSFET on (a) and off (b)

Based on the DC components obtained, the value of R_s can be estimated using the principle of Ohm's law. A simplistic update rule for resistance determination is shown by equation 6.12

$$R_s = \frac{V_{dc}}{I_{dc}} \tag{6.12}$$

Equation 6.12, however, needs to take into account the type of motor configuration. In [43], the update rule for R_s is derived under the assumption the machine is star connected. For the purpose of this thesis, the update rule for R_s estimation was adapted accordingly, such that this method could be applied to the delta connected machines. The derivation makes use of line voltages and currents, since these are easily accessible from the motor control centre. It should also be noted that the source impedance is assumed to be negligible and that the stator windings in each phase are approximately equal. The case for star and delta connected motors is based on Figure 6.1.

Star Connection

$$-V_{dc} = I_{dc}(R_{as} + R_{bs} \parallel R_{cs})$$

Assuming R_{as}=R_{bs}=R_{cs}=R_s and negligible source resistance

$$-V_{dc} = I_{dc}(R_s + \frac{R_s}{2})$$

$$-V_{dc} = I_{dc}(\frac{3R_s}{2})$$

$$R_s = \frac{-2V_{dc}}{3I_{dc}} = \frac{2V_{AB,dc}}{3I_{a,dc}} \qquad (6.13)$$

Delta Connection

$$-V_{dc} = I_{dc}(R_{ab} \parallel R_{ca})$$

Assuming R_{ab}=R_{bc}=R_{ca}=R_s and negligible source resistance

$$-V_{dc} = I_{dc}(\frac{R_s}{2})$$

$$R_s = \frac{-2V_{dc}}{I_{dc}} = \frac{2V_{AB,dc}}{I_{a,dc}} \qquad (6.14)$$

Based on equations 6.13 and 6.14, the values of R_s can be determined. In order to improve the accuracy of R_s estimation, it is necessary to remove any DC offsets that may inherently be contained prior to the estimation of R_s. These offset components are incorporated to eliminate the effects of the DC components inherent in the mains supply and instrumentation. Additionally, the effects of cable resistance need to be catered for [43]. Taking this into account, the amended equation used for calculating R_s is

$$R_s = \frac{2(V_{AB,dc} - V_{offset})}{(I_{a,dc} - I_{offset})} - R_{cable} \qquad (6.15)$$

In [43], it was shown that the accuracy of R_s increases with an increase in DC bias injection. An increase in the DC bias injection can be achieved by increasing the value of R_{ext}. The effects of increasing R_{ext} increases in the asymmetrical resistance during the 'on' and 'off' switching of the MOSFET. This, consequently, creates an increase in voltage asymmetry and larger DC current component. Despite the advantage of increased accuracy for R_s estimation, the increase in DC bias also contributes negatively to increased torque pulsations and additional power dissipation. This will be further discussed in the subsequent section.

6.4.3 Torque Pulsations and Power Dissipation

One of the main concerns surrounding DC signal injected R_s estimators is the level of torque pulsations and power dissipation associated with the additional circuitry and its connections.

Due to the signal injection of I_{dc}, the interaction between the flux linkage and the rotor causes a $-\omega_r$ current component to be induced in the rotor. The effects of the interactions between the AC and DC current components are seen to produce a distortion in the electromagnetic torque, as derived in [43] in the stationary reference frame. The electromagnetic torque is shown by

$$\begin{aligned} T_{em} &= \frac{3pL_m}{4}\left(i_{qs}^s i_{dr}^s - i_{ds}^s i_{qr}^s\right) \\ &= \frac{3pL_m}{4}\left\{\left(i_{qs,ac}^s i_{dr,ac}^s - i_{ds,ac}^s i_{qr,ac}^s\right) + \left(I_{a,dc}^s I_{dr,dc}^s\right)\right. \\ &\quad \left. + \left(i_{dr,ac}^s I_{s,dc}^s + i_{qs,ac}^s I_{dr,dc}^s - i_{ds,ac}^s I_{qr,dc}^s\right)\right\} \end{aligned} \tag{6.16}$$

Considering each of the terms in the electromagnetic torque equation, the first term is the torque without the DC injection, the second term being the braking torque and, lastly, the third term is the pulsating torque.

The power loss associated with the DC injection circuit needs to be considered for the design of circuit parameters and ratings of a heatsink. The average power dissipation of the DC injection circuit can be seen during both the MOSFET 'on' and 'off' mode in equation 6.17 and 6.18 respectively [43]

$$P_{avg,on} = \frac{R_{ds,on}\hat{I}_s^2}{2} \tag{6.17}$$

$$P_{avg,off} = \frac{4I_{a,dc}\hat{I}_s\left(R_{ext} - R_{ds,on}\right) + \pi\left(\frac{\hat{I}_s^2}{2} + I_{a,dc}^2\right)\left(R_{ext} + R_{ds,on}\right)}{2\pi} \tag{6.18}$$

As can be seen, the power loss due to the DC injection circuit is a function of $R_{ext,}$ $R_{ds,on}$, $I_{a,dc}$ and the peak of i_{as}.

Additionally, the effect of the DC injection current component contributes to the stator copper loss in the windings of the machine and thus needs to be accounted for. The additional power contribution to the total power for a star and delta connected motor is shown in equation 6.19 and 6.20 respectively.

$$P_{stator,star} = \frac{3R_s I_{ac}^2}{2} + \frac{3R_s I_{dc}^2}{2} \tag{6.19}$$

$$P_{stator,delta} = \frac{R_s I_{ac}^2}{2} + \frac{R_s I_{dc}^2}{2} \tag{6.20}$$

Considering the torque and power equations, it can be seen that they are highly dependent on the level of injected DC current, $I_{dc.}$ Due to the negative impact, the level of torque and power dissipation should be accounted for when designing the dc injection circuit. The level of I_{dc} can be controlled by the choice R_{ext}, therefore, as stated in [43] the value of R_{ext} should be chosen to ensure that the levels of torque pulsation and power dissipation are within tolerable ranges.

This method is considered to be intrusive, however once the required circuitry is installed, it can be thought of as non-intrusive. The installation process can be performed during motor installation or during a scheduled maintenance outage [7]. This makes the resistance estimator a dedicated device and not of a portable nature.

6.5 Rotor Speed Estimation

The method for speed estimation required for efficiency estimation is attained using vibration spectrum analysis. This method was chosen on the basis that it provides a simple, non intrusive and accurate means of rotor speed estimation. As indicated in [64], vibration analysis shows a strong signal for a wide range of loading conditions.

The basic functionality of the speed estimator incorporates the use of an accelerometer which measures the vibration of the machine. As shown in literature, vibration analysis is predominantly used for condition monitoring to detect machine unbalance and bearing faults but it can also be used to detect the rotor's speed. Once the vibration signal is obtained, an FFT process is applied to the signal and the frequency components are analysed. A distinguishable low frequency component exists and is associated with the rotational frequency of the machine. This frequency is present due to the mechanical imbalances of the rotating parts within the motor. These are inherent in the machine and are due to manufacturing processes. The mechanical vibration is a once per revolution force [65] and therefore the rotational speed can be calculated using

$$n_r = 60f_r \tag{6.21}$$

Where:

f_r is the rotational frequency.

For a 4-pole induction machine, the rotational frequency will be visible below 25Hz. An example of this is shown in Figure 6.4

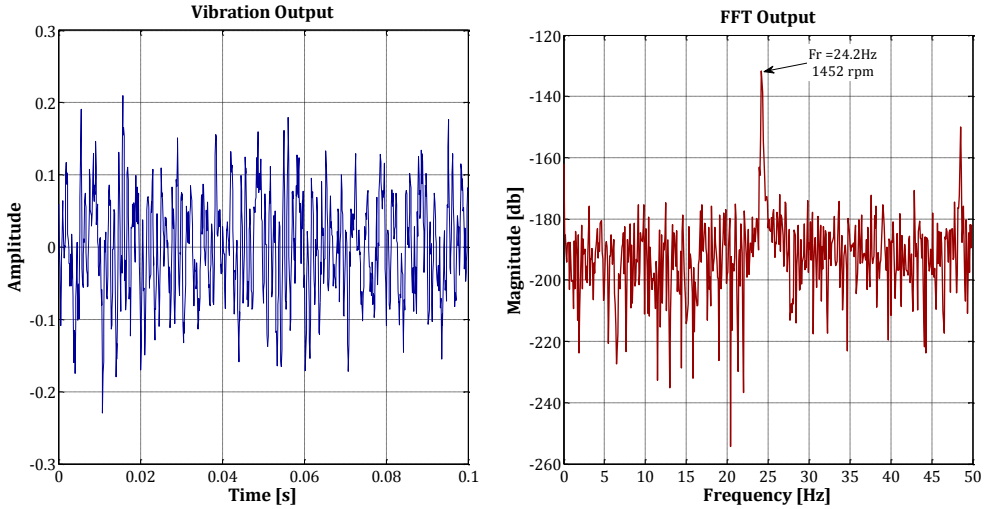

Figure 6.4: Example of vibration output signal and its corresponding FFT

As shown, the rotational frequency is easily detectable and clearly shows that the frequency component can be translated into the rotor speed.

6.6 Loss Estimation

6.6.1 No Load Losses

The no load losses consist of the friction and windage loss and the core loss and are considered to be constant and load independent. Typically, the no-load losses are obtained by conducting a no load test which requires the motor to be decoupled from its load and a variable supply connected to its terminals. This is highly intrusive and difficult to perform under field conditions when the machine is operating.

It can be argued that a no load test can also be performed before installation (for newly acquired motors) or during scheduled maintenance downtime. However, to avoid the interruption of already installed machines, it is required that no-load losses are estimated according to statistical methods. The combined value for the friction and windage and core losses can be assumed to be a fixed value of input rated power as suggested by the Ontario Hydro Modified Method E (OHME) [28]. Initially, a factor of 3.5% was proposed but was further revised for motors less than 50 hp (approx. 40kW). The refinement was based on the same ratio used by the IEEE Std 112 for which the stray load losses can be estimated. The improved empirical factor for no load loss estimation was adjusted to 4.2% of rated input power [3]. Therefore the no load losses are calculated according to

$$P_{NLL} = kP_{input} \tag{6.22}$$

Where:
k =3.5-4.2%

Additionally, 1.2% of the input power is due to the contribution of friction and windage loss [28].

For the purpose of this thesis, a value of 3.5% of rated input power will be used to obtain the no load losses as done in [7].

6.6.2 Stray Load Loss

The stray load losses are yet another component of the NAGT which needs to be calculated empirically. As discussed in Chapter 2, the IEEE Std 112 and IEC Std 34-2-1 allow for the stray load losses to be determined according to a fixed percentage of the rated output power or according to a predefined curve. For the purpose of this thesis the IEC Std 34-2-1 method for assigned values will be used. The general equation, based on the predefined curve for the range of motors tested (1kW<P_2<10000kW) can be calculated according to [24]

$$P_{SLL} = P_1 \times [0.025 - 0.005\log_{10}\left(\frac{P_2}{1kW}\right)] \qquad (6.23)$$

Where:
P_1 is the input power
P_2 is the rated output power

The equation depicted above is used to determine the stray load loss at rated load. At other than rated loads, the standard assumes the value of stray load loss to vary with the square of the rotor current (stator current minus the no load current). Since the NAGT method aims to reduce the intrusion levels associated with efficiency testing, the no load test is to be avoided and the no load current cannot be obtained. For the purpose of this thesis, the stray load loss values obtained at rated conditions (according to equation 6.23) will be used in the NAGT method for all load conditions.

6.7 Overall Non-Intrusive Air-Gap Torque Efficiency Estimation Method

Based on the above sections, the overall NAGT method can be combined as shown in Figure 6.5.

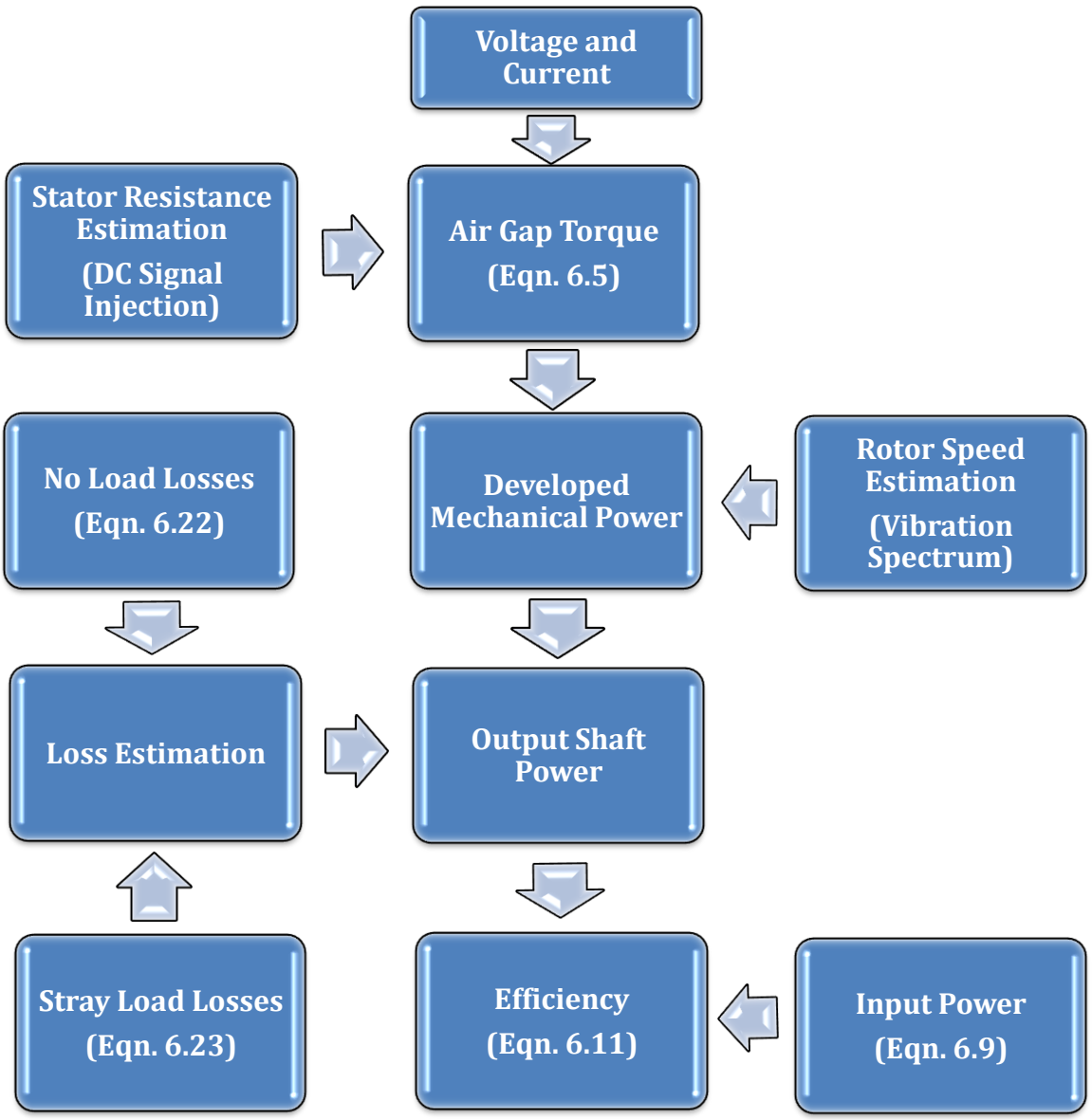

Figure 6.5: Overall NAGT procedure for efficiency estimation

6.8 Concluding Remarks

This chapter presented the development of the NAGT method for efficiency estimation. A detailed derivation of the air gap torque equation and it application to the NAGT method was discussed. In particular, the investigation of the discrepancies in literature of whether the core loss component is included in the equation was conducted. It was concluded that the core loss component is not included in this equation and therefore needs to be catered for in the overall efficiency equation.

The theory development of the candidate methods for stator resistance and rotor speed estimation was also presented. Since the stator resistance estimation theory was based on star connected machines, the derivation of the relevant equations for its application to delta connected motors was performed. The theory development of the rotor speed estimation process provided an indication to the manner in which the rotor speed can be detected. The empirical calculations of the no load loss and stray load loss estimation were also presented.

Based on the above, the relevant theory was combined and an overall NAGT method for efficiency determination was established.

CHAPTER SEVEN

LABORATORY IMPLEMENTATION AND METHODOLOGY

This chapter provides the laboratory implementation and methodology of the tests performed in this thesis. A description of the circuitry design and its required setup for stator resistance and rotor speed estimation is discussed. Furthermore, the instrumentation and measuring devices and the relevant software implementation are suggested.

7.1 Introduction

The implementation and conduction of the experimental procedures forms the basic foundation for which a hypothesis can be tested. The conduction of an experiment requires that a defined methodological procedure and apparatus setup be followed to ensure adequate structure, accuracy and safety.

7.2 Laboratory Setup for Induction Motor Efficiency Testing

The experiments conducted in this thesis took place in the machines laboratory at the University of Cape Town (UCT). The laboratory is equipped with a dedicated test bed for testing motors and contains sufficient measurement devices necessary for motor efficiency testing. Figure 7.1 shows an example of an induction motor coupled to a dynamometer situated on the motor test bed.

Figure 7.1: Test rig with dynamometer coupled to an induction motor

7.2.1 Specifications of Squirrel-Cage Induction Motors Tested

The motors considered for this thesis are the standard type motors with output power ratings of 7.5kW, 11kW and 15kW. Each of these motors are four-pole, 380/400V, 50Hz

and are totally enclosed fan cooled (TEFC) machines. The machines are connected in a delta configuration.

7.2.2 Motor Under Test (MUT) Setup

Various motor testing setup procedures need to be considered before the relevant tests can be conducted. The motor setup procedures will be discussed in more detail in the subsequent sections

- **Machine Alignment**

In order to conduct the relevant efficiency testing it is required that each motor is set up correctly to ensure the accuracy of the results obtained. Since the motor is coupled to a dynamometer, adequate care was taken to ensure that the motor shaft was precisely aligned. This was done to minimize the effects of vibration and motor eccentricities which negatively impact the efficiency by increasing the total losses of the motor. To ensure eminent alignment the motors were aligned using an alignment clock such that the centres of the motor and dynamometer shafts deviated by no more than 1mm. Figure 2.7 shows the alignment clock attached to the coupling of the induction machine.

Figure 7.2: Motor and dynamometer shafts with alignment clock

Furthermore, the motors were securely fastened to a set of base plates during the alignment process in order to keep the motor in place and further reduce the effects of vibration.

- **Machine Loading and Torque Calibration**

The induction motor was loaded using a separately excited DC machine operating as a generator (dynamometer) allowed for the motor to be loaded. The torque was controlled by adjusting the armature current, since torque is proportional to armature current. The reaction torque is then measured and displayed on a digital display via a torque transducer.

For accurate loading measurements, it was necessary to calibrate torque transducer. This was accomplished by attaching known weights to the torque arm and adjusting the amplification factor such that the display shows the expected torque. The expected torque was calculated using equation 7.1

$$\begin{aligned} T &= F \times d \\ &= m \times g \times d \end{aligned} \tag{7.1}$$

Where

m -is the mass of the weights applied

g = 9.796 m/s^2 is the gravitational force for Cape Town

d-is the distance of the torque arm

Figure 7.3 shows the dynamometer torque arm along with the weights that are used during the calibration process.

Figure 7.3: Dynamometer torque arm with weights

The calibration processes is a repetitive process that is required to ensure that linearity and hysteresis effects are resolved. This was done by loading and unloading the calibration arm with the calibration weights over the entire loading range and adjusting the amplification factor accordingly.

- **Load Cell**

A H3 200kg H961700 load cell from Load Cell Services [71] was configured in a manner whereby a force exerted on the motor's shaft can be converted into an electrical signal. The signal is fed into the digital display once the amplification factor is set during the calibration process (see section 7.2.2). The load cell has an accuracy of 0.02% of nominal range. The load cell and its corresponding torque display is shown in Figure 7.4.

Figure 7.4: Load cell and digital torque display

- **Additional load resistors**

Additional load resistors, as shown in Figure 7.5, were used in instances where additional loading from dynamometer was required. In particular, the additional load resistors become mandatory at the higher loading conditions for the 11kW and 15kW motors. It should be noted that due to the limitation in the rating of the dynamometer and additional loading resistors, only values of up to 125% of rated load can be achieved when testing the 15kW machine.

Figure 7.5: Additional load resistors

- **Motor Supply**

The voltage supply to the motor was attained using the mains supply from South Africa's power producer, ESKOM. The voltage unbalance and total harmonic distortion (THD) was monitored to ensure that it remained within tolerances set by the IEC Std 34-2-1 standard. The mains supply was chosen since ESKOM's conditions will reflect the supply to the majority of motors out in industry, therefore the effectiveness of the NAGT method can be tested under similar conditions.

7.2.3 Stator Resistance Estimation Circuit Setup

The resistance estimation circuit is based on the DC signal injection concept proposed in [43]. However, some adaptations have been made and will be discussed below. A schematic of the implemented circuitry is given in Figure 7.6.

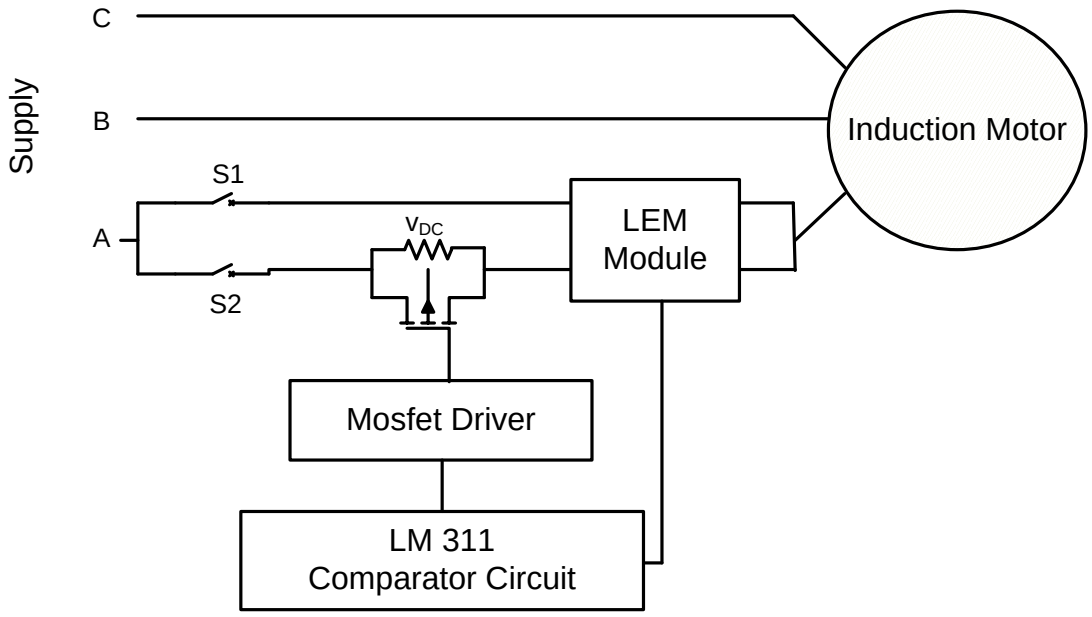

Figure 7.6: DC injection circuit setup for stator winding resistance estimation

The actual experimental circuitry was designed, built and tested in the laboratory. The choice of circuit components, its configuration and adaptation will be further discussed in the following sections. The experimental circuit implementation is shown in Figure 7.7.

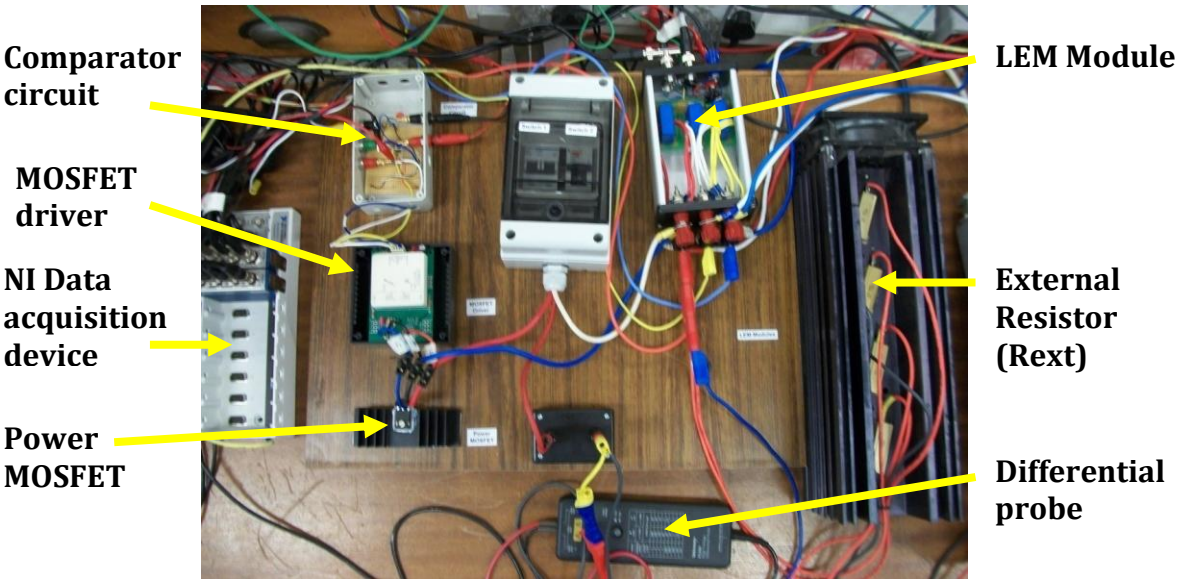

Figure 7.7: Experimental circuitry for resistance estimation

- **Comparator Circuit**

The comparator circuit consists of a LM311 voltage comparator [72] with the reference (V_{Ref}) set to the positive input (pin 2). The voltage output of the current LEM module (V_{in}) is then set to the negative input (pin 3). Thus, when the stator current is on its positive cycle $V_{in}>V_{Ref}$ and the output of the op-amp (pin 7) is low (OV) and the MOSFET is turned off. When the stator current is on its negative cycle, $V_{in}<V_{Ref}$ and the op-amp output is high (15V), tuning the MOSFET on. A pull-up resistor was incorporated into the design to ensure that a 'high' signal is fully 'high' (15V). Hysteresis resistors were also included into the circuit to ensure that the effects of switching oscillations and the effects of noise are eliminated.

- **MOSFET Driver**

A Semikron SKHI 21A Hybrid dual MOSFET Driver [73] is inserted between the comparator circuit and the MOSFET. Its advantages include built-in galvanic isolation so the secondary output side of the chip is separate from the primary input side.

- **Power MOSFET**

The power MOSFET chosen for this thesis is the IRFP064N HEXFET® Power MOSFET [74]. The MOSFET is rated at V_{DSS} =55V, $R_{DS(ON)}$=0.008Ω , I_D =100A and P_D=200W. The MOSFET was placed on a heat sink to ensure adequate dissipation of heat.

- **External Resistance (R_{ext})**

An external resistor bank, consisting of four 1Ω, 50W resistors, is connected in parallel with the MOSFET. The resistor bank contains additional wiring which allows for the resistors to be configured in parallel or in series combinations. For the purpose of this thesis, two resistors are connected in parallel, providing a R_{ext} of 0.5Ω. The value of 0.5Ω was chosen to be as large as possible, to improve accuracy when estimating R_s (as discussed in Chapter 6) but with the consideration of the power ratings of the resistors. In the case of the larger motors (15kW), higher stator current values flow through R_{ext} and by connecting two resistors in parallel, the resistors are able to share the current, thus not drastically exceeding the power rating. The resistance estimation circuit is not used for long periods of time, thus the resistors are able to tolerate these high currents. Additionally, the resistors are placed on a heat sink with an external fan so that they can be kept cool during operation. The value of R_{ext}= 0.5Ω was used in all cases of motor testing for comparison purposes. A differential voltage probe is connected across R_{ext} to measure the voltage across it.

- **Switching Modes**

The circuit design consists of two modes, normal mode and injection mode. To differentiate between the two modes, two switches are incorporated into the circuit design. In [43] the resistance estimation circuitry was connected continuously in one phase of the motor. The additional circuitry causes power dissipation, torque distortion and possible unbalanced motor winding conditions. As shown in [43] power dissipation occurs in both normal (to a lesser degree) and injection mode whereby it increases with increased loading conditions. Although the overall power dissipation was low, the torque pulsations may be

unacceptable in some applications. Thus, a suitable value of R_{ext} needs to be chosen to ensure a reasonable trade off between R_s accuracy and torque pulsations.

For the purpose of this thesis, the effects of power dissipation and torque pulsations during efficiency estimation were avoided. This was achieved by incorporating the use of two switches. The additional circuitry is switched in only when the stator resistance estimation is required. Thereafter, the additional circuitry is switched out so that its negative effects do not influence the remainder of the efficiency testing procedure. Additionally it can be argued that in order to do the relevant torque pulsation calculations (if the circuitry is not switched out), the motors magnetising inductance, rotor resistance and rotor inductance need to be known. To obtain these parameters the relevant blocked rotor, no load etc tests need to be performed. Since the thesis focuses on non intrusiveness, these tests are to be avoided.

To cater for the high current values of the larger machines, circuit breakers were used as switches. The current ratings for each of these breakers are 125 A and 100A.

7.2.4 Accelerometer Setup for Speed Detection

To detect speed using a vibration analysis, an accelerometer was built. Due to its availability, an ADXL202E dual axis accelerometer IC chip from Analog Devices [75] was used. The chip was soldered onto a circuit board along with a 0.1μF decoupling capacitor and a 5V voltage regulator.

For the purpose of this thesis, only single axis readings were used. In order to use the analog output of the chip, the output of X_{Filt} pin is exploited. The advantage of this method is that the entire bandwidth range of 5kHz is available. Additionally, a 0.001μF filter capacitor was connected to the output of the X_{Filt} pin for filtering. Figure 7.8 shows the internal components of the accelerometer device.

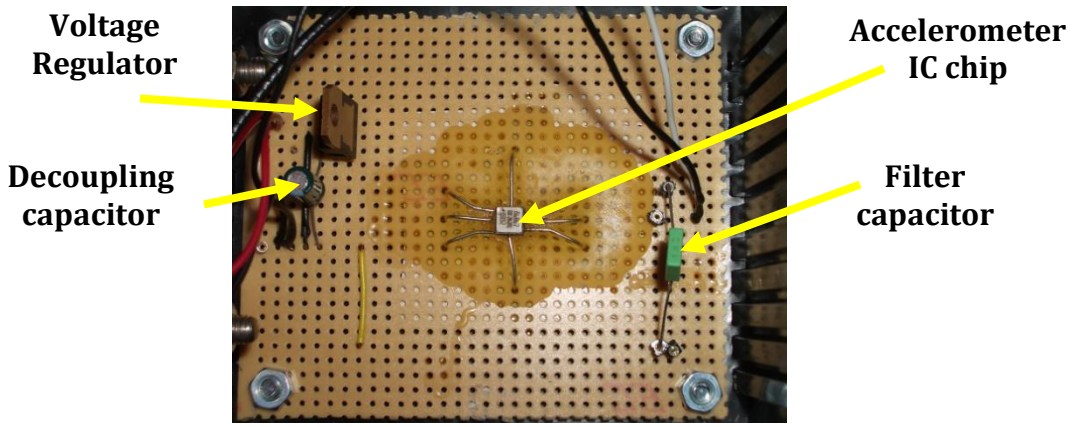

Figure 7.8: Internal circuitry of the accelerometer device

The entire circuit was encased inside a plastic box from which the signal is obtained from using a BNC connector. Strong magnets were affixed to the box so that it may be attached to the motor and held in any axial or radial position. A 9V battery may be used to power the device, making it portable. The external construction of the device is shown in Figure 7.9.

Figure 7.9: Front and side view of the accelerometer device

After completion of the design and construction of the accelerometer device, it was tested on an induction machine. Figure 7.10 shows the accelerometer placed on an induction machine during the test.

Figure 7.10: Accelerometer device placed on an induction machine

7.2.5 Voltage Unbalance Setup

In order to induce voltage unbalance, a three-phase variac connected to three single phase variacs were used. This allowed for individual voltage control in each of the three phases. The three phase variac is rated at 64A and is used to supply the motors up to 150% of its full load current. A schematic of the variac setup is shown in Figure 7.11. The individual single phase variacs were configured by connecting the brush voltage (G1) to the winding of the larger variac (G2) to allow for full control of the voltage output.

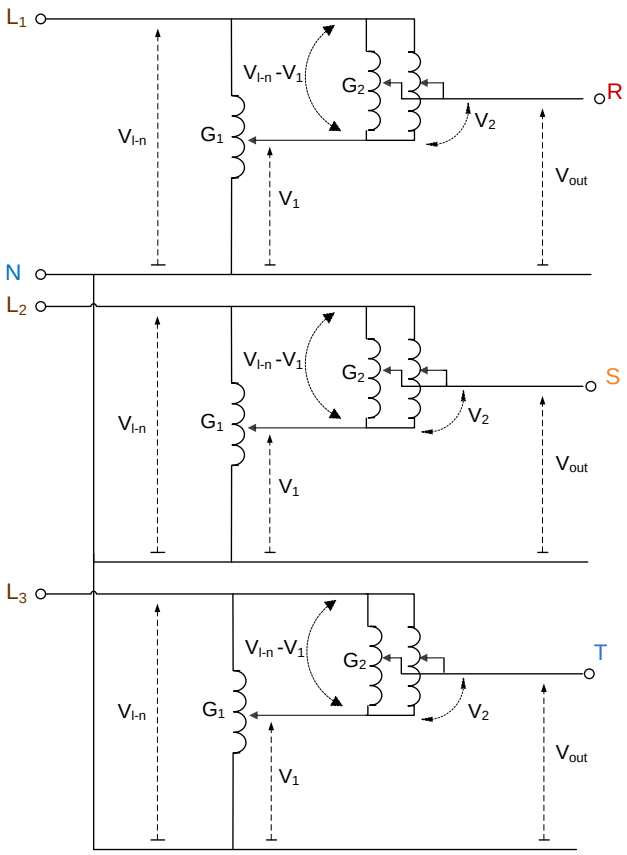

Figure 7.11: Variac configuration for implementing voltage unbalance

For the purpose of this thesis, only voltage magnitude unbalance (no phase unbalance) was considered. The voltage magnitude unbalance conditions were calculated according to the NEMA definition (section 2.3.3). The single phase variacs were adjusted to create 380V average voltage conditions with 0%, 2.5% and 5% unbalance.

It should be noted that a generator was used to generate the voltage supply. This was used in order to obtain voltage conditions greater than Eskom's mains supply. This is necessary when creating voltage unbalances where an individual line voltage is required to exceed Eskom's supply voltage while maintaining an overall average nominal voltage of 380V.

7.3 Data Capturing Devices and Instrumentation

The following sections will discuss the relevant data capturing devices.

7.3.1 Yokogawa WT1600 Power Analyser

A calibrated Yokogawa WT1600 Power Analyser was used to obtain the rms voltage, current, power, speed and torque measurements. The device allows for the data to be captured and stored during each test. The analyser was configured to a 3A3V wiring connection. The update rate was set to 1 second. The analyser has an accuracy of 0.1%.This is in accordance with the specifications set by the IEC Std 34-2-1.

Figure 7.12: Yokogawa WT1600 Power Analyser

7.3.2 Pico-technology Thermocouple Data Logger

To measure the effective temperature of the machine, three K-type thermocouples were installed on the drive-end side (opposite to the cooling fan) of the stator windings of each machine. The position of the thermocouples embedded in a motor is shown in Figure 7.13.

Figure 7.13: Thermocouple placement on stator end windings

The location of these thermocouples ensures that the temperature readings are at the highest temperature of each of the windings. For comparison purposes, all the thermocouples were positioned in the identical place for each of the motors.

A TC-08 Pico USB interfaced logger and its software was used to sample and record each of the winding temperatures during each of the tests conducted. Figure 7.14 shows the logger with the thermocouples connected.

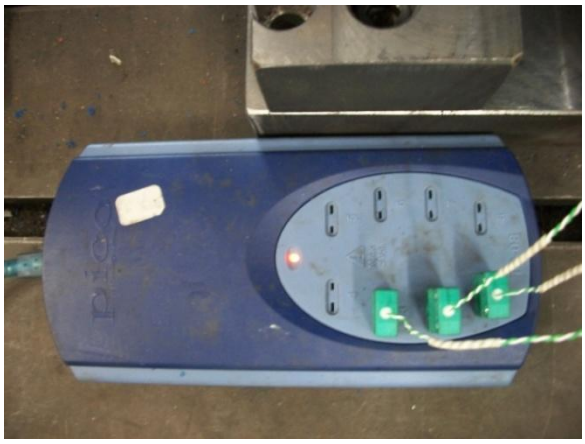

Figure 7.14: TC-08 Pico logger with thermocouples

The temperature was set to capture at a rate of one sample per second. The temperature accuracy associated with the logger is the sum of ±0.2% and 0.5°C.

7.3.3 Stator Winding Resistance Measurement

To determine the hot and cold stator winding resistance required for the IEC 34-2-1 standard an HP 3401A Digital Multimeter [76] was used. The multimeter was configured to measure the resistance using the four wire method. An advantage of this method is its accuracy. This is achieved since the four wire method compensates for the resistance associated with the measurement wires. The measurement accuracy of the multimeter is ± 0.0030% of reading + 0.0030% of range.

7.3.4 Proximity Speed Sensor

In order to compare the speed results obtained from the accelerometer device, the speed was also measured using an inductive proximity sensor. This is mounted approximately 2mm from the shaft coupling between the motor and the DC machine.

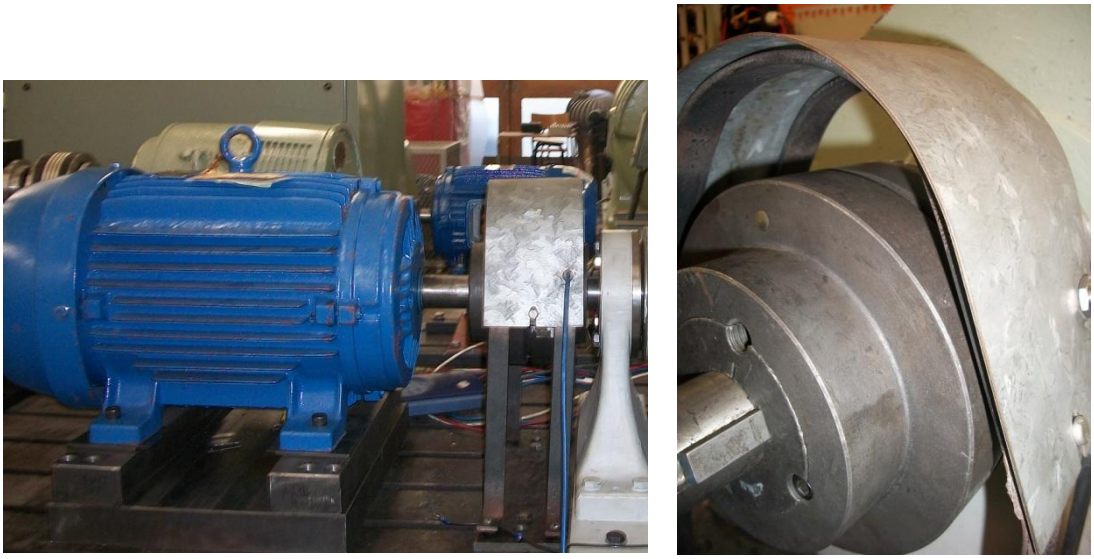

Figure 7.15: Proximity sensor placed over shaft coupling

The proximity sensor sends a pulse to the power analyser every time a change in inductance is detected. The coupling contains 30 metal teeth which cause a set of pulse signals to be triggered each time one of the teeth passes the sensor. Thus, one revolution equates to 30 pulses. An amplification factor is also necessary to ensure that the correct speed values are obtained. The speed obtained from the proximity sensor was calibrated

according to a hand-held photo digital tachometer (DT-2236) from Lutron Electronic. This tachometer has a resolution of approximately 1rpm and an accuracy of 0.05%.

An advantage of using the proximity sensor, as apposed to a hand-held tachometer, is that the signal can be captured and recorded automatically during a test.

7.3.5 LEM Current Transducer

Three LEM modules (one per phase) were used to measure the stator currents of the machine. These devices are known for their high precision, good linearity, low thermal drift, galvanic isolation and robustness. The LA 55-P [77] modules were chosen to cater for the high currents (36A rms at 125% of rated load) of the 15kW machine. They are connected with a 1:1000 conversion ratio and operated in the 50 A rms current range. The devices were supplied with ±15V from an external voltage supply and provides an accuracy of ±0.65%.

7.3.6 Differential Voltage Probes

Tektronix P5200 High Voltage Differential Probes were used to measure the terminal voltages of the motor. The range was set to an attenuation ratio of 1/500 to accommodate voltage ranges of 380/400V. The accuracy range of these probes is ±3%.

7.3.7 National Instruments Data Acquisition Device

An NI 9215 data acquisition device was used to capture the instantaneous voltage, current and speed signals. The device consists of two 4-channel, ±10V, 16-Bit Simultaneous Analog Input Modules embedded in a NI CompactDAQ chassis. The data captured using the device is then transferred to a personal computer.

The device was calibrated by adjusting all voltage and current measurements to match closely to that of the power analyser. This was done to account for the resistance tolerances of the measurement resistors in the LEM components. The calibration procedure was

achieved by a repetitive process of adjusting the gain (due to the turns ratio and measurement resistance) of the LEM modules.

7.4 Software Implementation

The simulations and calculations for this thesis were conducted in Matlab ® 2009 and NI Labview environments. A diagram of the Labview and Matlab Simulink models are provided in the Appendix.

7.5 IEC Std 34-2-1 and Direct Method as a Baseline for Comparison

The IEC Std 34-2-1 is the standard used in South Africa. This standard was officially approved by the South African Bureau of Standards (SABS) in 2008 [25]. This standard therefore forms the premise for which the results obtained from the NAGT method can be compared.

The procedures for efficiency testing of induction machines were followed according to the segregated loss method. Tests required for this procedure include rated load temperature test, variable load test and the no load test [24].

The method for which stator resistance values can be obtained was outlined in section 2.4.2. Since the motors available for testing already contained installed thermocouples, an alternative method which uses the temperature and resistance at rated conditions was employed. The value of rated resistance and temperature is obtained from a rated temperature test and is used as the known resistance and known temperature values. Using these values, the resistance at any other temperature (as measured using thermocouples) is obtained using equation 2.19.

The direct method incorporated was simply the ratio of output power (the product of the measured shaft torque and speed) to the input power.

7.6 Methodology for Efficiency Estimation Using the NAGT Method

It should be noted that the NAGT is developed to determine the efficiency of a machine, while in operation, at a specific operating point. For the purpose of this thesis, an efficiency curve obtained over a wide range of loads (25%-150% of rated load) for each of the machines. This allows for the investigation into the NAGT method over a wide range of loading conditions whereby meaningful comparisons can be made the IEC Std 34-2-1. The procedure for the NAGT method in this thesis follows as closely as possible to the procedures outlined by the standard. Measurements for the NAGT and IEC Std 34-2-1 methods are taken simultaneously such that the motor and supply conditions reflected in the results are identical This allows for the reduction of methodological errors when comparing the efficiencies obtained from measured and estimated results. However, there are a few discrepancies which will be identified below.

The suggested procedure for the NAGT method is outlined below.

1. **Run the machine until its rated temperature is achieved**

   Before an efficiency test is to be conducted, the machine should be run hot, until the stator winding temperature is within 5˚C of its rated temperature (obtained from a rated thermal test). It takes approximately 3 hours from start up for the machine temperature to stabilise. This is within accordance to the IEC Std 34-2-1.

   In field applications, however, the motor is presumed to be running and already stabilised at its operating temperature prior to efficiency determination, and therefore this step is not required.

2. **Estimate the stator winding resistance using the additional circuitry**

   For the NAGT method additional circuitry is required to determine the stator winding resistance non-intrusively. The procedure for resistance estimation is described below

Initially, it is necessary to determine the DC offset inherent in the mains supply such that compensations for these values can be made. This can be achieved by observing the DC offsets for a few cycles and an average of these values can be obtained. Thereafter, the resistance estimation circuit is switched in for a duration long enough to determine the values of the DC injected signals. Using these values, the estimated stator winding resistance can be calculated using equation 6.15. This process is repeated for each loading condition following a similar sequence to that of the IEC Std 34-2-1, which starts at the highest loading point and proceeds, in equal successions, to the lowest loading condition. During the efficiency testing, the standard requires that the measurements, at each successive loading point, are taken as quickly, and close to rated temperature, as possible in order to reduce the effects of changes in temperature. This means that the temperatures, and hence resistance values, are not stabilised at each load.

Under field conditions the estimation process is slightly different as the efficiency is only measured once i.e. at the machine's operating condition. It is assumed that the machine has been running under this condition for a long period of time, and suggests that the machine temperatures (and hence resistances) are stabilised.

3. **Determine the air gap torque, input power and rotor speed**

   At each loading condition, obtain the instantaneous voltage and current signals using the NI 9125 device. The measurements are fed into an NI LabView model and the air gap torque is calculated according to equation 6.5. Simultaneously, the input power is calculated according to equation 6.9.

   The sample rate was set to 10kHz. This provides high precision when sampling the required voltage and current signal. The increased sample rate also supports the accuracy of the dt increments in the integration process.

   The speed obtained from the vibration signal of the accelerometer is also captured simultaneously with the voltage and currents. However, since the speed requires a

FFT procedure, the length of the signal data becomes important. In order to obtain a sufficient resolution to determine the rotational frequency (f_r<30 Hz for a 4 pole machine), it was necessary to set the capture time to at least 10 seconds (100k samples). This provides a frequency resolution of 0.1 Hz

According to the standard, allowing a ten second capture time between each successive loading point is considered too long, especially at over rated conditions. However, if sufficiently accurate speed results are to be obtained this cannot be avoided. Since the measurements recorded for both the NAGT and IEC Std 34-2-1 are captured simultaneously, the effects of the lengthier capture time will be reflected in both efficiency curves. Under field conditions, however, this would not be problematic. Since only one load condition i.e. the operating condition, is being observed. Thus, lengthier acquisition times may be attained if the machine is running under steady state conditions.

4. **Use empirical estimation to obtain the no load and stray load losses**
   The combined no load losses are then calculated empirically at 3.5% of rated input power. The stray load losses are estimated according to equation 6.23.

5. **Determine the motor's efficiency**
   After completion of the above steps, the efficiency of the motor at each loading point is obtained using equation 6.11.

6. **Compare results with IEC Std 34-2-1 standard and direct method**
   The results obtained from the NAGT method are then compared to the results obtained from the IEC Std 34-2-1. The results are then analysed and discussed. Conclusions are drawn based on these results and recommendations are then proposed.

7.7 Methodology for Obtaining Efficiency during Voltage Unbalance

Traditionally, motor efficiency testing is conducted in laboratory conditions where the supply conditions can be monitored and adjusted to ensure that they are within specifications set by the motor testing standard. Due to these restrictions, the original test procedure is no longer applicable during unbalanced conditions. Therefore, in order to investigate the effect of voltage unbalance on the motor efficiency an appropriate test procedure needs to be defined.

There are two main areas of concern that become apparent during unbalanced conditions and these need to be clarified before the efficiency test can be performed. Firstly, the rated temperature of the machine is unknown. During unbalanced supply conditions, the motor cannot be left to stabilise as the increased temperatures associated with voltage unbalance may cause the motor to burn out or be permanently damaged. Secondly, since the IEC Std 34-2-1 is no longer applicable during unbalance conditions, the individual loss components cannot be calculated accordingly.

Therefore, in order to maintain some degree of conformity, the efficiency test will initially be conducted at the rated temperature established during balanced operation. The direct method (P_{out}/P_{in}) is to calculate the motor efficiency since it avoids the calculations of the individual loss components. The values obtained from this method forms the premise to which efficiency values obtained using the NAGT method can be compared.

The unbalanced conditions were implemented by adjusting the voltage from the individual single phase variacs (see Figure 7.11) such that the degree of required voltage unbalances is attained. The unbalance cases considered for this thesis were 2.5% and 5% voltage unbalance with an average nominal voltage of 380V and calculated according to the NEMA definition. The NEMA definition was adopted in this case because of its simplicity to calculate and implement.

7.8 Concluding Remarks

This chapter presented the laboratory setup and instrumentation required for motor efficiency testing. A detailed description of the motor installation, alignment, and calibration processes was provided. Furthermore, the chapter presented the design and implementation of the stator resistance estimation circuit and accelerometer device. Additionally, a detailed methodological procedure of how the experiments were conducted is also provided.

CHAPTER EIGHT

ANALYSIS AND VERIFICATION OF RESULTS

The results of the laboratory experiments are presented in this chapter. Initially, the development of the equivalent circuit for the 11kW machine is presented. Thereafter, the results for the stator resistance, rotor speed and loss estimation is provided. Based on these results, the final efficiency values are shown and a comparative analysis performed. The results of efficiency during unbalanced conditions are also presented.

8.1 Introduction

The subsequent sections will present the results of the experimental tests conducted. The focus of the experiments is aimed at the 11kW motor, however similar tests were performed on the 7.5kW and 15kW motors and serve to validate and/or compare whether the suggested estimation methods are applicable for different motor sizes.

8.2 Equivalent Circuit Parameters of the 11kW Induction Motor

The machine parameters were determined to develop a model in MATLAB Simulink. This model served to characterise the performance of the motor under ideal supply conditions.

8.2.1 No Load Test

The no load test was performed by applying rated voltage to the stator windings while decoupling the rotor from any mechanical load. The test provides information about the exciting current and rotational losses of the machine [1]. The results obtained from the no load test can be seen in Table 8.1. The rated conditions (blue) are used to obtain the equivalent circuit parameters while all the data is used to obtain the no load losses required to determine the motor's efficiency.

Table 8.1 Results obtained from the no load test

Voltage [V]	Current [A]	P_{input} [W]	$P_{no\ load\ loss}$ [W]	P_{FW} [W]	P_{Core} [W]
450.93	16.97	1504.75	1162.56	80.29	1082.27
424.68	13.71	1090.78	867.11	80.29	786.82
381.01	9.81	659.72	545.26	80.29	464.97
292.10	6.17	341.27	295.98	80.29	215.69
188.45	3.87	183.86	166.08	80.29	85.79
86.08	1.94	105.60	101.13	80.29	20.84

8.2.2 Locked Rotor Test

The blocked rotor test was performed by locking the rotor into a stationary position and applying rated current to the stator windings. This test provides information regarding the leakage impedances of the machine [1]. The results for the locked rotor test are shown in Table 8.2.

Table 8.2 Results obtained from the locked rotor test

Voltage [V]	Current [A]	P_{input} [W]
89.95	22.26	1557.01

8.2.3 Developed Equivalent Circuit

Based on the no load and locked rotor tests described in the previous sections, the equivalent circuit parameters for the induction machine can be obtained. The calculations involve an iterative process in which the values converge to a fixed value. A per phase equivalent circuit with its parameters is shown in Figure 8.1.

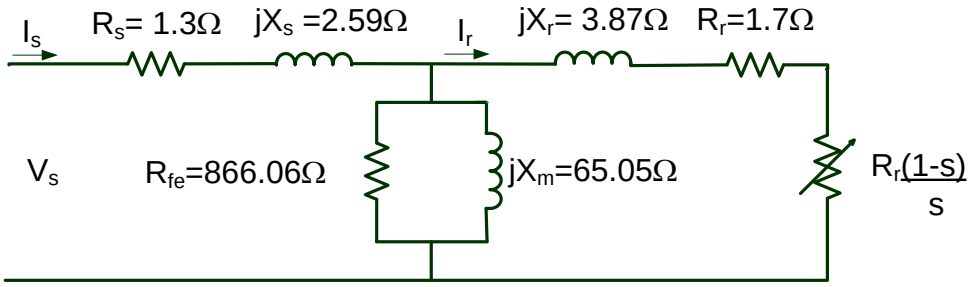

Figure 8.1: Equivalent circuit parameters of the 11kW induction machine

8.3 Stator Resistance Estimation

The proposed procedure for stator winding estimation was validated by both simulation and laboratory experimentation. The following graphs show a comparison of the simulated (see Appendix X) and experimental results of the 11kW motor obtained under rated load conditions with the external resistance (R_{ext}) set to 0.5Ω. As described in Chapter 6, the effect of the resistance estimation circuit is to inject DC components into the stator winding of the machine. The asymmetrical resistance obtained from the on-off switching effect of the MOSFET (in parallel with R_{ext}) is evident and is clearly shown by the corresponding asymmetrical voltage drop. The asymmetrical voltage waveform measured across R_{ext} and its effect on the stator current, $I_{a,}$ is shown in Figure 8.2. The resulting DC components created by the injection are also indicated.

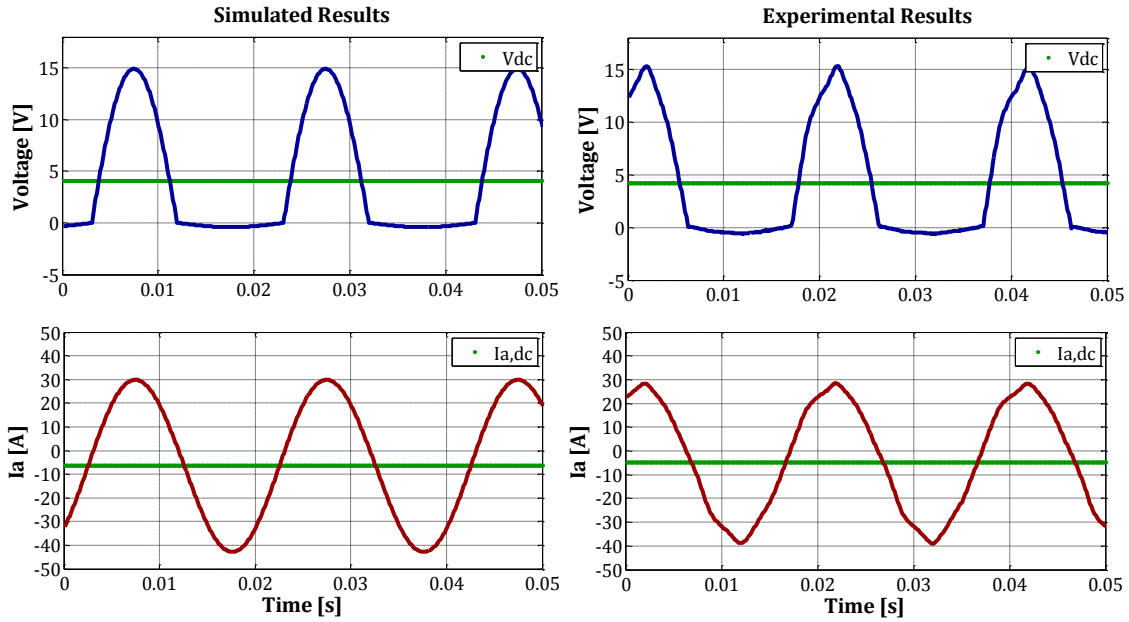

Figure 8.2: Waveforms of V_{Rext} and I_a during injection mode

As shown in the above figure, the experimental results obtained follow the same trends obtained from the simulation. The DC components injected into the stator winding are used to calculate the stator winding resistance according to equation 6.15. For completeness, the cable resistance was also accounted for and was measured to be 0.06Ω.For the purpose of

this thesis, the resistance values obtained from the estimation procedure are further corrected to a reference temperature of 25˚C according to equation 8.1 [24].

$$k_\theta = \frac{235 + \theta_w + 25 - \theta_c}{235 + \theta_w} \tag{8.1}$$

Where

k_θ is the temperature correction factor

θ_c is the inlet coolant temperature

θ_w is the winding temperature

This was done to allow for a more meaningful comparison of losses obtained according to the IEC Std 34-2-1. The efficiencies obtained from this standard are quoted at a reference value of 25˚C; therefore efficiencies quoted from the NAGT method should also be referred to this temperature if a direct comparison is to be made.

The resulting measured and estimated resistance values for each motor at the respective loads are shown below. Also indicated, are the average voltage and current offset values obtained during normal (non injection) mode.

8.3.1 11kW Motor Results

The average resistance results obtained for the 11kW motor is shown in Table 8.3.

Table 8.3 Estimated stator resistance results for the 11kW motor

Load [%]	$V_{dc,offset}$ [V]	$I_{dc,offset}$ [A]	Estimated R_s [Ω]	Expected R_s [Ω]	Relative Error [%]
150	0.540	-0.100	1.359	1.326	2.453
125	0.673	-0.108	1.405	1.363	3.063
100	0.494	-0.097	1.416	1.367	3.574
75	0.571	-0.097	1.379	1.348	2.272
50	0.596	-0.096	1.345	1.319	2.026
25	0.598	-0.092	1.347	1.304	3.319

As can be seen, the estimated resistance deviates from the expected results with a maximum of 0.049Ω (3.57% error) at 100% load and a minimum of 0.027Ω (2.03% error) at 50% load. In all loading cases the estimated R_s values are over estimated in comparison to the expected values.

8.3.2 15kW Motor Results

For the case of the 15kW motor, the estimated and expected the stator resistance values can be seen in Table 8.4.

Table 8.4 Estimated stator resistance results for the 15kW motor

Load [%]	$V_{dc,offset}$ [V]	$I_{dc,offset}$ [A]	Estimated R_s [Ω]	Expected R_s [Ω]	Relative Error [%]
125	0.893	-0.144	0.936	0.930	0.688
100	0.847	-0.154	0.948	0.925	2.506
75	0.992	-0.125	0.929	0.917	1.324
50	0.815	-0.121	0.923	0.910	1.416
25	0.803	-0.116	0.910	0.895	1.616

As seen above, the estimated R_s values show an over estimate in comparison to the expected R_s values. The maximum and minimum deviations are 0.023Ω (2.51% error) and 0.006Ω (0.68% error) and occur at 100% and 125% load respectively.

8.3.3 7.5kW Motor Results

The resulting stator resistance values for the 7.5kW machine are shown in Table 8.5 below.

Table 8.5 Estimated stator resistance results for the 7.5kW motor

Load [%]	$V_{dc,offset}$ [V]	$I_{dc,offset}$ [A]	Estimated R_s [Ω]	Expected R_s [Ω]	Relative Error [%]
150	0.420	-0.097	2.772	2.755	0.634
125	0.312	-0.100	2.892	2.841	1.815
100	0.461	-0.095	2.862	2.857	0.208
75	0.427	-0.099	2.841	2.825	0.544
50	0.436	-0.097	2.830	2.770	2.147
25	0.414	-0.154	2.727	2.716	0.414

The table shows a maximum deviation of the estimated results occurs at 50% load with a deviation of 0.059 Ω. (2.15% error) In contrast a minimum deviation of 0.006Ω (0.21% error) is evident at 100% load. The estimated resistance values are an overestimate when compared to the expected results.

8.3.4 Discussion of Results

As was shown, in all cases the resistance estimation resulted in values that are an over estimation when compared to the expected values. Notably, the amount by which the resistance is over estimated is not constant over the entire loading range for all three motors that were tested.

Although the value of the R_{ext} was set to 0.5Ω (two 1Ω resistors connected in parallel), tolerances of the resistors were not accounted for. For instance, at higher loading conditions, higher stator currents flow through R_{ext} causing it to heat up and thus affect the value of the resistance. In particular, the resistance estimation processes follow the same sequence as efficiency estimation (decrementing from 150% to 25% of rated load) and thus the higher currents cause the resistor to heat up and reflect higher R_{ext} values. Despite

the fact that R_{ext} is placed on a resistor bank with a fan, the resistors still reach high temperatures. Therefore, the effects of the higher currents heating up the resistors will consequently impact the resistor value during lower loading conditions. Additionally, the length of time the injection circuit is 'switched' is also a contributing factor to the heating of the resistor.

Another point to consider is that the stator winding temperature has not stabilized at each loading condition. This is not feasible since it takes a long time for the temperature to settle at a loading point (approximately. three hours) and during over loaded conditions, this may cause the motor to overheat and fail. The results indicate that the estimated R_s values follow closely with changes in loading conditions (and hence changes in temperature). For the case of all three motors, the resistance values are higher around the rated loading points for both the measured and expected resistances. This can be attributed to the methodology of the tests conducted. The IEC Std 34-2-1 requires that the sequence for which the load test is conducted, occur from the higher loading condition down to the lowest condition. Initially the machine is run until its rated hot stator winding temperature is stabilised. Thereafter, the machines load is increased to the highest loading point within a short period of time. Thereafter, the machine is left to run at this loading condition long enough for sufficient data to be captured. Due to the nature of the NAGT method, the required length of time between each consecutive load was 10 seconds. The effect of this at the higher load is to increase the stator winding temperatures. Thus, even when the succeeding loading point is set, the effects of the increased temperature is still apparent and the stator winding resistance measured at this temperature indicate higher values. This conforms to the results obtained in [43] where the authors investigated the effects of R_s estimation during abnormal cooling conditions. The authors showed that the R_s estimation trends followed closely to the changes in temperature. It is assumed, however, that in industrial applications the machine is running at its stabilized operating temperature and therefore at its stabilized stator winding resistance.

8.4 Speed Estimation

The speed estimation process requires the FFT of the vibration signal obtained from the accelerometer device. Based on the relevant literature, a frequency component related to the rotational frequency of the machine becomes prominent in the lower frequency range (below 30Hz) for a 4 pole machine. The voltage output of the accelerometer device (with the DC offset removed) and its FFT for the 11 kW motor, at rated condition, is shown in Figure 8.3.

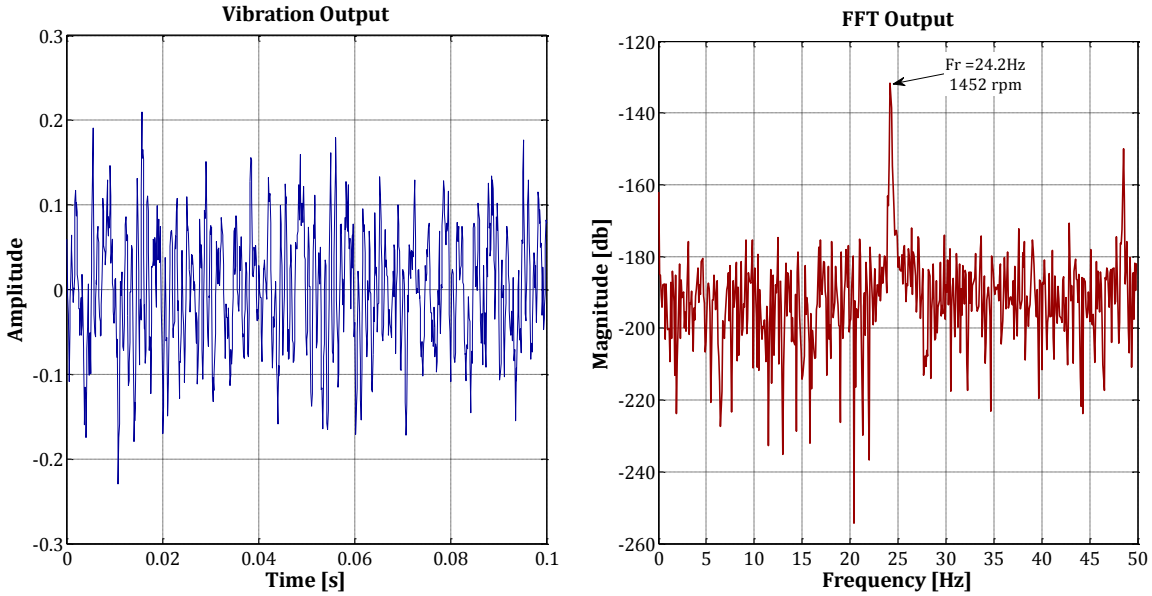

Figure 8.3: Vibration signal and frequency spectrum under rated conditions

As shown in Figure 8.3, the rotational frequency component is very dominant at 24.2Hz, which is below 30Hz. This makes using the vibration spectrum a simple method to use in situations where the motor speed is to be detected non-intrusively.

8.4.1 Speed Detection with Variation in Load

The changes in frequency of the rotational component are clearly depicted with variation of load and hence, the rotor speed. As the loading increases, so the frequency component shifts leftward to a lower frequency position i.e. lower frequency indicates a lower speed.

This variation of rotational frequency with changes in loading conditions is shown in Figure 8.4.

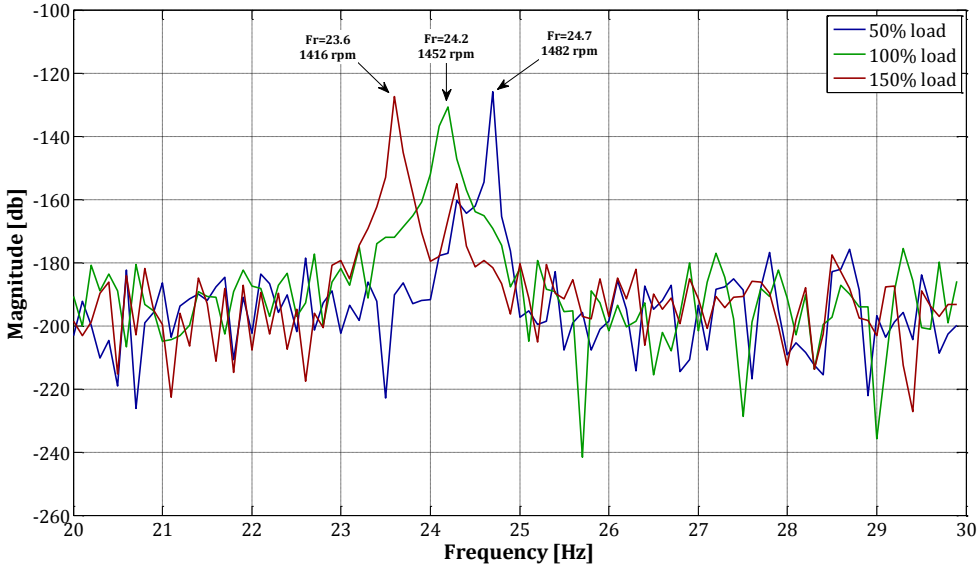

Figure 8.4: Variation of rotational frequency (F_r) with load

As shown above, the amplitude of the frequency component is not affected by the changes in speed and still remains dominant in the lower frequency ranges. Thus, the ability to detect this component is not affected by load (hence speed) and is detectable over the entire load/speed range.

The rotational frequencies and corresponding speed estimations for each of the motors at various loads will be shown in the subsequent sections. The accuracy of the estimated speeds will be assessed according to the measured speeds obtained from the proximity speed sensor and power analyser.

8.4.2 11kW Motor Results

The rotational frequency and corresponding estimated speed for the 11kW motor is shown in Table 8.6 below.

Table 8.6 Speed estimation results for the 11kW motor

Load [%]	F_{rot} [Hz]	Estimated Speed [rpm]	Measured Speed [rpm]	Relative Error [%]
150	23.6	1416	1417.2	-0.085
125	23.9	1434	1435.8	-0.125
100	24.2	1452	1449.8	0.152
75	24.4	1464	1465.7	-0.116
50	24.7	1482	1481.2	0.054
25	24.8	1488	1490.3	-0.154

As can be seen, the estimated speed values are closely related to the measured speed values. The maximum deviation of estimated speed is 2.3rpm (0.15% error) which occurs at 25% load while a minimum deviation of 0.8rpm (0.05% error) occurs at 50% load.

8.4.3 15kW Motor Results

The estimated and measured speed results, for the 15kW motor, is shown in Table 8.7 below.

Table 8.7 Speed estimation results for the 15kW motor

Load [%]	F_{rot} [Hz]	Estimated Speed [rpm]	Measured Speed [rpm]	Relative Error [%]
125	23.8	1428	1429.0	-0.069
100	24.1	1446	1446.1	-0.008
75	24.4	1464	1462.4	0.107
50	24.6	1476	1476.3	-0.023
25	24.8	1488	1490.4	-0.162

As shown above, the deviation of estimated speed from measured speed ranges between 0.12rpm (0.008% error) and 2.42rpm (0.16% error).

8.4.4 7.5 kW Motor Results

The corresponding estimated and measured speed results for the 7.5kW motor is indicated in Table 8.8.

Table 8.8 Speed estimation results for the 7.5kW motor

Load [%]	F_{rot} [Hz]	Estimated Speed [rpm]	Measured Speed [rpm]	Relative Error [%]
150	23.6	1416	1415.2	0.058
125	23.9	1434	1432.3	0.117
100	24.1	1446	1448.1	-0.145
75	24.4	1464	1462.4	0.113
50	24.6	1476	1476.6	-0.039
25	24.8	1488	1489.8	-0.123

Based on the above, the estimated speed results are within 0.6rpm (0.038% error) and 2.1rpm (0.145% error) when compared to the measured speed results.

8.4.5 The Effects of Frequency Resolution on Speed Detection

As mentioned in Chapter 6, in order to obtain an efficiency curve, it is required to conduct the experiment as quickly as possible. This causes a limitation on the length of data captured at any given load point. In this thesis, a sample length of 10 seconds at each loading point was used. With the sampling rate set at 10 kHz, the accuracy of the rotational frequency is limited to a frequency resolution of 0.1 Hz. This translates to a possible (not definite) deviation of ±6 rpm when calculating the rotor speed. For comparison purposes, capturing the vibration data for 60 seconds will provide an improved frequency resolution of 0.0166 Hz. This resolution translates to a possible deviation of ±1 rpm. Figure 8.5 shows the difference the vibration spectrum for an 11 kW motor operating at rated load. The case for a frequency resolution of 0.1 Hz (10 seconds) and 0.0166 Hz (60 seconds) is provided.

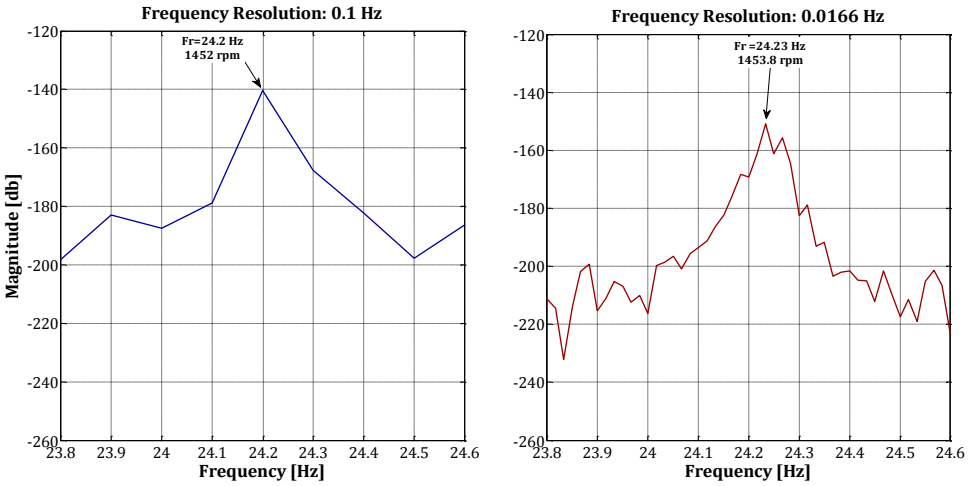

Figure 8.5: Differences in frequency resolution for speed detection

For the case above the difference in speed is 1.8rpm and shows the effect of frequency resolution in determining the accuracy of the speed.

Despite the fact that it is possible to obtain discrepancies of up to ±6 rpm using a frequency resolution of 0.1Hz, this was not the case for results obtained during testing.

8.4.6 Discussion of Results

Based on the results obtained in the previous sections, the resulting estimated speed shows a close relation to the expected measured results.

It is clearly evident that the rotational frequency is highly proportional to the speed and is indicated by the changes in frequency for each of the loading conditions. Notably, the accuracy of the speed results obtained using the vibration spectrum is not affected by the load. This has a significant advantage over other detection methods discussed in literature for which the accuracy of speed detection degrades at low speed operations.

The vibration signals provided conclusive results for all three motors, and hence the accelerometer device can be used for a range of motor sizes. The corresponding rotational frequencies range from 23.6 Hz to 24.8 Hz over the load range for each of the motors. This

is expected since all three motors are 4 pole machines and their corresponding operating speed ranges will be the same.

It should be noted that the results shown above are only indicative of a vibration spectrum obtained in the X-axis (radial) direction. Additionally, the accelerometer was placed on the top position of the machine (Figure 7.10). The accelerometer was placed in the same position for each of the tests conducted to ensure consistency when comparing results. Thus, no investigation of the effects of accelerometer position and orientation was conducted. Thus, possible improvements in speed estimation may alternatively be obtained.

8.5 No Load Loss Estimation

The no load losses are the constant, load independent losses associated with the motor. The IEC Std 34-2-1 calculated values are obtained from the conduction of a no load test and provide a basis for which the empirically estimated values can be compared. As described in Chapter 6, the estimated no load loss amounts to 3.5% of input power at rated load. Furthermore, the estimated friction and windage loss is assumed to be 1.2% of the rated output power. The experimental and estimated results for each of the motors are shown in the succeeding sections.

8.5.1 11kW Motor Results

The corresponding estimated and calculated no load losses for the 11 kW motor are shown in Figure 8.6 below.

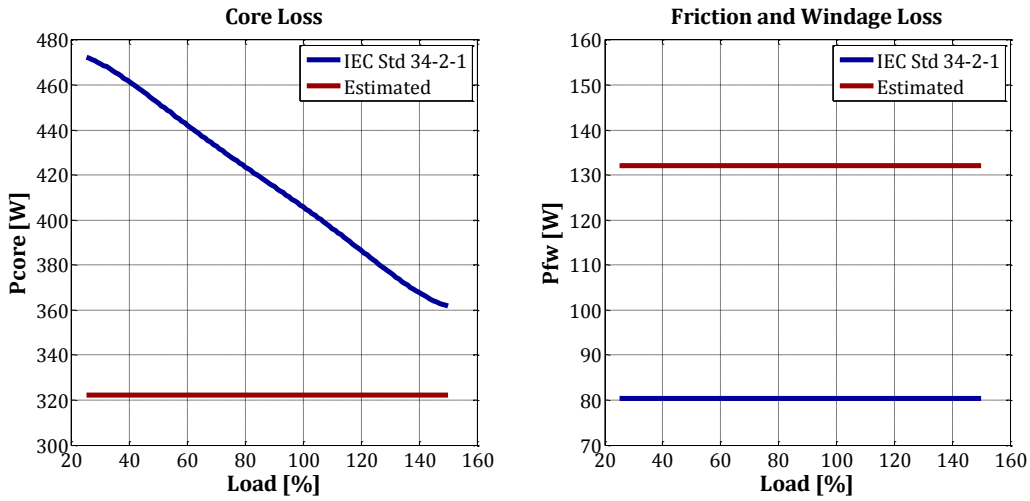

Figure 8.6: Core and friction and windage losses for the 11kW motor

Considering the core loss, the calculated values exceed the estimated values by approximately 150W at 25% load down to 40W at 150% load. In the case of the friction and windage loss, the estimated loss is greater than the actual values obtained, indicating an over estimate of approximately 52W.

The combined estimated and calculated no load loss results are shown in Figure: 8.7 below.

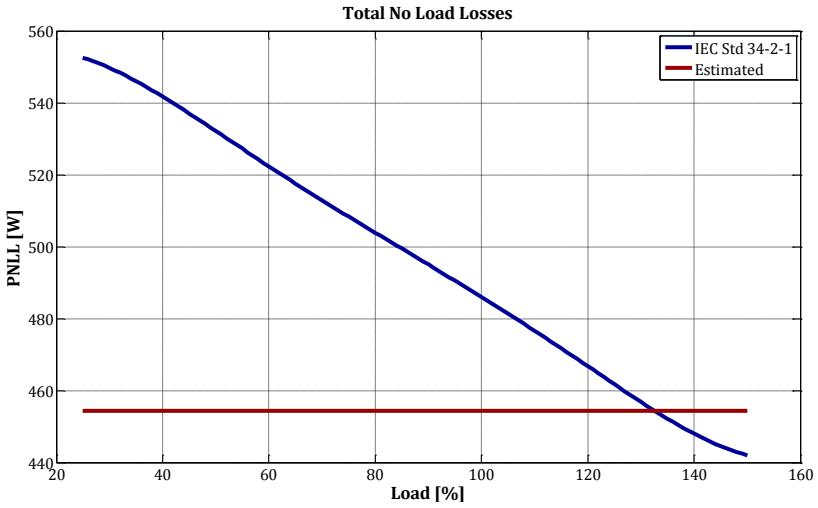

Figure: 8.7: Total no load losses for the 11kW motor

Based on the graph, the total measured no load loss values are greater than its estimated counterpart for loading conditions from 25% to 138% of rated load. After the intersection of the curves at 138% load (approx. 455W), the estimated values exceed the calculated values.

8.5.2 15kW Motor Results

The core and friction and windage loss for the 15kW motor is shown in Figure 8.8.

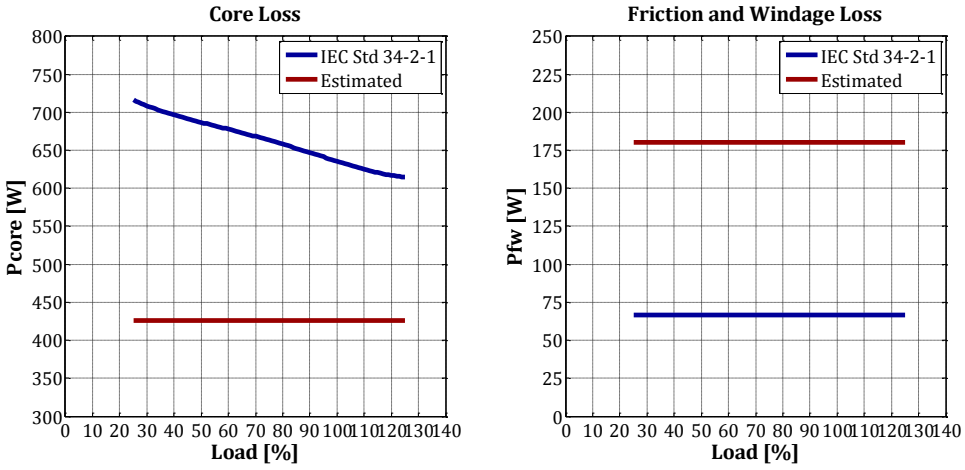

Figure 8.8: Core and friction and windage losses for the 15kW motor

The overall estimated core loss values show an underestimate in comparison to that of the calculated values. Considering the extreme cases, the calculated values exceed the estimated values by approximately 300W at 25% load and 185W at 150% load.
Considering the friction and windage losses, the estimated values exceed the actual calculated values by approximately 120W.

Taking into account the total combined no load losses, the resulting estimated and calculated results are shown in Figure 8.9.

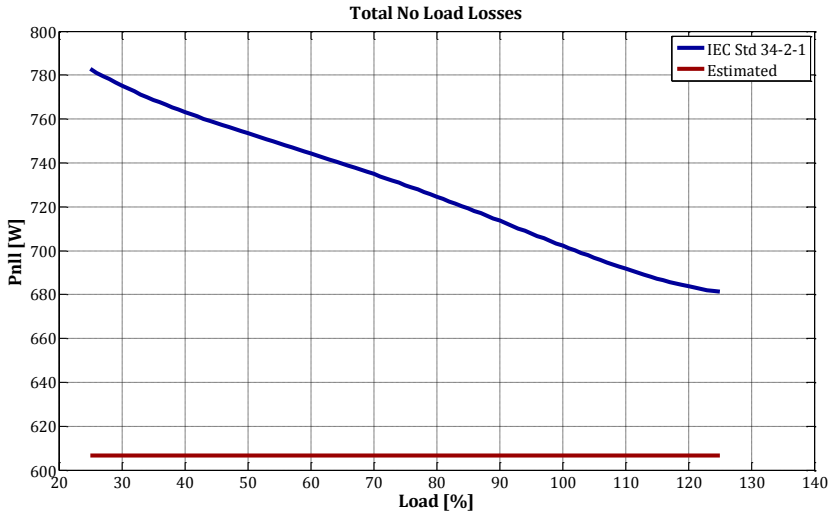

Figure 8.9: Total no load losses for the 15kW motor

As can be seen, the overall calculated no load loss values are higher than that of the estimated values, indicating that the overall estimation of no load losses is, in fact, an underestimate. Although the graphs do not intersect, as only values up to 125% load are indicated, it is expected that an interception will occur at higher ranges of loading by following the trend of the plots and extrapolation procedures.

8.5.3 7.5kW Motor Results

The results of the core loss and friction and windage loss for the 7.5kW motor is provided in Figure 8.10**.**

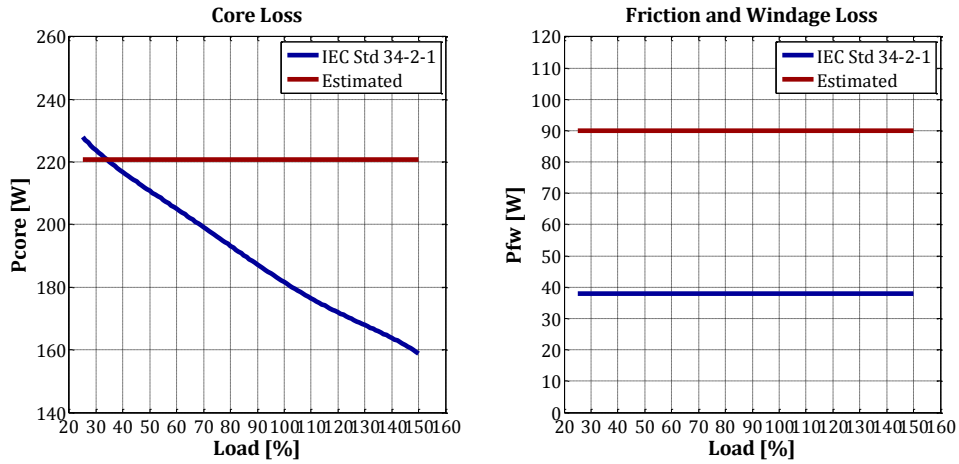

Figure 8.10: Core and friction and windage losses for the 7.5 kW motor

Considering the core loss component, the estimated results show an under estimated for the lower load operating points. The calculated results equal the estimated values at approximately 34% of rated load. Thereafter, the estimated results show an over estimate in comparison to the calculated results.

In the case of the friction and windage loss, the estimated results are over estimated by approximately 53 W. The total combined no load loss is shown in Figure 8.11 below

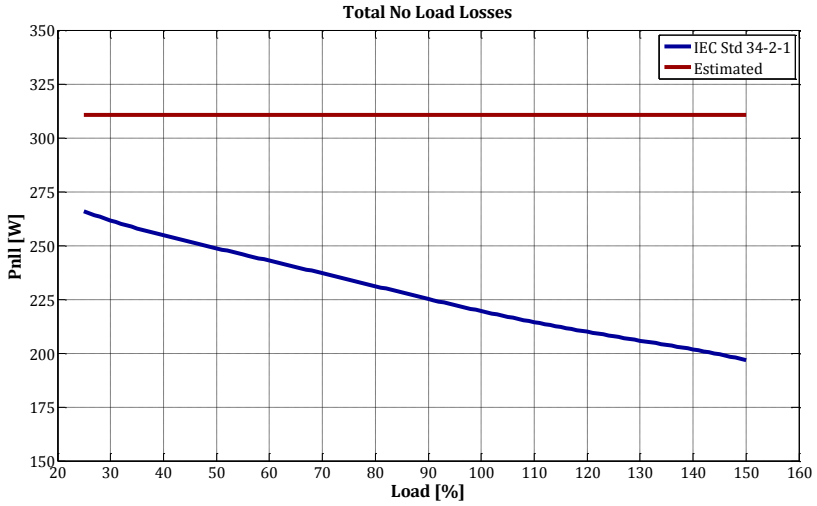

Figure 8.11: Total no load losses for the 7.5 kW motor

The overall combined estimated no load losses display an over estimate in comparison to the calculated values for the entire loading range. The degree of over estimation increases with an increase in load.

8.5.4 Discussion of Results

Based on the results provided, there is a general under estimation of core losses with an over estimation in friction and windage loss. Considering the total combination of the no load losses, the estimated values show an under estimate for the larger 11kW and 15kW motors. In contrast the estimated values display an over estimate in no load values for the 7.5kW motor. Consideration of this 7.5kW motor and observations of its core loss component, the estimated value amounts to an over estimate in comparison to the values obtained from the IEC Std 34-2-1. This applies to the load range above 30%. In addition, estimated friction and windage loss is also an over estimate. Consequently, the total no load loss represents the combination of these components and thus the over estimate in empirical values is emphasised. Additionally, the over estimate and under estimate conditions of the total no load loss estimation for each of the motors can be explained by considering the distribution of loss components. The total percentage of losses relative to the input power for the IEC Std 34-2-1 calculated results for each motor at rated load, is shown in Figure 8.12.

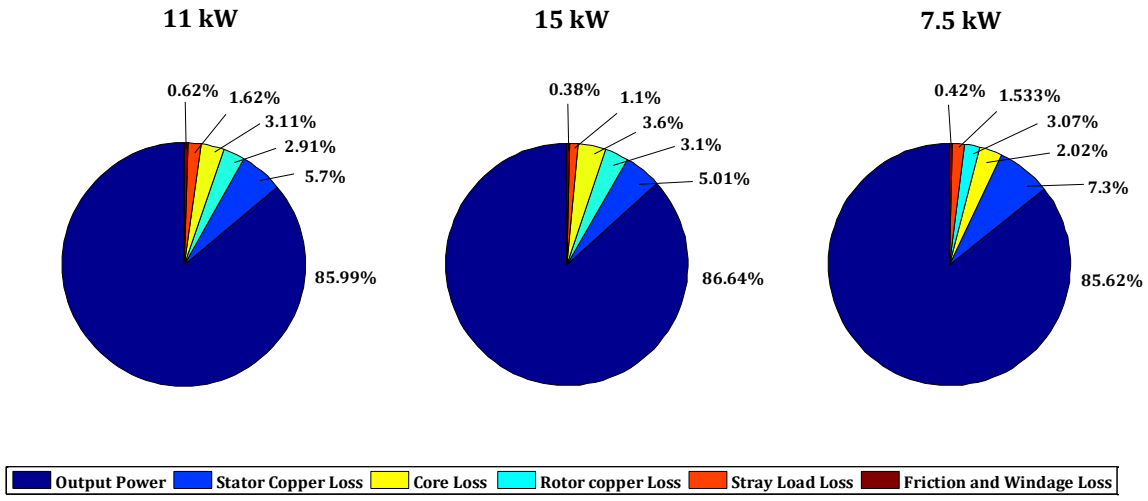

Figure 8.12: Loss distribution for each motor at rated condition

As depicted, the combined friction and windage loss and core loss for the 11kW and 15kW motors, amounts to 3.73% and 3.98% of rated input power respectively. Consequently, the empirically estimate of 3.5% of input power indicates an under estimate. For the 7.5kW motor however, the total no load loss contribution is 2.44% of input power. This is a lower value than the empirical 3.5% of input power and therefore, the empirical values provide on over estimate of no load losses. This suggests the questionability of the estimation of no load loss for smaller sized motors.

In general, the no load losses are considered to be constant, load independent losses. Based on the results shown in the previous section, it is evident that the IEC Std 34-2-1 calculated core losses are not constant over the load range, but rather decreases with an increase in load. As mentioned in Chapter 2, the IEC Std 34-2-1 compensates for the resistive voltage drop across the stator winding using equation 2.20, effectively relating the core loss to the induced stator voltage, $U_{r,}$ which decreases with an increase in load. This can further be explained by considering, the simplified equivalent circuit model of an induction machine shown in Figure 8.13 where U_r is the voltage that appears across the machine's core.

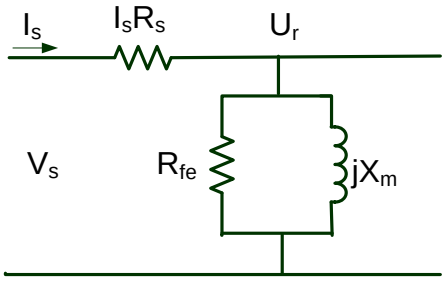

Figure 8.13: Simplified equivalent circuit of an induction machine

As the load increases, so the value of the stator resistive voltage drop increases due to the increase in stator current. As a consequence, the value of U_r decreases with this increase in load. This shows that the core loss obtained at lower loads is higher than that obtained at the higher loading conditions. The variation in core loss over the load range suggests that it is load dependant, i.e. not load independent as expected. For investigation purposes, the maximum variation of core loss for each motor over the load range is shown in Table 8.9.

Table 8.9 Maximum variation of core loss over load range

Load [%]	Core Loss [W]		
	15kW	**11kW**	**7.5kW**
150/125 %	720	470	225
25 %	620	360	160
Max. Variation	100	110	65

As shown, the variation in maximum and minimum core loss is 100W, 110W and 65W for the 15kW, 11kW and 7.5kW motors respectively.

8.6 Stray Load Losses

The stray load losses (SLL) account for the remaining losses in the machine. As mentioned in Chapter 2, SLLs, according to the IEC Std 34-2-1, is calculated by subtracting the output power and all the losses accounted for from the input power. These values are then smoothed using a linear regression technique as a function of the square of the torque. The estimated stray load loss components, as described in Chapter 6, are obtained using an assignment allowance based on a curve that relates the input power to the output power at rated load conditions. The estimated and calculated stray load loss components for each of the motors are shown in the following sections.

8.6.1 11kW Motor Results

The corresponding estimated and calculated SLL values for the 11kW machine are shown in Figure 8.14.

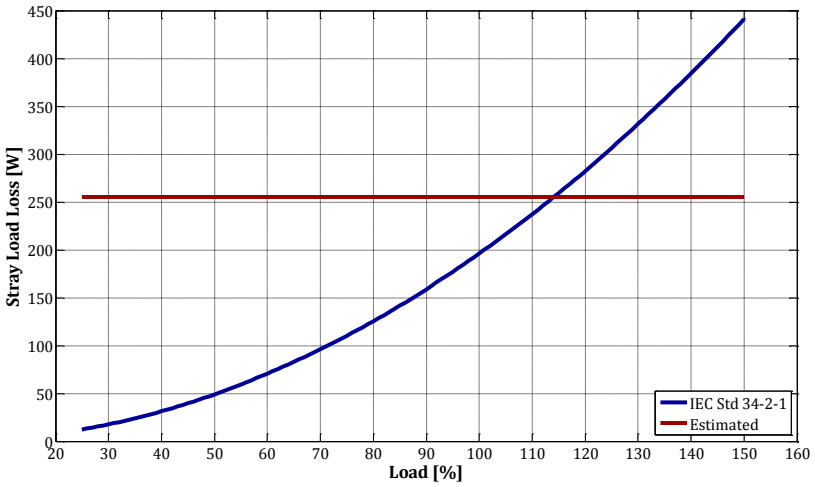

Figure 8.14: Stray load loss results for the 11kW motor

Observations of the above show that the estimated values are an over estimate up to 115% load and constant at 255.21W. This value of SLL represents 1.979% of input power at rated conditions. Thereafter, the calculated values exceed the estimated values. The calculated values follow a parabolic curve which ranges from approximately 10W at 25% load to 445W at 150% load.

8.6.2 15kW Motor Results

The SLLs for the 15kW is displayed in Figure 8.15 below.

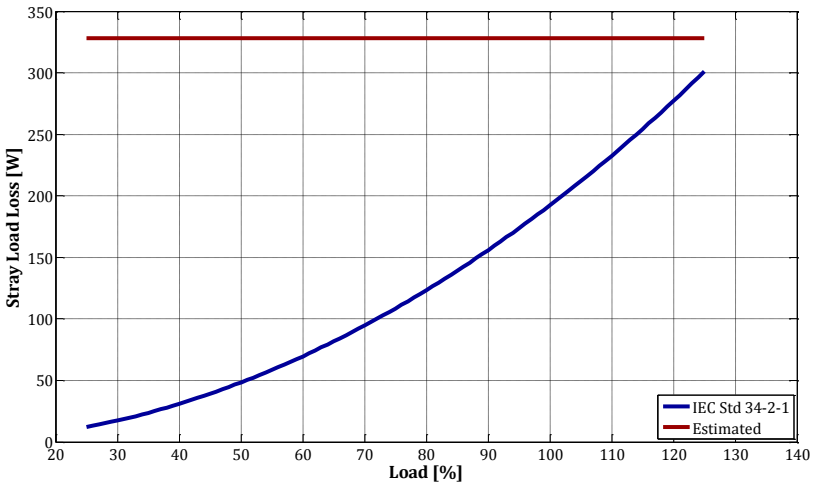

Figure 8.15: Stray load loss results for the 15kW motor

Based on the above, the estimated values of 327.94W present an over estimate in relation to the calculated values. This value represents 1.911% of the input power at rated conditions. The calculated values vary from 10W to 300W over the load range. An interception of the two plots is expected at higher loading conditions, as can be seen if the corresponding curves are extrapolated.

8.6.3 7.5kW Motor Results

Figure 8.16 below represents the estimated and calculated SLL values

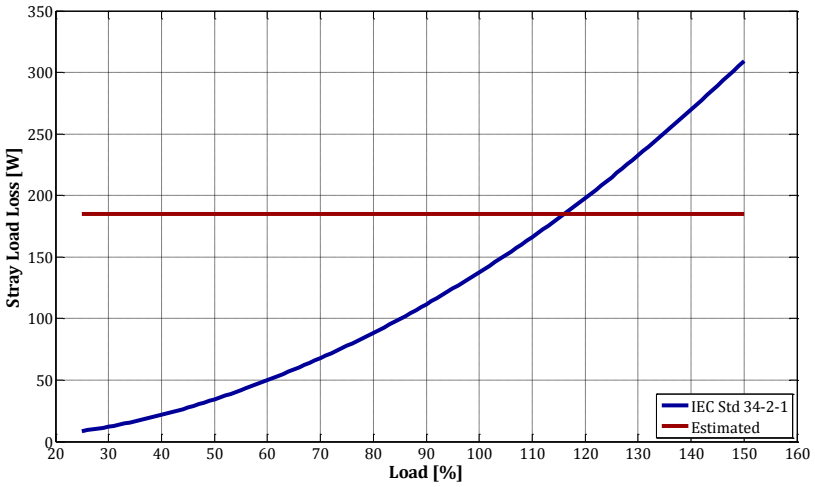

Figure 8.16: Stray load loss results for the7.5 kW motor

The plots above indicate an over estimation of SLL for loading ranges up to 115%. With the estimated SLL equating to 184.79W, the calculated values vary from approximately 10 W to 310W over the loading range. The 184.79W estimated SLL reflects 2.06 % of rated input power under rated conditions.

8.6.4 Discussion of Results

Considering the results shown in the previous sections, the estimated SLL exceed the measured values for loads ranging up to approximately 120% of rated load. The discrepancies of the estimated results lie with the governing equation (equation 6.23) used to obtain the SLLs at rated load. For other than rated loading condition the standard states

that the stray load loss varies with the square of the rotor current. This rotor current is obtained by

$$I_r = \sqrt{I_s^2 - I_{\text{No Load}}^2} \qquad (8.2)$$

Where:

I_s is the stator current

$I_{\text{No Load}}$ is the no load current

For the NAGT method, it is required that the no load test be avoided in order to eliminate the high intrusion associated with the no load test procedure. Thus, equation 8.2 cannot be used to obtain the SLL values at other than rated load conditions. Since the NAGT method provides an estimation of efficiency, the estimated stray load loss obtained at rated conditions is used for all other loading conditions. Therefore, the estimated SLL values do not vary with load (i.e. load independent), whereas the calculated values do (i.e. load dependant).

Additionally, the over estimation of SLL at rated conditions is as expected since the IEC Std 34-2-1 states that the assigned allowances represents an upper envelope of a large number of measured values, hence resulting in larger than expected SLL values. The effect of this over estimation (i.e. higher SLL values) is to decrease the overall output power and hence the efficiency of the machine.

The estimated SLL is dependant on both the input power and rated output power of the motor. A comparison of estimated SLL values between different motor sizes at 100% load is provided in Table 8.10 below.

Table 8.10 Comparison of estimated SLLs between different motor sizes

Motor Size [kW]	**P_{Input} [W]**	**SLL_{rated} [W]**	**% of P_{Input} [%]**
15	17152	327.94	1.911
11	12894	255.21	1.979
7.5	8959	184.79	2.062

As can be seen, the amount of power contributing to SLL varies according to the size of the machine. Although, larger motors are associated with higher SLL values, smaller motors contribute a larger percentage of their associated input power to SLLs.

8.7 Non-Intrusive Efficiency Estimation

The following section shows the efficiency results for the overall NAGT method. For comparison purposes the IEC Standard 34-2-1 and the direct method (P_{out}/P_{in}) results are also included. The percentage voltage unbalance and total harmonic distortion (THD) are also depicted to provide an indication of the supply conditions at which the efficiency values are quoted.

8.7.1 Repeatability of Tests and Averaged Results

The repeatability of a test can be described as the variation of test results when experiments are performed under similar conditions. These conditions include identical methodology, operator, and instrumentation. In order to convey the consistency of the results obtained in this thesis, each test conducted was repeated three times and an average value was obtained. To obtain the average, it is necessary that the results for each of the three tests are set to the exact same loading condition. This is a challenging task, since the exact values of loading cannot be obtained when using manual loading control. To overcome this, the efficiencies obtained during each test are plotted against the actual loading condition. This can be obtained by the ratio of the measured torque to the machine's rated torque as shown by

$$\%\text{Load} = \frac{T_{\text{Measured}}}{T_{\text{Rated}}} \times 100\% \tag{8.3}$$

The efficiency is then plotted against the load at six different loading points ranging from 25% to 150% of rated load. A polynomial curve of n-1 data points is fitted to these values and the equation of the curve is then obtained. The curve represents the efficiency values as a function of the load, allowing for the efficiency to be obtained at any loading point. The efficiencies for each of the tests are then plotted using its unique governing equation for exact loading conditions (eg at exactly 100%) and the average of the tests is obtained. The

following figures show the repeatability and average of the efficiency results for the motors tested.

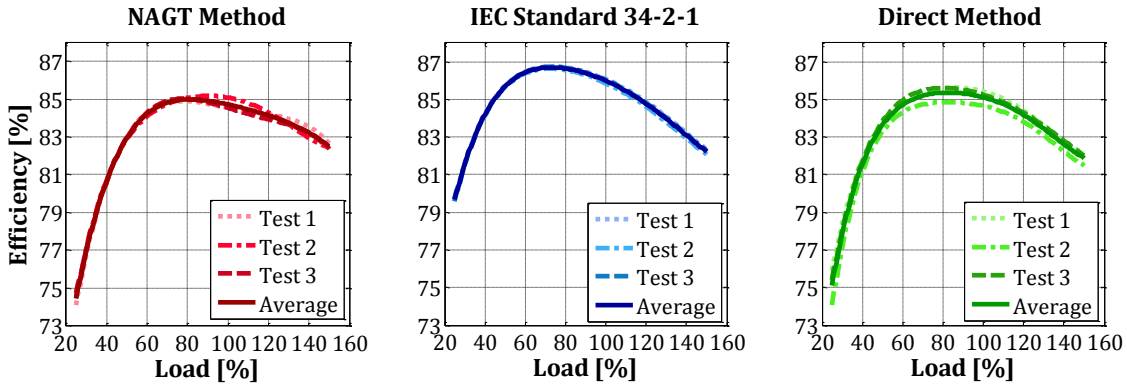

Figure 8.17: Repeatability of the 11kW motor results

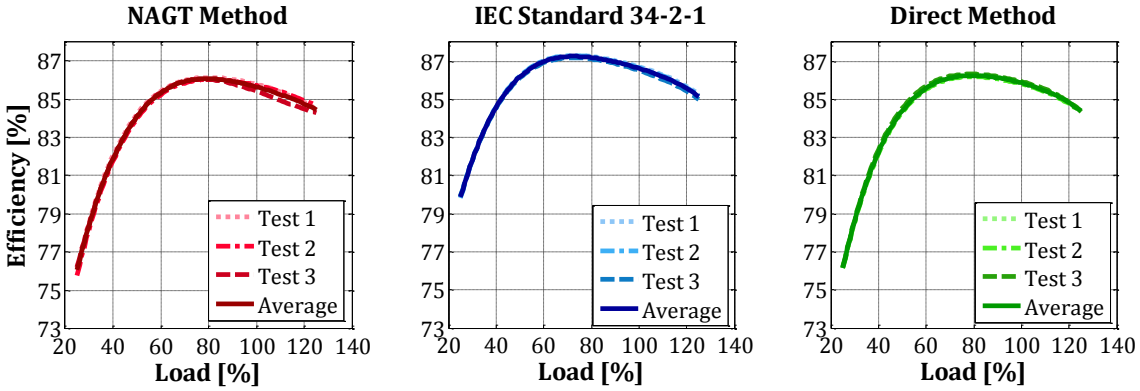

Figure 8.18: Repeatability of the 15kW motor results

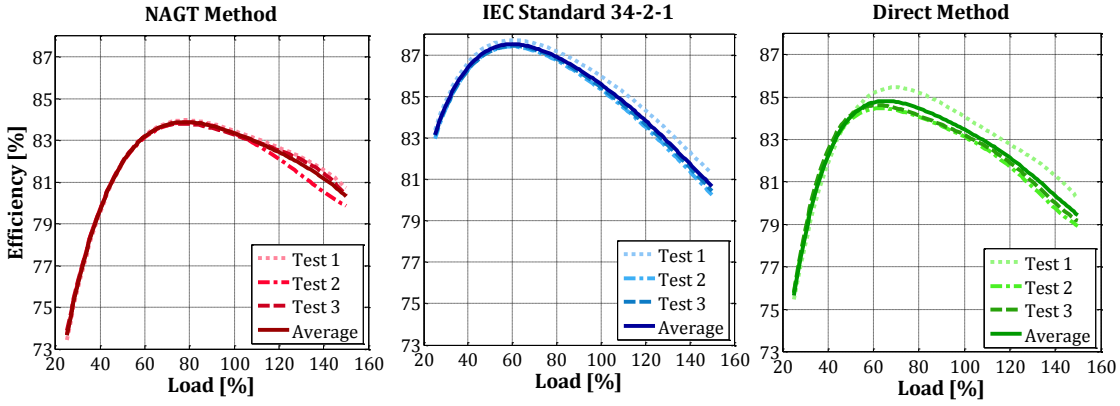

Figure 8.19: Repeatability of the 7.5kW motor results

As can be seen, the results show that there is a consistent trend when comparing tests 1, test 2 and test 3. This is evident in all three of the motors tested. For the remainder of this thesis, only the average values of the efficiency tests will be considered.

8.7.2 11kW Motor Results

The average efficiency results for the 11kW motor is shown in Figure 8.20 below. The efficiencies quoted here are obtained under 0.43% voltage unbalance and a THD of 2.33%, which is within the limits of the IEC Std 34-2-1 for conducting the efficiency test.

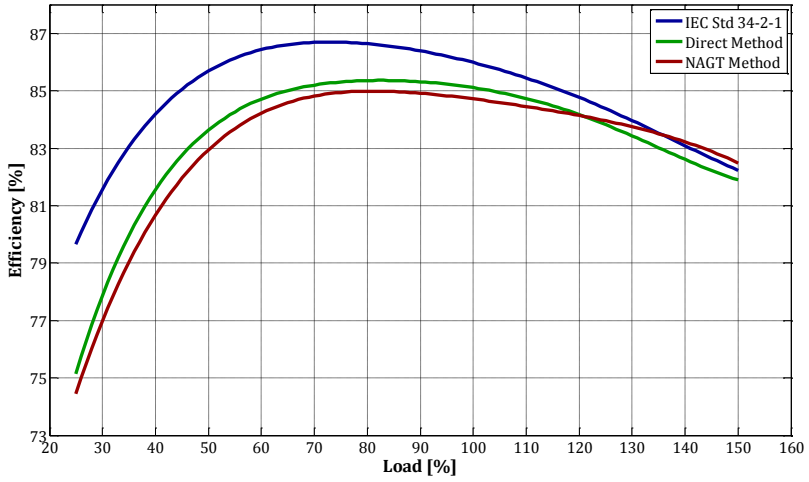

Figure 8.20: Efficiency results for the 11kW motor

Observing the above graph, one can see that the efficiency curves follow the same general trend for each of the three methods. Considering the IEC Std 34-2-1 method as the baseline for comparison, the NAGT and direct method efficiencies are lower over the entire loading range. The maximum efficiency values for the IEC Std 34-2-1, the direct method and the NAGT method are 86.70%, 85.36% and 84.99% and occur at 73%, 82% and 81% of rated load respectively. The actual efficiency values obtained at the six loading points are provided in Table 8.11.

Table 8.11 Efficiency results of the 11kW motor

Load [%]	IEC Std 34-2-1 [%]	Direct [%]	NAGT [%]
150	82.228	80.1054	82.484
125	84.378	84.0122	83.955
100	85.987	85.4470	84.716
75	86.695	85.7173	84.943
50	85.688	83.8005	82.947
25	79.658	75.4474	74.445

Based on the table, the efficiency results of the NAGT method deviates from the IEC Std 34-2-1 results by a maximum of 5.12% at 25% load and a minimum of 0.256% at 150% load. In comparison to the direct method, the NAGT efficiency results are within 2.3% efficiency.

8.7.3 15kW Motor Results

The average efficiency results for the 15kW motor are shown in Figure 8.21. Due to limitations in the loading for the 15kW machine, only values of up to 125% of rated load were obtained. The supply conditions contained 0.251% unbalance and 2.66% THD

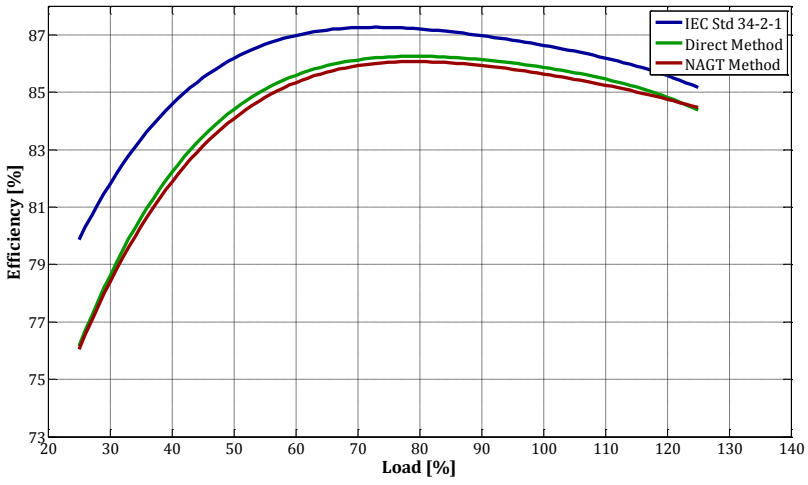

Figure 8.21: Efficiency results for the 15kW motor

The curves indicated in the above figure show that the NAGT efficiency values obtained are lower when compared to the IEC Std 34-2-1 and direct method results. Incidentally, the NAGT results are closely related to the values obtained using the direct method. Despite

this, all three curves show a similar trend in results, with the maximum efficiencies of 87.26%, 86.25% and 86.06% occurring at 73%, 79% and 79% of rated load respectively. The actual efficiency values for the five loading points are shown in Table 8.12.

Table 8.12 Efficiency results of the 15kW motor

Load [%]	IEC 34-2-1 [%]	Direct [%]	NAGT [%]
125	85.1596	84.3797	84.4600
100	86.6329	85.8678	85.6369
75	87.2535	86.2253	86.0358
50	86.1832	84.3995	84.0834
25	79.8703	76.1495	76.0493

The NAGT efficiency results, in relation to the IEC 34-2-1, show a maximum deviation of 3.82 % at 25% load and a minimum deviation of 0.699 % at 125% load. When comparing the NAGT results with the results obtained from the direct method, the efficiencies are within 0.3 % efficiency over the entire loading range.

8.7.4 7.5kW Motor Results

The efficiency results for the 7.5kW motor are shown in Figure 8.22. The supply conditions for which these efficiency results were obtained were 0.43% voltage unbalance and 2.5% THD.

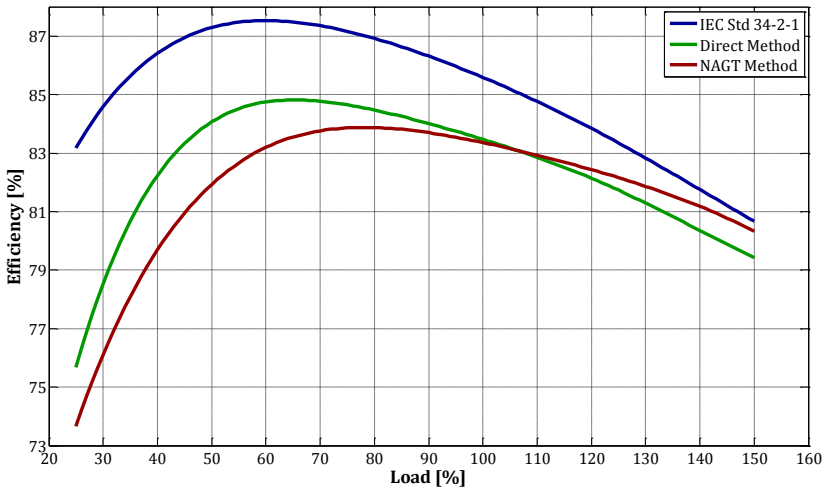

Figure 8.22: Efficiency results for the 7.5 kW motor

The curves above show the IEC Std 34-2-1 representing higher efficiency values, followed by the direct method and the NAGT method. The maximum efficiency for each of the methods can be seen in decreasing order at 87.53%, 84.82% and 83.87% at 60%, 65% and 78% loading respectively. A more detailed comparison of efficiency results obtained is provided in Table 8.13 below.

Table 8.13 Efficiency results of the 7.5kW motor

Load [%]	IEC 34-2-1 [%]	Direct [%]	NAGT [%]
150	80.6710	79.4300	80.316
125	83.3465	81.7300	82.159
100	85.5880	83.4720	83.359
75	87.1616	84.6466	83.861
50	87.2936	84.0685	81.933
25	83.1653	75.6638	73.663

Notably, there is a large discrepancy between the curves, especially at the lower loading ranges. In comparison, the NAGT efficiencies diverge from the IEC Std 34-2-1 values by 9.5 % and 0.36% at 25% and 150% loading respectively. Alternatively, the NAGT efficiency values are within 2.135% of the values obtained by the direct method.

8.7.5 Discussion of Results

For each of the tests performed on a specific motor, the results indicate consistency relative to each other. This strong correlation indicates that the test procedures are highly repeatable. Additionally, the supply (voltage unbalance and THD) conditions for each of the tests conducted were all within accordance of the IEC Std 34-2-1 standard. This shows that Eskom's mains supply can be used for motor efficiency testing since it falls within the specifications of the standard.

Consideration of the air gap torque equation and its relation to the core loss showed that there is a need to cater for the core loss component in the efficiency equation. This suggests that the air gap power calculated using the air gap torque equation is merely the input

power less the stator copper loss which coincides with the theory and lays to rest the uncertainty identified in the literature. In this case, the calculations using the air gap torque equation can be avoided. Since similar results can be obtained by merely calculating the input power from the motor's stator voltages and current (equation 6.9) and subtracting the stator copper loss. This indicates a simpler and less computationally tedious procedure.

The efficiency results obtained from the NAGT method consistently shows the lowest efficiency values for the case of all three motors under test. It is difficult to identify which component is the main contributing factor to the deviations in efficiency, due to the sources of error in estimating the various parameters. Another aspect to consider is that the efficiency values show higher deviations at the lower load ranges. Based on this observation, further investigation into the deviations of the efficiency results over the load range was conducted.

This was done by applying the NAGT methodology to the IEC Std 34-2-1 calculated results and comparing the efficiencies to the original IEC Std 34-2-1 results. The effects of individual estimated components on the overall efficiency were observed by introducing the estimated components independently of the others. For example, to investigate the effects of estimated rotor speed on the efficiency, the estimated rotor speed values were used while using the IEC Std 34-2-1 calculated results for the remaining components i.e. stator resistance, no load loss and stray load loss. This was repeated for the each of the measured stator resistance, no load loss and stray load loss components which were compared to the original efficiencies of the IEC Std 34-2-1. Based on this, it was observed that the effects of stray load loss contributed most significantly to deviations in efficiency, i.e. approximately 10 % at 25 % load.

Considering the discussion made in section 6.6.2 and section 8.5.4, the estimated stray load loss is obtained at rated load (equation 6.23) and the value obtained is applied for all loading ranges. Consequently, the stay load losses are not load dependant which transgresses the load dependant values seen in the IEC Std 34-2-1 results. In order to improve the estimated stray load loss results, a linear regression technique similar to that

of the IEC Std 34-2-1 was applied. This process involves expressing the stray load loss as a function of the square of the torque for each load. The corrected stray load loss is then obtained by shifting the linear curve to go through the origin while maintaining the slope of the curve. Since the empirically estimated stray load loss is obtained at rated conditions, a straight line passing through this point and the origin gives the 'improved' values for stray load loss estimation.

The corrected stray load loss components for the IEC Std 34-2-1, the estimated (equation 6.23) and the 'improved' estimate is shown in Figure 8.23. The subsequent results for the 11 kW motor is reflected for the remainder of this investigation.

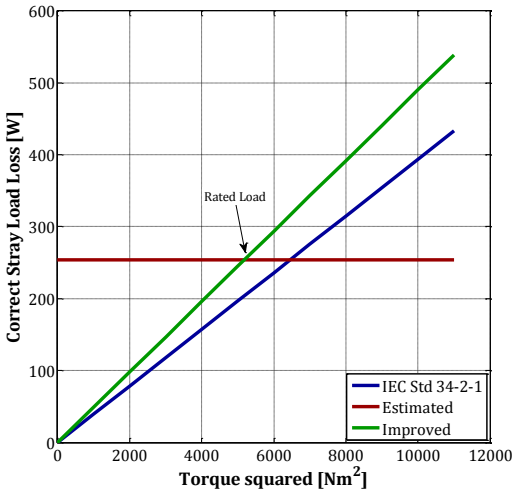

Figure 8.23: Corrected stray load loss

As can be seen, the gradient of the 'improved' SLLs is steeper than the IEC Std 34-2-1 indicating that higher stray load loss values will be obtained. Based on this, the stray load losses can be obtained for a range of load conditions as shown in Figure 8.24.

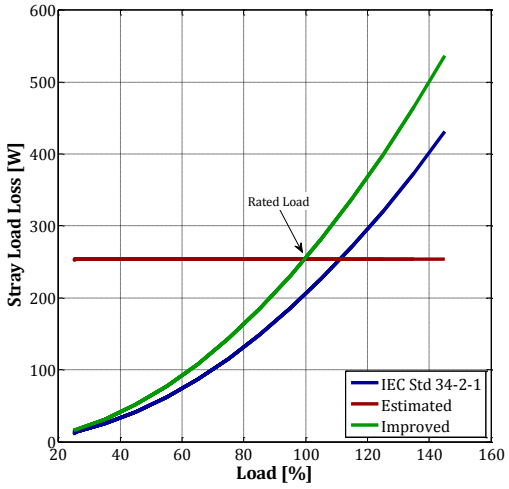

Figure 8.24: Stray load loss variation with load

As can be seen, the improved results are load dependant and follow the same trend as the IEC Std 34-2-1. Despite showing an over estimate in relation to the IEC Std 34-2-1 results, particularly at the higher loading conditions. The 'improved' stray load loss results reflect a more realistic trend than the original estimated results.

The effects of using the improved stray load loss results on the NAGT method can be seen in Figure 8.25.

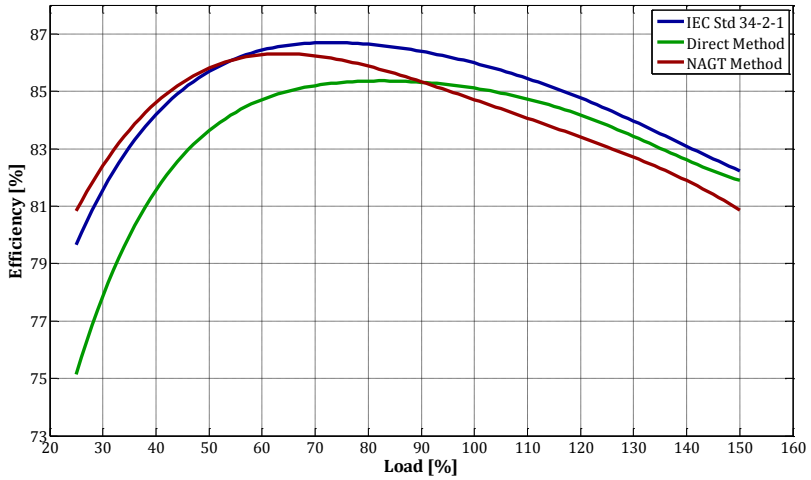

Figure 8.25: Efficiency obtained using improved SLL estimation

As can be seen, the NAGT method efficiencies show an improvement in the lower load ranges in relation to the IEC Std 34-2-1. However, the deviations at the higher loading range have increased. This is due to the over estimate of the improved stray load loss values at higher loads. Overall, the new NAGT efficiencies are within 2% of the IEC Std 34-2-1 which is an improvement to the original NAGT efficiencies.

8.8 Effects of Voltage Unbalance on Motor Efficiency

The efficiency results of the NAGT and direct method under unbalanced conditions is presented in the following subsections. As mentioned in Chapter 7, there is not standard procedure for the calculation of efficiency under unbalanced supply conditions. In particular, complications arise when calculating the individual loss components. Therefore the direct method will be used to which the NAGT results can be compared. The investigation of voltage supply unbalances is limited to the case of magnitude unbalance with nominal (380V) average voltage. The case of 2.5 % and 5% voltage unbalance defined according to the NEMA definition is presented.

8.8.1 Unbalanced Supply Conditions

The experimental supply voltages and currents obtained from the generator during unbalanced conditions are shown in Figure 8.26. Only the case for the 11 kW under rated load is represented and is merely for demonstration purposes.

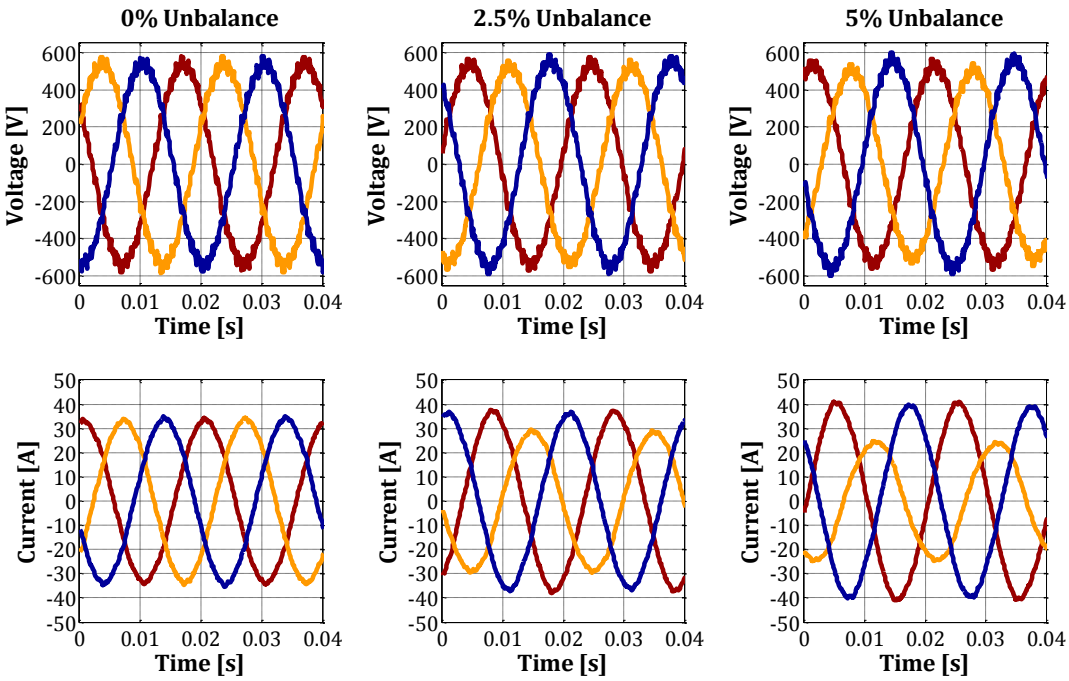

Figure 8.26: Motor supply voltages and currents during unbalanced conditions

The effects of voltage unbalance can be clearly seen by the corresponding unbalanced currents. During 0% voltage unbalanced conditions, each of the line voltages and currents are equal in magnitude with amplitudes 580.23 V and 34.6 A respectively. As the severity of magnitude unbalance increases, so the magnitude of the corresponding voltages and currents changes. For the case above, the variac combination caused the voltage and current magnitudes of phase A (red) and phase C (blue) to increase while the magnitude of phase B (yellow) decreased with increasing unbalanced conditions.

The efficiency for each of the motors tested during unbalanced conditions is presented in the following sections

8.8.2 11kW Motor Results

The air gap torque values and their corresponding NAGT efficiencies are shown in Figure 8.27.

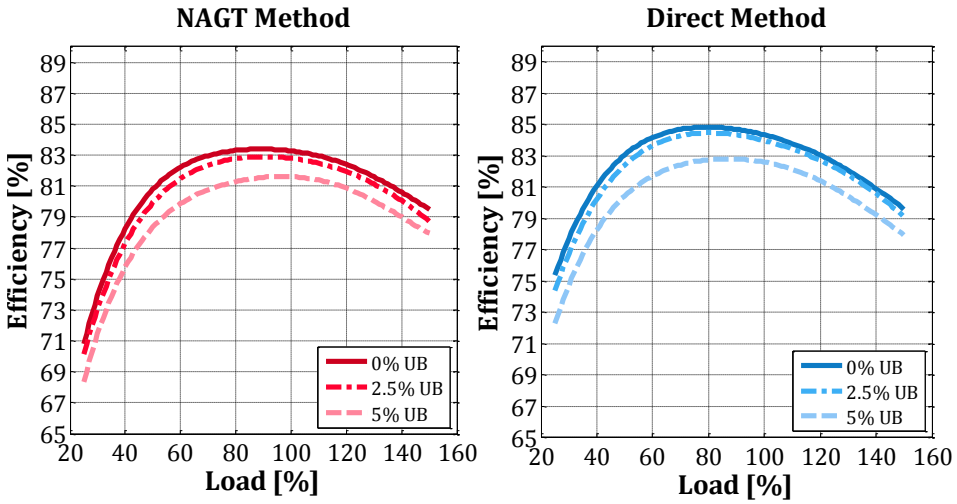

Figure 8.27: Overall unbalanced efficiency curves for the 11 kW motor

As expected, the unbalance efficiency values for both the NAGT and the direct method show a decrease with an increase in voltage unbalance.

A more explicit comparison of the NAGT and direct method efficiencies for each of the unbalance cases are shown in Figure 8.28

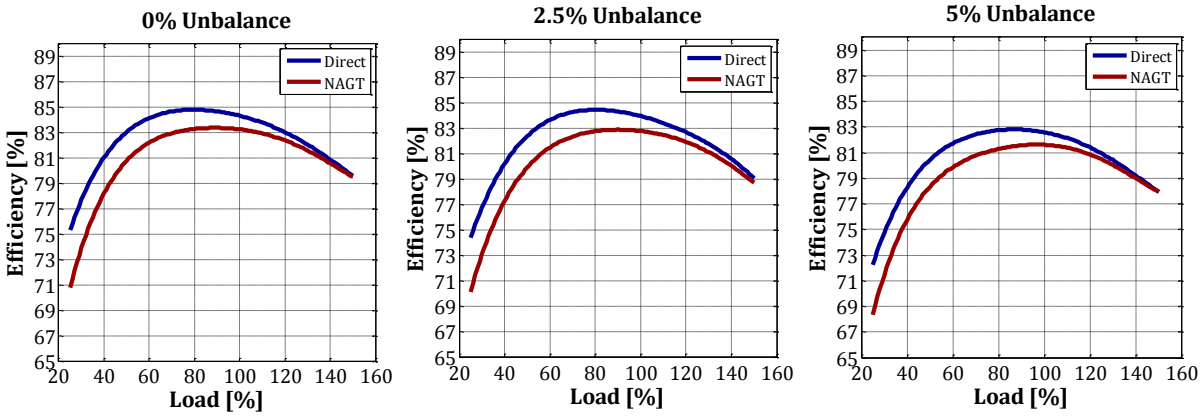

Figure 8.28: Efficiency results for the 11 kW motor under unbalanced conditions

For all unbalanced cases, the NAGT efficiencies are lower than the direct method values. The efficiency curves follow the same trend for each of the unbalance cases. As with the results shown in the previous section, the deviation of the NAGT results is higher at the lower loading points.

8.8.3 15kW Motor Results

The unbalanced efficiency results for the 15 kW motor is shown in Figure 8.29 below.

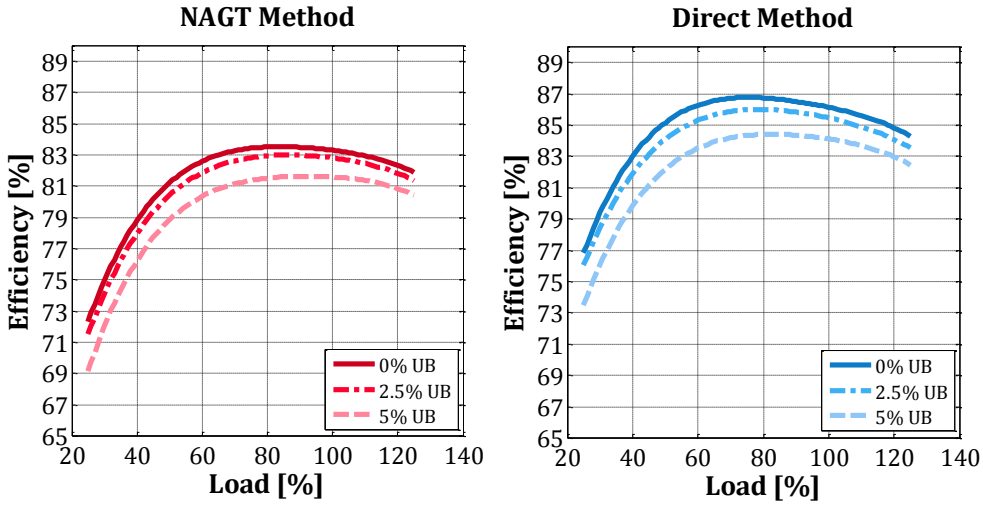

Figure 8.29: Overall unbalanced efficiency curves for the 15 kW motor

The efficiency values for both the NAGT and direct method are as expected and decrease with an increase in voltage unbalance.

The individual cases for each of the unbalanced conditions are shown in Figure 8.30 below.

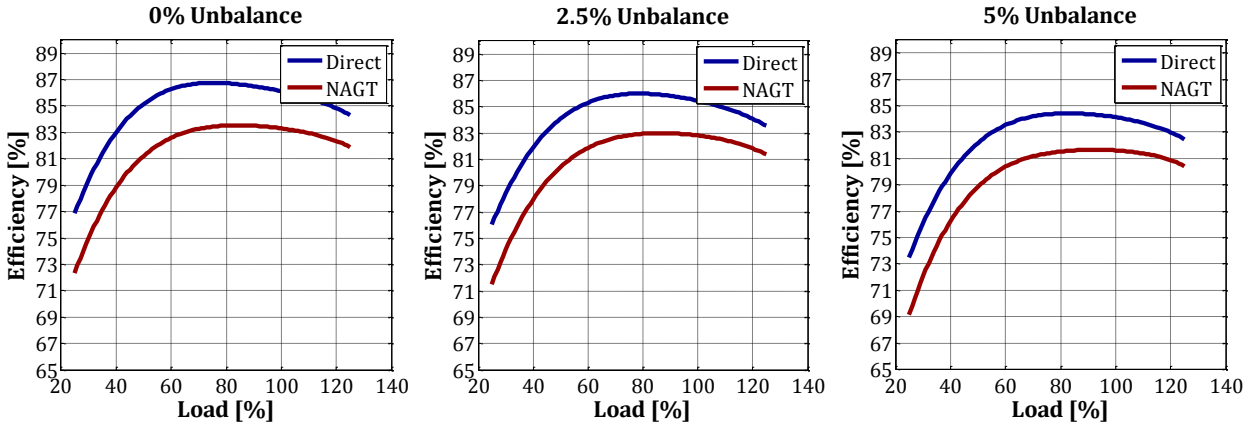

Figure 8.30: Efficiency results for the 15 kW motor under unbalanced conditions

As shown, the NAGT efficiency values represent lower efficiency values when compared to the values obtained from the direct method. The estimated NAGT efficiencies do however follow the same trend as the direct method. Similarly, the maximum deviation occurs at the lower loading range.

8.8.4 7.5kW Motor Results

The air gap torque values and the resulting efficiencies for each of the unbalanced conditions is displayed in Figure 8.31.

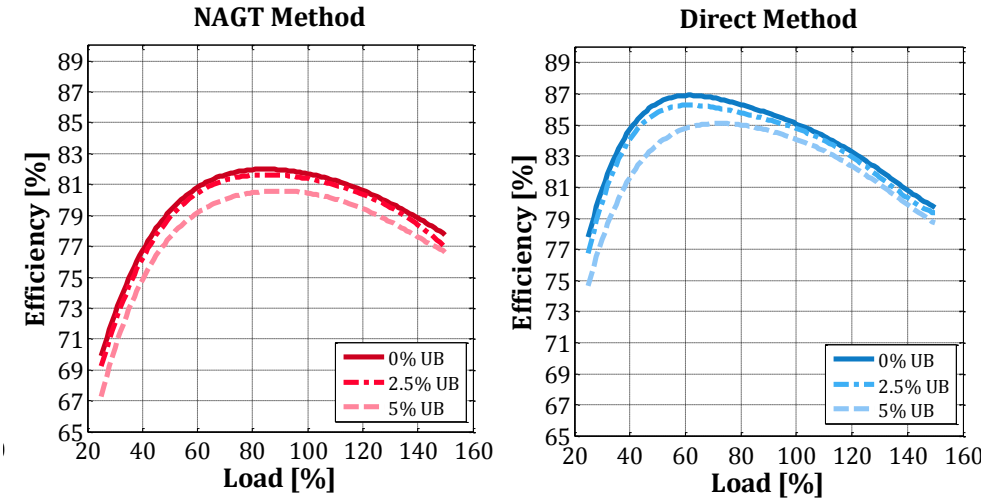

Figure 8.31: Overall efficiency curves for the 7.5 kW motor

The efficiency results are as expected and show a decrease in values with an increase in voltage unbalance for both the NAGT and direct methods. A representation of the differences in the acquired results for each of the unbalanced conditions for the NAGT and direct method is shown in Figure 8.32 below.

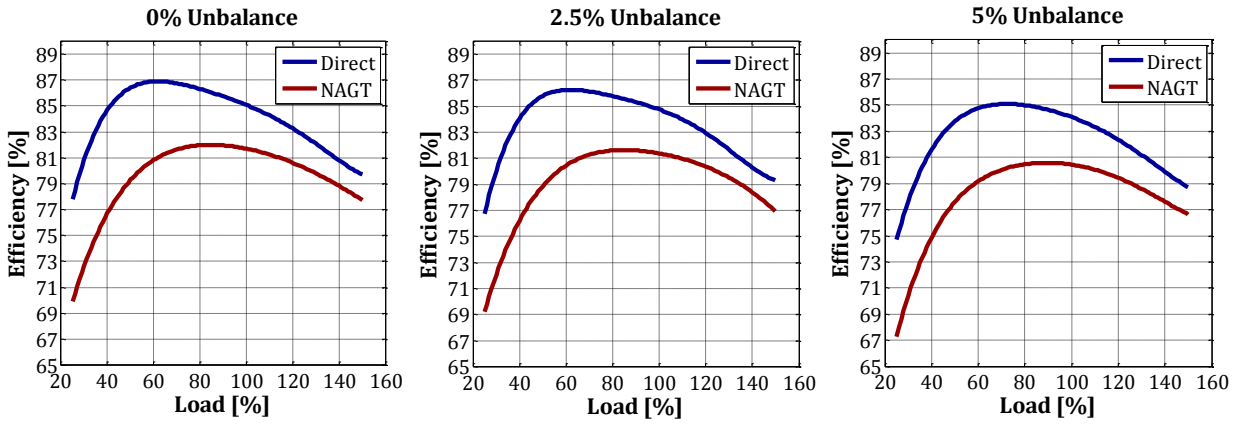

Figure 8.32: Efficiency results for the 7.5kW motor under unbalanced conditions

The NAGT efficiency results show lower values in comparison to the direct method efficiencies. Although the results show the same trend in each of the above cases, there is a large discrepancy in the actual efficiency values i.e. more that 5% difference between the two methods, particularly at the lower load range.

8.9 Discussion of Results

As expected, the effects of supply unbalance have a negative impact on the motor's efficiency. The results presented in the above sections showed that an increase in the degree of supply unbalance further decreases the motors efficiency. The unbalanced condition causes further losses within the motor and therefore increases the operating temperature. This is evident in the increase in stator winding temperatures and therefore stator copper loss as the motor draws more current.

The results for the NAGT shows that it can be used to determine the motor's efficiency during unbalanced conditions. The results consistently showed lower efficiency values for all tested machines in comparison to the direct method efficiencies. This is also the case for efficiency values obtained under balanced conditions and therefore suggests that the NAGT method consistently underestimates the machine's efficiency in relation to the direct method. This is indicative of the advantage of the air gap torque method above other methods in that it accounts for the effects of the negative torque associated with the unbalanced conditions.

8.10 Concluding Remarks

In this chapter, the experimental results are presented and discussed. In particular a detailed analysis of the individual estimated parameters for the NAGT method and their performance is assessed.

The stator resistance estimation results showed an over estimate in comparison to the expected resistance values. Additionally, the percentage error between these values is not consistent over the entire loading range and this variation is also extended across different motor sizes. The stator resistance values, did however vary with load and hence temperature.

For the case of the speed estimation technique, the results proved to be successful in comparison to the measured values with accuracy within 0.16% for all three motors. The rotational frequency components, from which the speeds can be obtained, were dominant and easily detectable over the entire load range making speed estimation highly dependable. Due to the required signal processing (FFT) techniques, the effects of frequency resolution was also investigated. The results indicated that higher accuracy levels for speed estimation can be achieved by increasing the acquisition time.

The estimated no load losses proved to be an under estimate for the 11kW and 15kW motors. On the other hand, an over estimate was indicated for the 7.5kW motor. This led to the investigation of the individual loss contribution in relation to the input power. Furthermore, the effects of the variation of the IEC Std 34-2-1 calculated core losses with load were explored. It was seen that the variation of core loss is due to the effects of stator voltage drop compensation which is unique to the IEC Std 34-2-1.

The comparison between the IEC Std 34-2-1 calculated results and estimated values of SLLs were also presented. In general the estimated values show a constant overestimate in SLL over the loading range.

Based on the above, the efficiency estimation based on the NAGT method was obtained. These values were compared to the efficiencies obtained using the IEC Std 34-2-1 and direct method and were, for the most case, lower in magnitude. In particular, the deviations in efficiencies at the lower loading points were substantially larger than at the higher loading range. To address this issue, the effects of the SLL estimation on the NAGT efficiencies were investigated and subsequently lead to the development of an 'improved' estimation technique. The SLLs obtained from this improved technique differs from the original estimated values in that it provides SLLs that are load dependant. The SLL results obtained from this 'improved' method reflects the values obtained from the IEC Std 34-2-1 more closely despite being an over estimate. The introduction of the 'improved' SLL results, showed an improvement in the NAGT efficiencies to within 2% relative to the IEC Std 34-2-1 results.

Lastly the effect of magnitude voltage unbalance on the NAGT method was investigated. It was observed that a decrease in efficiency is related to an increase in voltage unbalance. This is attributed to the increase in motor losses and hence increases in the operating temperature. The efficiency results obtained using the NAGT method indicated lower values for each of the unbalanced cases in comparison to the direct method.

CHAPTER NINE

ERROR ANALYSIS OF EFFICIENCY DETERMINATION

This chapter investigates the accuracy of measured and estimated efficiency results. In particular the effects of instrumental errors associated with experimental testing are investigated. To accomplish this, the worst case error estimation (WCEE) and realistic error estimation (REE) techniques are incorporated. Based on this, the effects of errors associated with individual parameters on the overall motor efficiency are explored.

9.1 Introduction

When quoting the results of any experimental procedure, there is often a question around the credibility of the values stated. In general, the conduction of an experimental investigation requires amongst other things, a test bed with the relevant measuring devices, a methodological test procedure and experienced personal to carry out the study. Due to the nature of these aspects, the results obtained often contain a certain degree of uncertainties and it is important that these uncertainties are accounted for if the outcome is to be creditable. The following sections will provide detailed analysis of the errors associated with the motor efficiency testing process.

9.2 Definition of Basic Terms and Concepts

The process of *measuring* involves the determination of these measurable quantities with the aid of measuring devices or instrumentation [78]. The measurement process is often outlined by a set procedure or methodology according to a specific standard.

A *measuring instrument* is regarded as a highly specialized piece of equipment used to detect the value of the measurable quantity. These instruments should be regularly calibrated. This is done to avoid the effects of drifting and to ensure a reliable level of accuracy defined by the accuracy class.

The term *measurable quantities* can be used to describe the physical quantities that are measured during an experiment, for example voltage, current, resistance etc. These measured quantities can also be referred to as the *measurand* [78].

The *true value* of the meaurand is considered to be the values obtained from the experiment that would ideally represent the measurable quantity with 0 % error. It should be noted that in practice the true value of a measurand is unknown. Alternatively, if the true value was known there would be no need for measurement [78]. Thus, the 'true' values are denoted by the measured (IEC Std 34-2-1) or estimated (NAGT method) values obtained from the conducted experiment. Due to the nature of these methods, i.e. the

required personnel and the instrumentation used, the values obtained contain unavoidable degrees of inaccuracies.

The *inaccuracy* of a measurement represents the degree of deviation or imperfections of the true value in relation to the measurand. This inaccuracy is attributed to the measurement uncertainty or measurement error associated with the experiment.

The term *uncertainty* (in terms of measurement) can be regarded as the interval within which the true value is expected to lie with a given probability [78]. In contrast, the *error* (of measurement) is merely the deviation of the measured or estimated value from the true value of the measurand. The measurement error can be expressed in absolute or relative form, as shown in equation 9.1 and 9.2 respectively [78].

$$\zeta_{\text{Absolute}} = \widetilde{A} - A_t \tag{2.25}$$

$$\varepsilon_{\text{Relative}} = \frac{\widetilde{A} - A_t}{A_t} \tag{2.26}$$

Where:

ζ_{Absolute} is the absolute error

$\widetilde{A}$ is the estimated value

A_t is the true value

$\varepsilon_{\text{Relative}}$ is the relative error

With reference to the absolute error, it is expressed in the same unit as the measured quantity and its value can take the form of a positive or negative value. In contrast, the relative error is represented as a ratio of the true value and is expressed as a percentage [78].

The following sections will discuss the different sources of experimental error with its focus on efficiency determination.

9.3 Sources of Experimental Errors

The conduction of an experiment is generally associated with three sources of errors. These include methodological errors, human errors and instrumentation errors, which may be expressed as

$$\zeta_{\text{Absolute}} = \zeta_{\text{m}} + \zeta_{\text{h}} + \zeta_{\text{i}} \qquad (2.27)$$

Where:

ζ_{Absolute} is the absolute measurement error

ζ_{m} is the methodological error

ζ_{h} is the human error

ζ_{i} is the instrumental error.

All three of the above sources of error are contributing factors in induction motor efficiency testing. The following section will describe these errors in more detail.

9.3.1 Methodological Error

As the name applies, the methodological errors are a consequence of the errors in the testing procedure or methodology. In terms of motor loss and efficiency measurements, the methodological errors are due to the routine of the measurement method conducted. These experimental tests are usually performed by following a set method, according to an accepted standard or established procedure. As mentioned in Chapter 2, there are many established motor efficiency standards that exist globally and their major differences in testing procedures were highlighted. Due to these discrepancies, the efficiency results quoted from these standards will show slight differences despite the tests being conducted on the same motor. This indicates that the methodology of efficiency testing each contains its own set of associated methodological errors. One solution to avoid these discrepancies is to adopt a single worldwide motor testing efficiency testing procedure.

Many of the motor testing standards are based on the equivalent circuit model of the machine. These models also contain their own level of assumptions and simplifications [79]. Since the efficiency calculations are based on the relationship between the components depicted in the model, they too will contain errors. For example, considering the separation of loss method in IEC Std 34-2-1, the stray load loss component is not accounted for in the equivalent circuit model [79]. In contrast the other four loss components (stator copper loss, rotor copper loss, core loss and friction and windage loss) are modelled by a set of resistive and inductive components. The standard, therefore, assumes a value of stray load loss to be the loss remaining after the subtraction of the output power and other loss components from the input power (see equation 2.8).

Additionally, the level of intrusion of the applied method is linked to the amount of errors (and hence accuracy) associated with the methodology [80]. As mentioned in Chapter 3, there is a trade off between the accuracy and level of intrusion when it comes to efficiency estimation techniques. In an attempt to make the efficiency estimation techniques less intrusive, more assumptions are made, which introduces a greater degree of error.

9.3.2 Human Error

Human errors are a consequence of errors associated with inaccurate readings, incorrect calculations and misuse of instrumentation. Despite this, even the most experienced operator cannot avoid the inevitable errors due to the nature of being human. Additionally, no two operators are identical, and hence the results obtained by these two operators will differ, even if the same methodological procedure is followed. The individual judgement of the operator plays a role in determining sufficient machine operating stability, load condition, the time taken between subsequent readings, and adequate experimental setup, all of which contributes to the final errors in efficiency values.

The interpretation and understanding of a given testing standard or procedure is also a contributing factor to human errors. This is particularly evident in cases where there are ambiguities in the test procedure. For example, the IEC Std 34-2-1 does not define a

preferred position for temperature sensors [81]. Consequently the position of the temperature sensors will lead to different temperature reading of which affects the calculation of stator copper losses and the overall efficiency.

9.3.3 Instrumentation Error

Instrumentation errors are considered to be the main contributing factor to the errors in measurement [80]. In terms of efficiency determination, the effects of instrumentation errors have an influence on the measurement of voltage, current, speed, torque and stator winding resistance. Errors in these measurements, consequently contribute to the inaccuracies of loss determination and overall motor efficiency.

The instrumentation error can be calculated using error evaluation techniques. The three most common techniques include the following [80]

- Maximum Error Estimation (MEE)
- Worst Case Error Estimation (WCEE)
- Realistic Error Estimation (REE)

For the purpose of this thesis, emphasis will be placed on instrumental error, since these are considered to be the largest contributor to errors associated with measurement. Additionally, the effects of these errors can be calculated and subsequently reduced by incorporating the choice of more accurate instruments. In contrast, the methodological and human errors cannot easily be quantified by empirical equations and it can be assumed that the operator is highly experienced and follows the methodological procedure as strictly as possible. Therefore, the effects of human and methodological errors are minimal and will not be considered.

A more detailed discussion of these error estimation techniques in terms of instrumentation error will be provided in the following sections.

9.3.4 Error Estimation Techniques for Instrumental Error

The motor testing system can be represented by a set of variable inputs and its associated output, as shown in Figure 9.1 [79].

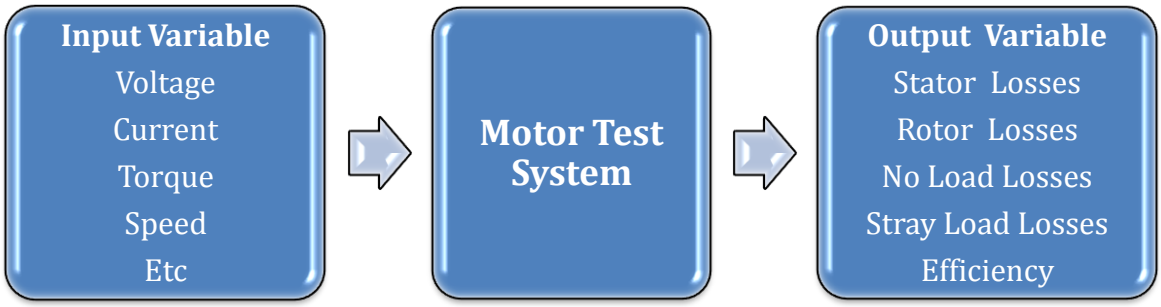

Figure 9.1: Motor testing procedure [79]

The relationship between the input variables and the output can be represented by a transfer function which reflects the methodology or test procedure upon the motor under test. This transfer function is considered to be highly complex, non linear and is often difficult to model [79].

The errors in instrumentation used to measure the input variables (or measurands) can be determined by the techniques presented below.

9.3.5 Maximum Error Estimation (MEE)

The maximum error estimation (MEE) technique accounts for the most extreme case of estimation error associated with the measurement system. In this case, the maximum measurement error is seen to occur in addition to the maximum uncertainties of all the instrumentation used in testing [80]. The maximum error can be represented by

$$\varepsilon_{\eta} = \max \left| \frac{1 \pm \varepsilon_{\text{Poutput}}}{1 \pm \varepsilon_{\text{Pinput}}} \right| - 1 \qquad (2.28)$$

Where:

ε_{η} is the relative error in efficiency

$\varepsilon_{Poutput}$ is the relative error in output power

ε_{Pinput} is the relative error in input power

The assumption that the maximum errors will occur simultaneously is not a realistic reflection of the errors associated with the measurement system at any given time. This method therefore provides an over estimate of the errors associated in with the system.

9.3.6 Worst Case Error Estimation (WCEE)

The worst case error estimation (WCEE) technique also assumes the extreme case of maximum measurement error occurring simultaneously with the maximum errors in the instrumentation. However, this technique differentiates itself from the MEE technique by accounting for each of the individual sources of errors independently [80].

The absolute and relative error calculations were presented in equations 9.1 and 9.2. Considering these equations and Figure 9.1, the effects of small perturbations placed on the input variables in relation to the output can be expressed mathematically using a Taylor series [80]. For practical purposes, only the first term in the Taylor series is considered with the assumption that the resulting output, (y) has a linear relation to the effective perturbations of the input variables (x) [78], [80]. This is valid if the perturbations of the input variable are small. The resulting error in output can be written in simplified form as [80]

$$\zeta_y = f(\Pi, x_i, z_j) - f(\Pi, x_{i,t}, z_{i,t}) \approx \sum_{i=1}^{n}\left[\zeta_{x,i}\frac{\partial f(\Pi, x_{i,t}, z_{j,t})}{\partial x_i}\right] + \sum_{j=1}^{m}\left[\zeta_{z,i}\frac{\partial f(\Pi, x_{i,t}, z_{j,t})}{\partial z_i}\right] \quad (2.29)$$

Where:

$\zeta_{y,}$ is the absolute errors in the output

Π is the system parameter

$x_{i,t}$ is the true value of the input parameter

$z_{i,t}$ is the true value to the additive noise

$\zeta_{x,i}$, is the absolute errors in the input

$\zeta_{z,i}$, is the absolute errors in the additive noise

The contribution of each individual input component in the measurement system and its impact upon the output variable can be expressed as [80]

$$\varepsilon_y = \frac{\zeta_y}{y} = \frac{1}{y}\frac{\partial f}{\partial x_p}\zeta_{x_p} = \frac{x_p}{y}\frac{\partial f}{\partial_{x_p}}\varepsilon_{x_p}, \quad 1 \le p \le n \tag{2.30}$$

An influence coefficient can be used to indicate the sensitivity of the contribution of errors in the input variable upon the final output variable. The influence coefficient can be expressed as [80]

$$I_{x_p} = \frac{\varepsilon_y}{\varepsilon_{x_p}} = \frac{x_p}{y}\frac{\partial f}{\partial x_p} \tag{2.31}$$

The influence coefficient of the noise contribution, z_j can be expressed as

$$W_{z_j} = \frac{\partial f}{\partial z_j} \tag{2.32}$$

Based on the above, the maximum relative error can be determined by equation 9.9 [80]

$$\varepsilon_y = \sum_{i=1}^{n} I_{x_i}\varepsilon_{x_i} + \frac{1}{y}\sum_{j=1}^{m} W_{z_j} z_j \tag{2.33}$$

Due to the separation of the effects of each of the error sources, this method simplifies the error analysis procedure. Additionally, the influence coefficient provides an indication of the impact of the error source on the final measurement result. This method, however is still considered to be an over estimate of the measurement uncertainty due to the assumption of the probabilities of the errors occurring equally and simultaneously [79], [80], [81]. An improvement to the WCEE technique is proposed in the next section.

9.3.7 Realistic Error Estimation (REE)

Observing that the MEE and WCEE techniques provide an unrealistic over estimation of the effects errors associated with the input variables, the realistic error estimation (REE) technique is introduced. The general derivation of the governing equation for the REE is similar to that of the WCEE technique and is therefore not presented. The resulting absolute and relative error in the output variable can be expressed in equation 9.10 [80].

$$\varepsilon_y = \sqrt{\sum_{i=1}^{n} (I_{x_i} \varepsilon_{x_i})^2 + \frac{1}{y^2} \sum_{j=1}^{m} (W_{z_j} z_j)^2} \qquad (2.34)$$

Based on the above, the effects of the individual instrumentation errors are discriminately accounted for in relation to its associated influence coefficient by quadrature addition [81]. Thus, the overall measurement error is a more realistic reflection of the errors that occur in measurement systems.

9.4 Methodology for Error Analysis on Experimental Data

Since the MEE is considered to be an extreme over estimation and the least likely to occur in practice, it is not included in the analysis. Therefore, the results for the error analysis techniques presented here will consist of the WCEE and REE methods.

The experimental data obtained from the laboratory experiments were fed into a MATLAB motor efficiency determination program and the relative WCEE and REE errors were obtained. Figure 9.2 shows the overall error analysis determination procedure.

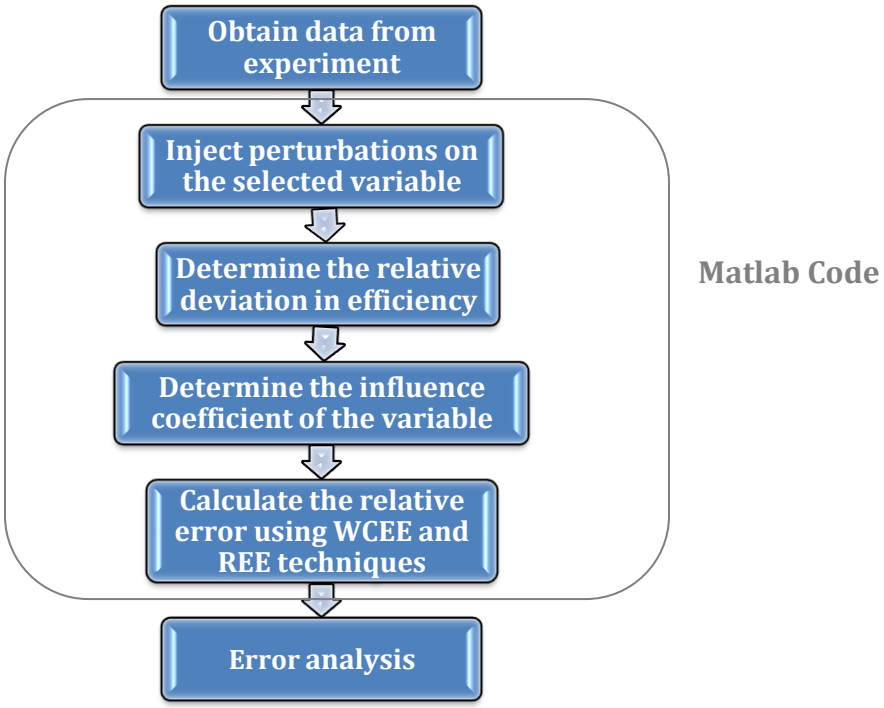

Figure 9.2: Overall error analysis procedure

In complex systems, such as motor testing, it is difficult to obtain the expressions of the derivatives found in equation 9.7 [80]. Therefore, to determine the influence coefficients of each input variable (voltage, current etc), small perturbations were injected onto of the collected data. It is assumed that variables such as voltage, current, torque, speed and resistance, contain small errors [80] and hence perturbations of -5% to +5% were implemented. For the case of the no load loss and stray load loss component used in the NAGT, they are assumed to have large errors and perturbations ranging from -100% to +100% were used [80]. The relative deviations in the efficiency were recorded for each perturbation and the corresponding influence coefficient was obtained by finding their ratio as shown in equation 9.7. As mentioned, the changes in the output efficiency are assumed to be linearly related to the small changes in the input variable. Therefore, a

straight line regression implemented to determine the relationship of the aforementioned changes. The gradient of the straight line equation represents the influence coefficient.

Once the influence coefficients were obtained, the relative errors for the WCEE and REE estimation techniques were calculated using equations 9.10 and 9.12 respectively. By multiplying the influence coefficient with the relative error in instrumentation, the relative significance of the input variable can be obtained. This permits the use of a ranking system in which these variable can be placed with respect to each other.

The error analysis process was applied to each of the motors tested and the results are presented in the following section.

9.5 Results and Discussion

The error analysis of the experimental results is presented in the following sections. The analysis was performed on the test results obtained from each of the test methods, namely the IEC Std 34-2-1, the direct and the NAGT methods.

The various instruments used in this thesis were presented in Chapter 7. As indicated their accuracy levels fall within the limits set by the IEC Std 34-2-1. However, for the purpose of error analysis conducted in this thesis, the maximum tolerances of relative errors set by the standard is used in order to reflect the worst case instrument error associated with the IEC Std 34-2-1 and direct methods. The maximum relative instrumentation tolerances set by the IEC Std 34-2-1 were presented in Chapter 2. In contrast, the relative instrumentation errors for the NAGT method take into account the stator resistance estimation circuit, the accelerometer, the current LEM modules and the voltage probes. The relative instrument errors associated with stator resistance circuit and accelerometer represents the worst case error obtained between the estimated and measured results of all three motors. Similarly, the relative errors used for the no load and stray load loss components were obtained by the worst case error found between the calculated and estimated values.

The influence coefficient for all the variables of the 11kW motor at rated load is shown in the Appendix. The corresponding results for the 15kW and 7.5kW motors show similar trends and are therefore omitted.

9.5.1 11kW Motor Results

The sources of error and their corresponding influence coefficients for the IEC Std 34-2-1 applied to the 11kW motor under rated conditions is shown in Table 9.1. Based on the aforementioned error analysis techniques, the relative WCEE and REE errors are also presented.

Table 9.1 Instrumental error for the 11kW motor using the IEC Std 34-2-1

Error Source	Relative Error [%]	Absolute Influence Coefficient	WCEE [%]	REE [%]	Rank
Shaft Torque	±0.2	0.521	±0.10420	±0.0108576	1
Input Power	±0.2	0.460	±0.09200	±0.0084640	2
Rotor Speed	±0.05	1.013	±0.05065	±0.0025654	3
Input Current	±0.2	0.005	±0.00100	±0.0000010	4
Stator Resistance	±0.2	0.004	±0.00080	±0.0000006	5
Input Voltage	±0.2	0.003	±0.00060	±0.0000004	6
Total			**±0.249**	**±0.148**	

According to the relative WCEE and REE results, the source of error can be ranked in relation to each other. As depicted, the major source of error contribution is due to the errors associated with the shaft torque. In contrast, the input voltage is the least contributing error source in the overall efficiency measurement system. However, considering, the influence coefficients, it can be seen that the rotor speed is by far the most influential component in efficiency determination. Despite this, it is only ranked in third place in terms of percentage error in terms of the WCEE and REE technique. This is due to the multiplication process contained within the WCEE and REE techniques. Therefore, due

to the higher accuracy levels of the tachometer, its multiplicative effect on the influence coefficient causes its contribution to the WCEE and REE values to be reduced.

The overall errors obtained from the contributions of all the error sources are ±0.249% for the WCEE technique and ±0.148% for the REE technique. As expected the REE represents smaller tolerances of error and hence reflects errors associated with the measurement process more realistically.

The direct method only requires the measurement of shaft torque, rotor speed and input power to calculate the motor's efficiency. The instrumental error for the direct method is indicated in Table 9.2 below.

Table 9.2 Instrumental error for the 11kW motor using the direct method

Error Source	Relative Error [%]	Absolute Influence Coefficient	WCEE [%]	REE [%]	Rank
Input Power	±0.2	1.001	±0.2	±0.04	1
Shaft Torque	±0.2	1	±0.2	±0.04	2
Rotor Speed	±0.05	1	±0.05	±0.003	3
Total			**±0.450**	**±0.287**	

According to the results shown above, the influence coefficients show that the contributions of each measurand are equal. Furthermore, it indicated that a 1% error in the measurand proportionally translates to a 1% error in efficiency. This can be explained by considering that the efficiency is equal to the ratio of the product of torque and speed to the input power, where each variable is measured independently of each other. For example, a small error injected onto the torque measurement is proportional to the error in efficiency with a proportionality constant equal to the ratio of rotor speed and input power. Since the changes in torque do not affect other variables, the proportionality constant remains unchanged irrespective of the perturbations placed on the torque measurement. This concept can also be applied to the other parameters. The overall WCEE and REE errors are ±0.450% and ±0.287% respectively.

The NAGT method contains many sources of errors due to the inherent nature of the assumptions and empirical estimations it is associated with. The effects of instrumentation error for the 11kW motor at rated conditions can be seen in Table 9.3 below.

Table 9.3 Instrumental error for the 11kW motor using the NAGT method

Error Source	Relative Error [%]	Absolute Influence Coefficient	WCEE [%]	REE [%]	Rank
Stray Load Loss	±26.164	0.023	±0.6018	±0.3621	1
Estimated Stator Resistance	±3.570	0.070	±0.2499	±0.0625	2
Input Voltage	±3.000	0.070	±0.2100	±0.0441	3
Estimated Rotor Speed	±0.160	1.064	±0.1702	±0.0290	4
Input Current	±0.650	0.070	±0.0455	±0.0021	5
No Load Loss	±0.367	0.041	±0.0150	±0.0002	6
Total			**±1.292**	**±0.707**	

The table above indicates a relative error of ±1.292% and ± 0.707% for the WCEE and REE techniques respectively. As can be seen, the most dominant error source is due to the estimation of stray load loss. Thereafter, the contribution the influence of stator resistance error is ranked in second place. This is followed by the input voltage and estimated rotor speed. The contributions of the estimated no load loss is ranked in the lowest positions of the rank list.

Consideration of the influence coefficient shows that the estimated speed contributes more than ten times in comparison to the other parameters. As in the case of the IEC Std 34-2-1 and the direct method results, the accuracy level of the instrumentation affects the overall contribution of the parameter to the final value of WCEE and REE. The overall error associated with the NAGT method for the WCEE and REE techniques is ±1.292% and ±0.707% respectively.

In summary, the overall WCEE and REE results for each of the efficiency determination methods are shown in Table 9.4.

Table 9.4 Overall WCEE and REE results for each method

	WCEE [%]	REE [%]
IEC Std 34-2-1	±0.249	±0.148
Direct Method	±0.450	±0.287
NAGT Method	±1.292	±0.707

Based on the above, the NAGT method contains a higher degree of instrumentation errors i.e. approximately 5.2 times more than the IEC Std 34-2-1. Since the IEC Std 34-2-1 indirect method is considered to be highly intrusive, it suggests that a compromise between accuracy and intrusiveness is inevitable when selecting a test procedure for determining efficiency.

Comparison of results between the IEC Std 34-2-1 and the direct method indicates that the manner in which the efficiency is calculated contributes to the value of WCEE and REE. Despite the fact the same instruments were used in each method (and hence same instrument tolerances), the WCEE and REE values were higher for the direct method in comparison to the IEC Std 34-2-1 values. This was further emphasised by the contribution of errors associated with each measurable parameter, which is affected by the influence coefficients. In the direct method efficiency equation, the influence of errors in the measurable parameters (torque, speed and input power) have the same contributing effect on the overall efficiency due to the linear relationship between the parameter and the efficiency producing similar influence coefficients. This is not the case for the IEC Std 34-2-1 as the governing separation of loss equation reflects a more complicated relationship between the individual measurable parameters and the overall efficiency. The lower values of WCEE and REE for the IEC Std 34-2-1 further emphasises that the method for efficiency determination is more accurate than that of the direct method.

Additionally, the choice of instrumentation plays a vital role in its contribution to the overall WCEE and REE results. Since the relative instrumentation error has a multiplicative effect on the influence coefficient, special attention should be given to the parameters with

larger influence coefficients. In particular, investing in instruments with higher accuracy levels used to measure speed, torque and input power will significantly reduce the overall WCEE and REE results.

To validate the above, the requirement for instrumentation accuracies for the respective parameters, in accordance with the IEC Std 34-2-1, was placed on the NAGT method. The results at rated loading conditions are shown in Table 9.5.

Table 9.5 Effects of IEC Std 34-2-1 relative instrumental errors on the NAGT method

Error Source	Relative Error [%]	Absolute Influence Coefficient	WCEE [%]	REE [%]	Rank
Stray Load Loss	±26.164	0.023	±0.6018	±0.3621	1
Estimated Stator Resistance	±0.2	0.070	±0.0140	±0.0002	4
Input Voltage	±0.2	0.070	±0.0140	±0.0002	4
Estimated Rotor Speed	±0.05	1.064	±0.0532	±0.0028	2
Input Current	±0.2	0.070	±0.0140	±0.0002	3
No Load Loss	±0.367	0.041	±0.0150	±0.0002	2
Total			**±0.7120**	**±0.6048**	

As expected, the effects of introducing lower tolerances on the relative instrument errors, reduce the WCEE and REE values. For the case above, the WCEE and REE values were improved to ±0.712% and ±0.6% respectively. Despite the improvement the instrument errors associated with the NAGT method are still higher than those obtained from the IEC Std 34-2-1 due to the estimated SLL and no load loss components

Further investigation of the effect of loading on the values of WCEE and REE was conducted. The results showing the variation of WCEE and REE with load for each of the methods for the 11kW motor is depicted in Table 9.6.

Table 9.6 Variation of WCEE and REE with load for the 11kW motor

	IEC Std 34-2-1		Direct Method		NAGT Method	
Load [%]	**WCEE [%]**	**REE [%]**	**WCEE [%]**	**REE [%]**	**WCEE [%]**	**REE [%]**
150	±0.3644	±0.2275	±0.4502	±0.2874	±1.5250	±0.7990
125	±0.3051	±0.1860	±0.4502	±0.2874	±1.3795	±0.7351
100	±0.2493	±0.1479	±0.4502	±0.2874	±1.2925	±0.7071
75	±0.1915	±0.1108	±0.4502	±0.2874	±1.1443	±0.6537
50	±0.1827	±0.1189	±0.4502	±0.2874	±1.1136	±0.6431
25	±0.1052	±0.0631	±0.4502	±0.2874	±1.1786	±0.6595

For the case of the IEC Std 34-2-1 and the NAGT, the WCEE and REE errors show a decrease in values with a decrease in load. Since the instrumentation is the same for each load, the variation indicates that the influence coefficients vary according to the load. This is due to the progressive increase in magnitude of power, current, resistance and torque associated with the increase in load. In contrast, there is no variation of the WCEE and REE results with load for the direct method. This can be attributed to the linearity and proportionality of the changes in efficiency with torque, speed or input power, as previously mentioned.

In order to validate this, a comparison of the absolute influence coefficients for the 100% and 25% loading conditions was performed. The respective coefficient values are shown in Table 9.7.

Table 9.7 Comparison of influence coefficients at 100% and 25% load

Error Source	**Absolute Influence Coefficient**	
	100 % Load	**25 % Load**
Shaft Torque	0.521	0.124
Input Power	0.460	0.128
Rotor Speed	1.013	1.04
Input Current	0.005	0.007
Stator Resistance	0.004	0.0001
Input Voltage	0.003	0.007

As can be seen in Table 9.7, there is a large discrepancy in influence coefficient values for the shaft torque and input power under different loading conditions. The value of the influence coefficients for shaft torque and input power are approximately 4.2 and 3.59 times larger for 100% load condition in comparison to the values at 25% load. Further investigation of this observation was conducted based on the torque component. In the IEC Std 34-2-1 segregation of loss method, torque values are only used for determining the SLLs. The proportion of SLLs, relative to the input power, obtained at the higher load conditions are greater than the proportions obtained during lower loading conditions. In particular, the proportion of SLLs at full load was 4.6 times larger than at 25% load. This greater proportion can be expected since the calculation of SLL, according to the IEC Std 34-2-1, has a linear relationship with the square of the torque. Notably the influence factor of the torque component at full load is 4.2 times larger than at 25% load. These observations indicate that as the ratio of losses to input power varies over load, so does the influence coefficient of the measuring variable to which the loss is associated, hence changing the overall error.

The upper and lower efficiency limits due to the errors in instrumentation can be compared with the 'true' efficiency values. Figure 9.3 and Figure 9.4 shows this relationship for the WCEE and REE techniques respectively for each of the methods and its variation over the load range.

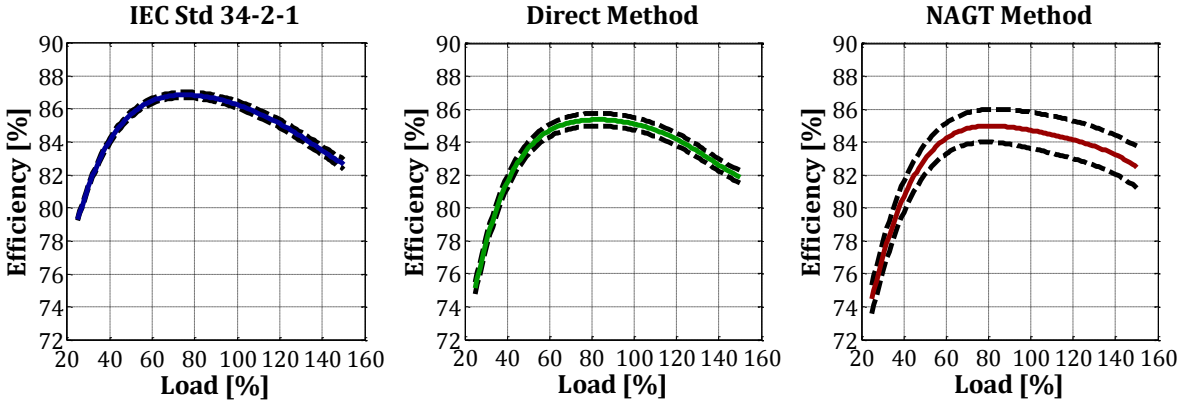

Figure 9.3:Variation of instrument errors with load for the WCEE technique for the 11kW motor

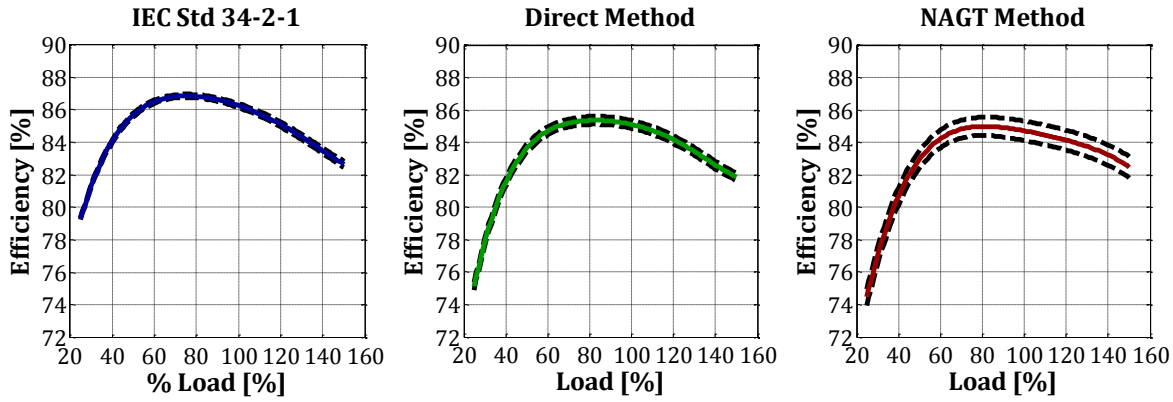

Figure 9.4: Variation of instrument errors with load for the REE technique for the 11kW motor

As shown, the possible errors in determining the efficiency at the 25 % load are relatively small. However, at the higher loading points the relative errors becomes larger. For the case of the WCEE technique, the maximum possible interval in which the efficiency lies, at 150 % load, is 0.72%, 0.9% and 3.05% for the IEC Std 34-2-1, the direct method and the NAGT method respectively. For the case of the REE technique, the uncertainty of each of the methods at 150% load is 0.44%, 0.574% and 1.598% respectively. As expected, the values for the REE technique are lower than those obtained from the WCEE since the REE values represent a more realistic indication of the errors associated with instrumentation.

The error analysis discussed above was conducted on a set of data obtained for the 15kW and 7.5kW motor and is presented in the following sections for completeness.

9.5.2 15kW Motor Results

The sources of error and their corresponding influence coefficients for the IEC Std 34-2-1 applied to the 15kW motor under rated conditions is shown in Table 9.8. The relative WCEE and REE errors are also presented.

Table 9.8 Instrumental error for the 15kW motor using the IEC Std 34-2-1

Error Source	Relative Error [%]	Absolute Influence Coefficient	WCEE [%]	REE [%]	Rank
Shaft Torque	±0.2	0.620	±0.1239681	±0.0153681	1
Input Power	±0.2	0.562	±0.1124450	±0.0126439	2
Rotor Speed	±0.05	1.008	±0.0504234	±0.0025425	3
Input Voltage	±0.2	0.002	±0.0004214	±0.0000002	4
Stator Resistance	±0.2	0.002	±0.0003969	±0.0000002	5
Input Current	±0.2	0.002	±0.0003728	±0.0000001	6
Total			**±0.288**	**±0.175**	

Based on the above, the ranking of the individual parameter is similar to that indicated for the 11kW motor, however values are for the WCEE and REE are higher.

The impact of instrumental errors on the direct method for the 15kW motor is presented in Table 9.9 below.

Table 9.9 Instrumental error for the 15kW motor using the direct method

Error Source	Relative Error [%]	Absolute Influence Coefficient	WCEE [%]	REE [%]	Rank
Input Power	±0.2	1.002	±0.2	±0.040	1
Shaft Torque	±0.2	1.000	±0.2	±0.040	2
Rotor Speed	±0.05	1.000	±0.05	±0.003	3
Total			**±0.450**	**±0.287**	

The results reflected above are identical to the 11kW and indicate that the errors associated with measurement, when using the direct method, is not dependant on the size of the motor. This can be attributed to the same linear relationship between the efficiency and individual error in parameters.

The effect of instrumentation errors on the NAGT method for the 15kW motor is shown in Table 9.10 below.

Table 9.10 Instrumental error for the 15kW motor using the NAGT method

Error Source	Relative Error [%]	Absolute Influence Coefficient	WCEE [%]	REE [%]	Rank
Stray Load Loss	±26.164	0.023	±0.60201	±0.3624204	1
Estimated Stator Resistance	±3.570	0.058	±0.20611	±0.0424826	2
Input Voltage	±3.000	0.058	±0.17351	±0.0301068	3
Estimated Rotor Speed	±0.160	1.064	±0.17019	±0.0289651	4
Input Current	±0.650	0.058	±0.03753	±0.0014083	5
No Load Loss	±0.367	0.041	±0.01493	±0.0002230	6
Total			**±1.204**	**±0.682**	

In comparison to the 11kW motors, the values of WCEE and REE are slightly lower than the 15kW motor. This can be attributed to different influence coefficient associated with each motor. As previously mentioned, the influence coefficients vary according to motor size due to the variation in proportionality of the loss components in relation to the input power. The variation of WCEE and REE for different loading conditions is presented in Table 9.11.

Table 9.11 Variation of WCEE and REE with load for the 15kW motor

Load [%]	IEC Std 34-2-1		Direct Method		NAGT Method	
	WCEE [%]	REE [%]	WCEE [%]	REE [%]	WCEE [%]	REE [%]
125	±0.355	±0.221	±0.450	±0.287	±1.319	±0.725
100	±0.288	±0.175	±0.450	±0.287	±1.204	±0.682
75	±0.220	±0.130	±0.450	±0.287	±1.105	±0.649
50	±0.149	±0.087	±0.450	±0.287	±1.047	±0.631
25	±0.099	±0.061	±0.450	±0.287	±1.062	±0.632

The upper and lower efficiency limits due to the errors in instrumentation can be compared with the 'true' efficiency values. Figure 9.5 and Figure 9.6 shows this relationship for the WCEE and REE techniques respectively for each of the methods

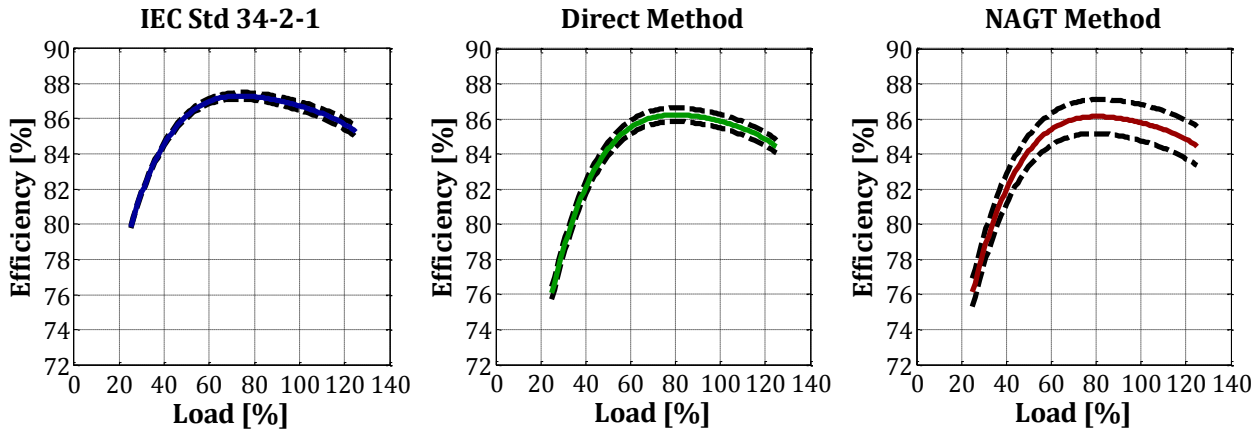

Figure 9.5:Variation of instrument errors with load for the WCEE technique for the 15kW motor

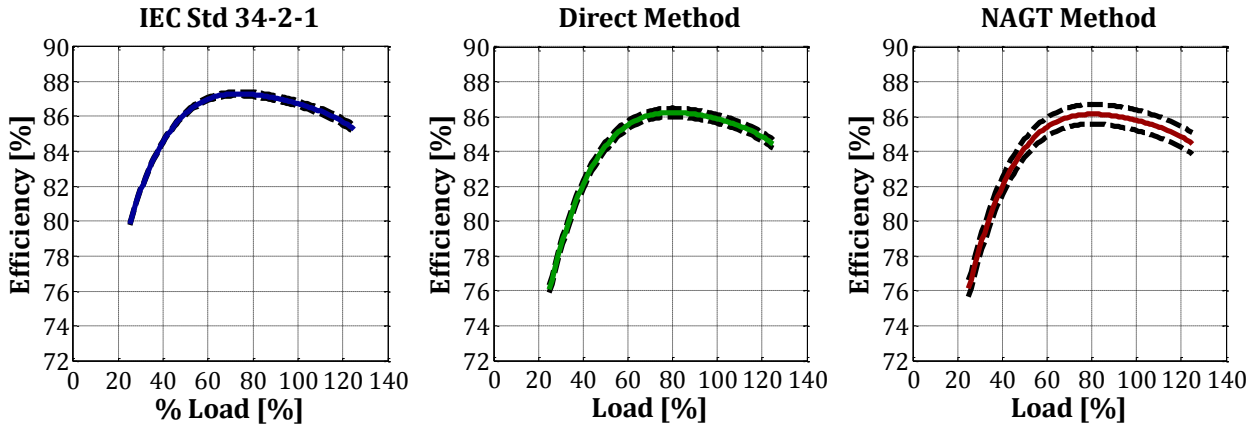

Figure 9.6:Variation of instrument errors with load for the REE technique for the 15kW motor

The results shown above show similar trends to that of the 11kW motor. For the WCEE, the For the case of the WCEE technique, the possible interval in which the 'true' efficiency lies at 125 % load is 0.71%, 0.9% and 2.638 % for the IEC Std 34-2-1, the direct method and the NAGT method respectively. For the case of the REE technique, the uncertainty of each of the methods at 125% load is 0.44%, 0.574% and 1.45% respectively.

9.5.3 7.5kW Motor Results

The results for the instrument error of the 7.5kW motor for the IEC Std 34-2-1 is shown in Table 9.12

Table 9.12 Instrumental error for the 7.5kW motor using the IEC Std 34-2-1

Error Source	Relative Error [%]	Absolute Influence Coefficient	WCEE [%]	REE [%]	Rank
Shaft Torque	±0.2	0.515	±0.1029566	±0.0106001	1
Input Power	±0.2	0.475	±0.0950040	±0.0090258	2
Rotor Speed	±0.05	1.012	±0.0505845	±0.0025588	3
Input Current	±0.2	0.007	±0.0014058	±0.0000020	4
Stator Resistance	±0.2	0.006	±0.0011134	±0.0000012	5
Input Voltage	±0.2	0.004	±0.0008216	±0.0000007	6
Total			**±0.252**	**±0.149**	

The results depicted above show similar trends to that seen in the 11kW results. However, the overall WCEE and REE are slightly higher.

The instrumental error for the 7.5 W motor for the case of the direct method is presented in Table 9.13.

Table 9.13 Instrumental error for the 7.5kW motor using the direct method

Error Source	Relative Error [%]	Absolute Influence Coefficient	WCEE [%]	REE [%]	Rank
Input Power	±0.20	1.002	±0.2	±0.0401	1
Shaft Torque	±0.20	1.000	±0.2	±0.0400	2
Rotor Speed	±0.05	1.000	±0.05	±0.0025	3
Total			**±0.450**	**±0.287**	

As expected, the final values of WCEE and REE are identical to the values obtained for the 11kW and 15kW for reasons previously mentioned.

The instrument errors for the 7.5kW motor for the NAGT method is shown in Table 9.14 below.

Table 9.14 Instrumental error for the 7.5 kW motor using the NAGT method

Error Source	Relative Error [%]	Absolute Influence Coefficient	WCEE [%]	REE [%]	Rank
Stray Load Loss	±26.16	0.024	±0.61652	±0.3800917	1
Estimated Stator Resistance	±3.57	0.084	±0.30059	±0.0903524	2
Input Voltage	±3.00	0.084	±0.25304	±0.0640315	3
Estimated Rotor Speed	±0.16	1.065	±0.17044	±0.0290487	4
Input Current	±0.65	0.084	±0.05473	±0.0029952	5
No Load Loss	±0.37	0.042	±0.01529	±0.0002338	6
Total			**±1.41**	**±0.753**	

As can be see, the relative WCEE and REE values for the NAGT method is 1.41% and 0.753%. Respectively

The variation of WCEE and REE with load for the 7.5 kW motor is presented below.

Table 9.15 Variation of WCEE and REE with load for the 7.5kW motor

Load [%]	IEC Std 34-2-1		Direct Method		NAGT Method	
	WCEE	REE	WCEE	REE	WCEE	REE
150	±0.3644	±0.2273	±0.4504	±0.2875	±1.7488	±0.8989
125	±0.3067	±0.1867	±0.4504	±0.2875	±1.5855	±0.8251
100	±0.2519	±0.1490	±0.4504	±0.2875	±1.4106	±0.7528
75	±0.1977	±0.1135	±0.4504	±0.2875	±1.2762	±0.7013
50	±0.1366	±0.0787	±0.4504	±0.2875	±1.1935	±0.6728
25	±0.0889	±0.0576	±0.4504	±0.2875	±1.2072	±0.6754

Based on the above WCEE and REE values the upper and lower bounds of errors in efficiency can be seen in Figure 9.7 and Figure 9.8 below.

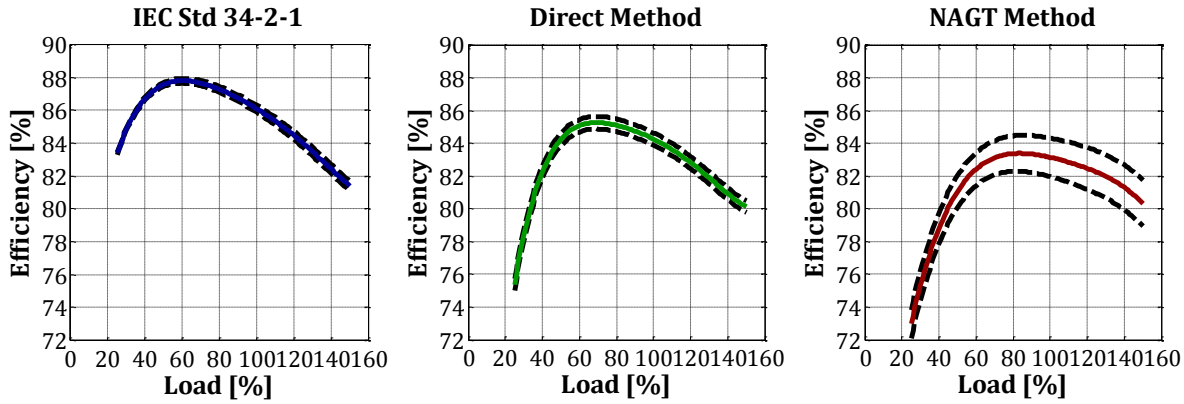

Figure 9.7:Variation of instrument errors with load for the WCEE technique for the 7.5 kW motor

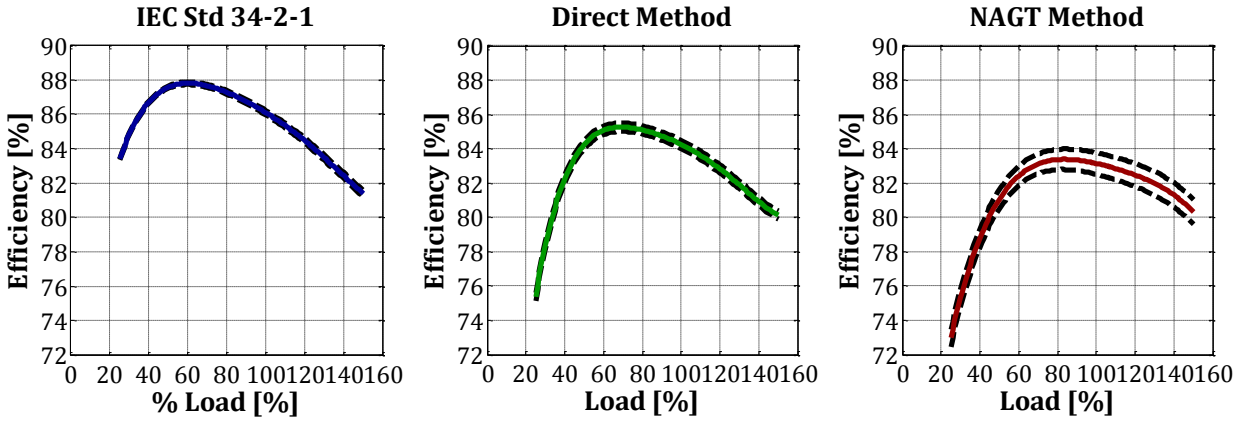

Figure 9.8:Variation of instrument errors with load for the REE technique for the 7.5kW motor

The maximum range in which the 'true' efficiency can exist occurs at 150% and is 0.72%, 0.9% and 3.49% for the IEC Std 34-2-1, the direct method and the NAGT method respectively using the WCEE technique. For the case of REE, the maximum interval in which efficiency can be seen at 150% load is 0.44%, 0.57% and 1.79% respectively.

9.6 Concluding Remarks

This chapter presented the error analysis of efficiency determination for the IEC Std 34-2-1, the direct method and the NAGT method on the 11kW, 15kW and 7.5kW motors.

The focus of the error analysis was aimed at investigating the effects of instrumentation errors in parameter measurements on the efficiency value of the motor. In order to conduct this investigation, WCEE and REE techniques were employed. These techniques are advantageous in that they cater for the effects of errors in individual parameters independently of each other. This is achieved by the inclusion of an influence coefficient. The error associated with the REE technique is smaller than that of the WCEE and provides a more realistic representation of the errors associated with measured data based on the effects of instrument errors.

The results presented confirm that the IEC Std 34-2-1 method is more accurate than the direct and NAGT methods. The IEC Std 34-2-1 method is the most intrusive (due to the requirements of no load and variable load test) yet provides the highest accuracy. This emphasises the trade off between accuracy and level of intrusion when considering efficiency testing procedures.

For the case of the 11kW motor at rated load, the associated WCEE and REE errors of the IEC Std 34-2-1 and NAGT method were summarised in Table 9.4. As shown, the uncertainties of the NAGT method are approximately five times higher than the IEC Std 34-2-1. Since the purpose of efficiency estimation is merely to provide an indication of the operating efficiency, a ±0.7% uncertainty does not significantly impact the operator's judgment of the status of the machine. For example, if the true value of a motor's efficiency is 80%, an uncertainty of ±0.7% indicates that the machine is between 80.85% and 79.15% efficient. This variance is, therefore, small enough to make a reasonable deduction whether the machine operating with an appropriate efficiency level. Therefore, decisions as to

whether to replace or repair the machine is not drastically affected by the uncertainty of 0.7% but rather the efficiency range the machine is operating in.

However, the effects of tolerance on instrumentation play an important role in the overall WCEE and REE. This was demonstrated by the improvement in WCEE and REE values when incorporating the stricter instrument tolerance, according to the IEC Std 34-2-1, on the parameters used in the NAGT method. This emphasises the importance of accurate and calibrated in efficiency testing. Therefore, special attention in instrumentation should be given to parameters showing higher influence coefficients in order to reduce the overall WCEE and REE values.

Lastly, it was observed that the WCEE and REE values vary with changes in load. This was attributed the disparity of the influence coefficients with varying load conditions. This was due to the variation of the loss distribution, in relation to the input power over the loading range. Based on this it was established that the values of WCEE and REE become larger with an increase in load. Additionally, the values of WCEE and REE for the IEC Std 34-2-1 and the NAGT method showed variation in relation to the size of the motors.

CHAPTER TEN

CONCLUSIONS AND RECOMMENDATIONS

This chapter present the conclusion and recommendations based on the experimental results and work carried out in this thesis.

10.1 Conclusions

This thesis has proposed a non-intrusive efficiency estimation method for induction machines. The main focus was based on the investigation, implementation and analysis of the NAGT method. This method is based on the air gap torque method however it combines various non-intrusive methods to estimate the parameters that are traditionally measured in a highly intrusive manner. This includes the stator winding resistance, rotor speed, no load and stray load losses.

Efficiency tests were conducted on three different motors with power ratings of 7.5kW, 11kW and 15kW in the Machine's Laboratory at the University of Cape Town. The test conducted followed the methodology based on the IEC Std 34-2-1, the direct method and the proposed NAGT method.

Based on the results and error analysis of the experiments presented, the following conclusions can be made.

10.1.1 Stator Winding Resistance Estimation

The stator winding resistance of an induction machine is traditionally determined by performing an unpowered test which involves shutting down the machine and ensuring the rotor is at standstill measuring the stator winding resistance. This method is considered to be highly intrusive and hence unsatisfactory for the NAGT method. Therefore, a low intrusive means for stator winding resistance determination was required.

The stator resistance estimation technique adopted for this thesis was based on a DC signal injection technique proposed in [43]. The technique is based upon the asymmetrical resistance created by the 'on'-'off' switching of a MOSFET connected in parallel to an external resistor. The DC voltage and current components associated with this switching was used to calculate the stator winding resistance. In order to make the resistance

estimation as accurate as possible, compensation for the DC offset components associated with the mains supply and the cable resistance was made before the final value of stator resistance was obtained.

The above method, however, is associated with the increase in stator unbalance, additional power loss and torque pulsations. In order to avoid this during efficiency testing, the use of two switches allowed for the circuit to be switched in only when the estimation of resistance is requires, thereafter the additional circuitry was bypassed. This eliminated the negative impact of unbalance, torque pulsations and additional power loss during efficiency testing.

Based on the implementation and tests conducted, it can be concluded that the stator winding resistance can be estimated using DC signal injection. The results for stator resistance estimation obtained from experimentation proved to be an over estimate for the case of all three motors tested. The accuracy of the estimated resistance was within 3.57% in relation to the expected resistance values. The impact of this stator winding resistance estimation on motor efficiency, using the NAGT method, is to affect the value of air gap torque obtained using equation 6.5. An overestimation of R_s was shown to decrease the air gap torque value and vice versa. This subsequently affects the overall efficiency value obtained using equation 6.11. Therefore, it can be concluded that the accuracy of the signal injection circuit needs to be improved in order to attain an accurate efficiency estimation value.

In terms of field applications, the installation of the resistance estimation circuit can be considered as intrusive. However, once the circuit has been installed it can thereafter be regarded as non-intrusive. To avoid any disruption to the motor during operation, the circuit can be installed simultaneously with scheduled maintenance procedures. This does, however, suggest that the resistance estimation circuit is not portable but rather a dedicated device.

10.1.2 Rotor Speed Estimation

The shaft rotor speed is yet another parameter required for many motor efficiency determination methods. Traditionally, the rotor speed is obtained by the use of shaft mounted speed encoders or highly advanced tachometers. These instruments require direct access to the motor's shaft yet, in many field applications, the motor's shaft may not be easily accessible. Therefore, the NAGT method required that the rotor speed is detected in a non-intrusive manner.

To achieve this, the rotor speed was detected by exploitation of the inevitable mechanical vibration associated with a motor in operation. The process of speed detection incorporated the use of an accelerometer to measure the motor's vibration therefore applying a signal processing technique (FFT) to the acquired signal. Observing the frequency spectrum in the range of 0-30Hz, the rotational frequency components were detected. This frequency component was then translated to rotational speed.

Based on the results provided, it can be concluded that the rotor speed can be detected in a non-intrusive manner with a high level of accuracy (within 0.16%.). The rotational frequency component proved to be the most dominant component in the low frequency range which made its detection unquestionable. This was evident under all loading conditions. Therefore, it can be concluded that the rotor speed can be estimated non-intrusively, reliably and accurately using machine vibration spectrum analysis. The high accuracy levels attained using the vibration spectrum analysis suggest that it does not significantly degrade the value of efficiency obtained using the NAGT method.

Due to the use of spectrum analysis techniques, the frequency resolution plays an important role in the accuracy of speed diction. As was shown, by increasing the sample time, the frequency resolution can be improved from 0.1Hz (10 seconds) to 0.0167Hz (60 seconds). In terms of speed, a 0.1Hz frequency resolution translates to speed detection of within ±6rpm whereas a 0.0167Hz resolution translates to speed detection within ±1rpm. In this thesis the data capturing time was limited to a maximum of 10 seconds due to the

requirements contained in the methodology. Fortunately, this did not impede the accuracy of the speed detection results as all the results indicated are within 2.42 rpm relative to the measured speed.

The speed estimation technique can easily be implemented in field applications. The requirements for speed detection only require access to the outer casing of the motor, an accelerometer and sufficient software to perform the FFT. These requirements can easily be fulfilled both effortlessly and cost effectively.

10.1.3 Loss Estimation

The NAGT method employs empirical calculations in order to determine the no load losses. This eliminates the need to conduct a no-load test which requires that the motors load be removed and that a variable voltage supply be readily available. The total no load loss contribution was empirically estimated to be 3.5% of the rated input power. For the case of the 11kW and 15kW motors this proved to be an underestimation, in relation to the expected values over most of the loading range. In contrast, for the case of the 7.5kW motor it proved to be an overestimate. It was shown that this discrepancy was due to the relative loss distribution, in relation to the input power, which differs according to motor size. The impact of the no load loss estimation affects the overall efficiency. An over estimate in loss translates to an underestimate in overall efficiency estimation, while an under-estimate translates to higher efficiency values. Therefore, it can be concluded that no load loss estimation should be estimated as accurately as possible in order to obtain an accurate estimate of efficiency.

In terms of SLL estimation, an assigned allowance according to the IEC Std 34-2-1 can be used to estimate the SLLs at rated conditions. For the purpose of this thesis the value obtained at rated conditions was employed over the entire loading range. By doing so, these estimated values are not load dependant, which is not the case presented in reality. This proved to be an over estimate in SLLs for the most part of the loading range for all three motors tested. It can therefore be concluded that this is an insufficient means of SLL

estimation. The effects of this over estimate in SLLs are to reduce the overall estimated efficiency values. This suggests that the motor is perceived to be operating at a lower efficiency value, which, in reality may not be the case.

To rectify this, an improved SLL estimation technique was suggested. The improved estimation technique incorporated a linear regression technique to the plot of SLL against the square of the torque. This process provides a straight line passing through the origin and the value of SLL obtained empirically at rated conditions. Based on this, the 'improved' values of SLLs can be obtained at any load condition. Therefore, a more realistic approach to SLL estimation can be achieved since the SLL values are now load dependant. Despite remaining an overestimate in comparison to the of the IEC Std 34-2-1 values this method of SLL is superior than using a fixed value for all load conditions.

10.1.4 Non-Intrusive Efficiency Estimation

Initially the air gap torque equation used in NAGT method was questioned, due to the discrepancies in literature, as to whether it accounts for the core loss component. This investigation was resolved by simulation and it was concluded that the air gap torque equation does not account for the core loss component and therefore it needs to be included in the final efficiency equation. This indicates that the air gap power, as defined by the air gap torque equation, is merely the input power less the stator copper loss. This suggests that the computation of the air gap torque can be avoided by simply calculating the air gap power i.e. input power (using instantaneous currents and voltages) and subtracting the stator resistance loss (obtained by using stator winding resistance estimation).

It can be concluded that the air gap torque method can be used to determine the efficiency of a motor non-intrusively by measuring the line voltages and currents and adopting non-intrusive stator winding resistance and rotor speed estimation techniques. This is referred to as the non-intrusive air gap torque (NAGT) method. Furthermore, the values of no load

and stray load losses can be calculated empirically. However, in general, the efficiencies obtained from the NAGT method were lower than that obtained using the IEC Std 34-2-1 and direct method. In particular, the deviations in efficiencies at the lower loading points were substantially larger than at the higher loading range indicating that the performance of the method degrades at lower load conditions. This discrepancy was investigated by introducing the values of the estimated components independently of the others. Based on this, it was concluded that the effect of SLL estimation was the main contributor to the deviation in efficiency, particularly at the lower loading points. An 'improved' estimation of SLL was implemented to examine its effect on efficiency. This showed improvements in efficiencies to within 2% of the values obtained from the IEC Std 34-2-1. Based on the above it can be concluded that the NAGT method can be used to determine the efficiency under any load condition. However, if the accuracy is to be improved, revisions of the accuracy of the stator resistance, rotor speed and loss estimation need to be conducted. The efficiency trends of the NAGT method showed lower efficiency values in relation to the IEC Std 34-2-1 and direct method results for all three of the motors tested. This suggests that the NAGT method can be applied to a wide range of induction motors and is not restricted by the motor's size.

The air gap torque method can be used in field applications, to determine the efficiency of an induction machine non-intrusively. Furthermore, the technique is easily implemented in industrial applications and its purpose is relevant in a South African context. Under these conditions however, the efficiency is obtained at one point, i.e. the operating point. Additionally, the load of the machine, at this operating point, remains unknown and therefore there is no indication of where along the motor's efficiency curve the motor is operating. For example, the machine could be operating with a high efficiency but under low load conditions. Therefore, in order to make the NAGT estimation more accurate, the load condition must also be known. To resolve this, the value of current can be used to provide an indication of the loading conditions. Since the stator current is related to the loading of the machine, it can be compared to the rated current (obtained from the motor's nameplate) in order to provide an indication of whether the machine is operating above or below rated load

10.1.5 Effects of Voltage Unbalance on Motor Efficiency

The effects of magnitude voltage unbalance on the efficiency and its detection using the NAGT was investigated. Based on the results presented, it can be concluded that the effect of voltage unbalance is to reduce the overall motor efficiency. This can be attributed to the increase in the machine's operating temperature associated with the increase in motor losses.

The results for the NAGT showed that its technique can be used to determine the motor's efficiency during unbalanced conditions since it also varied in accordance to the direct method with changes in unbalanced conditions. The results consistently showed lower efficiency values for all tested machines in comparison to the direct method efficiencies. This is also the case for efficiency values obtained under balanced conditions and therefore suggests that the NAGT method consistently underestimates the machine's efficiency in relation to the direct method.

10.1.6 Error Analysis

The effects of instrumentation errors are known to be the major contributor to sources of errors in the measurement system. This prompted the investigation of the effects of instrument errors on the quoted efficiency of a motor. The techniques used for this analysis was the WCEE and REE techniques. These techniques incorporate the use of an influence coefficient so that the contribution of error due to a parameter is individually assessed. These influence coefficients provide an indication of the degree of contribution an individual parameter has to the overall accuracy of the measurement system.

The results presented indicate that the IEC Std 34-2-1 method is the most accurate in comparison to the direct and NAGT methods. However, due to the fact that this method is the most intrusive of them all, it can be concluded that there is a trade off between accuracy and intrusion, as to be expected.

Additionally, the choice of instrumentation is considered to have a major contribution to the overall WCEE and REE tolerances. In particular, the effect of introducing lower tolerances in instrumentation of the NAGT method was to significantly improve the accuracy levels of the WCEE and REE values. Therefore it can be concluded that it is necessary to employ instrumentation with lower tolerances if accuracy is to be improved. In particular, it can be suggested that parameters containing higher influence coefficients, should be given special attention.

It was also concluded that the associated WCEE and REE values varied according to changes in the machine's loading conditions. This was attributed to the variation of influence coefficient with load, since the instrumentation and its respective relative errors remain unchanged. Furthermore, it can be concluded that the changes in magnitude of the influence coefficient is associated with the level of loss distribution in relation to the input power.

10.2 Recommendations on Further Research

Based on the above conclusions, the following recommendations can be made.

10.2.1 Stator Winding Resistance Estimation

As previously mentioned, the stator resistance showed over estimated values in relation to the expected values. In order to improve this, it is suggested that a higher resistance value for R_{ext} should be employed. As stated in [43], the choice of R_{ext} is dependant on the tolerable levels of torque pulsations. Since, in this thesis, the effects of torque pulsations were eliminated during efficiency testing, it stands to reason that a higher value of R_{ext} can be used. Further investigation should therefore be conducted in order to validate whether an improved stator winding resistance estimate can be achieved. This should be applied for all the motors tested

In addition, the stator resistance estimation circuit should be implemented in all three phases. If the same circuit components are used in each line, the effects of unbalance due to the circuitry can be reduced. Furthermore, the stator winding resistance can be measured in all three phases and an average stator winding resistance be obtained.

10.2.2 Rotor Speed Estimation

The speed detection process in this thesis incorporates the use of signal processing techniques in order to obtain the required rotation frequency component required for speed estimation. This was done by post processing only once the required data was captured.

The methodology used in this thesis can be improved by allowing for an online means of speed detection. This can be achieved by employing a frequency detection algorithm applied to the vibration spectrum, whereby the rotational frequency component is identified. Since the rotational frequency component is dominant and easily detectable at

the low frequency range (<30Hz), a peak detection algorithm will indicate the largest frequency component within this frequency range. Thereafter, the frequency component can be translated into speed and an online speed estimation topology can be established.

One disadvantage of the speed estimation technique is that it requires a minimum data acquisition time of 10 seconds in order to achieve sufficient frequency resolution to ensure successful speed estimation. Considering the high accuracy levels of the estimated speed values obtained using the accelerometer, they can be considered as approximately equal to the measured values obtained using the tachometer. Therefore, under laboratory conditions, the use of the tachometer readings can be used in place of the estimated speed when using the NAGT method. This is to avoid the 10 second delay in data acquisition between two successive loading points when conducting an efficiency test

10.2.3 Loss Estimation

As already mentioned, the improvement of the loss estimation technique should be employed in order to determine the associated loss more accurately in order to achieve an improved means of efficiency estimation

In particular, an improved method of SLL estimation was suggested however further investigation into this should be conducted.

10.2.4 Non-Intrusive Efficiency Estimation

Since many of the parameters required for efficiency estimation in the NAGT method i.e. voltage, current, speed and resistance are also required for condition monitoring, a combination of an efficiency estimation and condition monitoring techniques can be employed. This allows for a multipurpose device that is relevant for motors installed in industry.

In this thesis the trapezoidal method was used to calculate the flux linkage integrals in the air gap torque equation. Due to the high sampling rate (10kHz), the accuracy level of the

trapezoidal deemed sufficient. However, more accurate integration methods, such as Simpsons Rule or Gauss' Rule, should be investigated.

10.2.5 Effects of Voltage Unbalance on Motor Efficiency

In reality, the voltage supply is polluted with voltage unbalance and harmonics with varying degrees and combinations. In this thesis, only the effects of voltage magnitude unbalance were investigated. Since this is not a true reflection of the supply conditions obtained in industry, the effects of other polluted conditions should be reviewed. This includes voltage phase unbalance, voltage variation, magnitude over/under voltage unbalance and harmonics. The success of the NAGT method under these conditions can then be considered

10.2.6 Error Analysis

The main focus of error analysis was aimed at instrument errors. However, other sources of error are known to exist, namely methodological errors and human errors. Therefore, in order to obtain a true reflection of the total error contained in efficiency tested, all sources of errors need to be accounted for.

Additionally, other statistical methods such standard deviation, sample mean, variance and probability distribution should also be incorporated into the error analysis process.

REFERENCES

[1] P.C Sen, *Principles of Electric Machines and Power Electronics*, 2nd ed.: John Wiley and Sons, Inc., 1997.

[2] H. M. Mzungu, A. B, Sebitosi, M. A Khan, "Comparison of Standards for Determining Losses and Efficiency of Three-Phase Induction Motors," in *IEEE PES Power Africa*, July 2007.

[3] E. Romero, L.F. Mantilla S. Corino, "How the Efficiency of an Induction Machine is Measured?," in *International Conference on Renewable Energy and Power Quality (ICREPQ)*, 2008.

[4] B. Reiner, K.Hameyer, R, Belmans, "Comparison of Standards for Determining Efficiency of Three Phase Induction Motors," *IEEE Trans. Energy Conversion*, vol. 14, no. 3, pp. 512-517, September 1999.

[5] A. Boglietti, A. Cavagnino, M. Lazzari, M. Pastorelli, "International Standards for the Induction Motor Efficiency Evaluation: A Critical Analysis of the Stray-Load Loss Determination," *IEEE Trans. on Industry Applications*, vol. 40, no. 5, pp. 1294-1301, September/October 2004.

[6] Electrical Apparatus Service Association. Understanding Energy Efficient Motors. [Online]. https://smtp.cpuaid.com/easa/resources/cgis/displayitem.cgi?category=2&name=Promotional+Material&Item=5

[7] B. Lu, T. Habetler, R. Harley, "A Nonintrusive and In-service Motor Efficiency Estimation Method Using Air-Gap Torque With Considerations of Condtion Monitoring," *IEEE Trans. Industry Applications*, vol. 44, no. 6, pp. 1666-1674, November/ December 2008.

[8] P.G. Cummings, W.D Bowers, W.J. Martiny, "Induction Motor Efficiency Test Methods," *IEEE Trans. on Industry Application*, vol. IA-17, no. 3, pp. 235-272, May/June 1981.

[9] Reliance. AC Motor Efficiency- A guide to Energy Savings-Part 3. [Online].. http://www.reliance.com/prodserv/motgen/b7087_5/b7087_5_3.htm

[10] Bureau of Energy Efficiency. Electric Motors. [Online]. http://www.energymanagertraining.com/GuideBooks/3Ch2.pdf

[11] A.T.de Almeida, F.J.T.E Ferreira, J.F Busch, P,Angers, "Comparative Analysis of IEEE 112-B and IEC 34-2 Efficiency Testing Standards Using Stray Load Losses in Low-Voltage Three-Phase Cage Induction Motors," *IEEE Trans. on Industry Application*, vol. 38, no. 2, pp. 608-614, March/April 2002.

[12] P. Giridhar Kini, R.C. Bansal, R.S Aithal, "Impact of Voltage Unbalance on the Performance of Three-Phase Induction Motor," *South Pacific Journal of Natural Science*, vol. 24, pp. 45-50, 2006.

[13] K.V Vamsi Krishna, "Effects of Unbalanced Voltage on Induction Motor Current and its Operation Performance," Lecon Systems,.

[14] R. Belmans, W. Deprez, O. Gol, "Increasing Induction Motor Drives Efficiency: Understanding the Pitfalls," in *Electotechnical Institute*, Warsaw, 2005, pp. 7-25.

[15] M. Manyage, "EEE4099F Course Notes-Voltage Unbalance," University of Cape Town, 2008.

[16] A. Bonnett, "Understanding Efficiency in Squirrel Cage Induction Motors," *IEEE Trans. Industry Application*, vol. IA-16, no. 4, pp. 476-483, July/August 1980.

[17] B. Lu, T.G Habetler, R.G Harley, "A Survey of Efficiency-Estimation Methods for In-Service Induction Motors," *IEEE Trans. on Industry Applications*, vol. 42, no. 4, pp. 924-933, July/August 2006.

[18] W.Cao, K. Bradley, "Assessing the Impacts of Rewind and Repeated Rewinds on Induction Motors: Is an Opportunity for Re-Designing the Machine Being Wasted?," *IEEE Trans. Industry Application*, vol. 42, no. 4, pp. 958-964, July/ August 2006.

[19] Motor Challenge Fact Sheet. Determining Electric Motor Load and Efficiency. [Online]. http://www1.eere.energy.gov/industry/bestpractices/pdfs/10097517.pdf

[20] J. Custodio. (2007) Pump-Zone. [Online]. http://www.pump-zone.com/motors/motors/the-impact-of-rewinding-on-motor-efficiency.html

[21] B. Gibbon A. Bonnett, "The Result Are In: Motor Repair's Impact on Efficiency," Electrical Apparatus Service Assosiation, 2002.

[22] Cao, W., "Comparison of IEEE 112 and New IEC Standard 60034-2-1," *IEEE Trans. on Energy Conversion*, vol. 24, no. 3, pp. 802-808, 2009.

[23] IEEE Standard 112, IEEE Standard Test Procedure for Polyphase Induction Motors and Generators, 2004.

[24] IEC 60034-2-1, Rotating Electrical Meachines-Part 2-1, 2007, Standard method for determining losses and efficiency from tests (excluding machines for traction vehicles).

[25] SABS-South African Bureau of Standards. (2010) List of Published Standards. [Online]. hhttps://www.sabs.co.za/Business_Units/Standards_SA/Controls/Published_Standards/PS61.PDF

[26] J.S Hsu, J.D Kueck, M.Olszewski, D.A Casada, P.J Otaduy, L.M Tolbert, "Comparision of Induction Motor Field Efficiency Evaluation Methods," *IEEE Trans. on Industry Applications*, vol. 34, no. 1, pp. 117-125, January/February 1998.

[27] J.S Hsu, P.L Sorenson, "Field Assessment of Induction Motor Efficiency Through Air-Gap Torque," Oak Ridge National Laboratory, Tennessee, Conf-960111--3 1995.

[28] J.D Kueck, M. Olszewski, D.A Casada, J.Hsu, P.J Otaduy, L.M. Tolbert, "Assessment of Methods for Estimating Motor Efficiency and Load Under Field Conditions," Oak Ridge National Laboratory, 1996.

[29] J.D Kueck, "Development of a method for estimating motor efficiency and analysing motor condition," in *Pulp and Paper Industry Technical Conference*, Portland, 1998, pp. 67-72.

[30] R. Castillon, J. Oslinger, J Pakacios, "In-Field Induction Motor Efficiency Determination Methods in the Scope of Efficiency-Based Maintenance," Energy Research Group Gien and Energy Research Convergia, Columbia,.

[31] S.B. Lee, T.G Habetler, R.G Harley, D.J. Gritter, "An Evaluation of Model-Based Stator Resistance Estimation for Induction Motor Stator Winding Temperature Monitoring," *IEEE Trans. on Energy Conversion*, vol. 17, no. 1, pp. 7-15, March 2002.

[32] S. Mir, M. Elbuluk, D. Zinger, "PI and Fuzzy Estimators for Tuning the Stator Resistance

in Direct Torque Control of Induction Machines," *IEEE Trans. on Power Electronics*, vol. 13, no. 2, pp. 279-287, March 1998.

[33] E. Akin, H.B Ertan, M.Y Uctug, "A Method for Stator Resistance Measurement Suitable for Vector Control," in *International Conference on Industrial Electonics, Control and Instrumentation, IECON*, 1994, pp. 2122-2126.

[34] L. Zhen, L. Xu, "Sensorless Field Orientation Control of Induction Machines Based on a Mutual MRAS Scheme," *IEEE Trans. On Industrial Electronics*, vol. 45, no. 5, pp. 824-831, October 1998.

[35] A.V Pavlov, A.T. Zaremba, "Real-time Rotor and Stator Resistances Estimation of an Induction Motor," Department od Mechanical Engineering, Eidenhoven University of Technology, 2001.

[36] L.Umanand, S.R Bhat, "Online Estimation of Stator Resistance of an Induction Motor for Speed Control Applications," in *IEE Proceedings-Electric Power Applications*, 1995, pp. 97-103.

[37] G. Guide, H. Umida, "A Novel Stator Resistance Estimation Method for Speed-Sensorless Induction Motor Drives," *IEEE Trans. on Industry Application*, vol. 36, no. 6, pp. 1619-1627, November/December 2000.

[38] I.Ha, S.Lee, "An Online Identification Method for Both Stator and Rotor Resistances of Induction Motors Without Rotational Transducers," *IEEE Trans. on Industrial Electronics*, vol. 47, no. 4, pp. 842-853, August 2000.

[39] B. Bose, N. Patel, "Quasi-Fuzzy Estimation of Stator Resistance of Induction Motor," *IEEE Trans. on Power Electronics*, vol. 13, no. 3, pp. 401-409, May 1998.

[40] S.Lee, T.G Habetler, R.G Harley, D.J. Gritterr, "A Stator and Rotor Resistance Estimation Technique for Conductor Temperature Monitoring," in *IEEE Industry Application Conference*, 2000, pp. 381-387.

[41] L. de Souza Ribeiro, C.B Jacobina, A.M.N Lima, "Linear Parameter Estimation for Induction Machines Considering the Operating Conditions," *IEEE Trans. on Power Electronics*, vol. 14, no. 1, pp. 62-73, January 1999.

[42] C.B Jacobina, J. Filho, A.M.N Lima, "On-line Estimation of Stator Resistance of Induction Machines Based on Zero-Sequence Model," *IEEE Trans. on Power Electronics*, vol. 15, no. 1, pp. 346-353, March 2000.

[43] S.B Lee, T.G Habetler, "An Online Stator Winding Resistance Estimation Technique for Temperature Monitoring of Line-connected Induction Machines," *IEEE Trans. on Industry Application*, vol. 39, no. 3, pp. 685-694, May/June 2003.

[44] Y. Wu, H. Gau, "Induction Motor Stator and Rotor Winding Temperature Estimation Using Signal Injection Method," in *IEEE Internaltional Conference on Electric Machines and Drives*, 2005, pp. 615-621.

[45] M. Stiebler, Y. Plotkin, "Superposition Methods for On-line Determination of A.C Machine Winding Resistance," in *International Symposium on Power Electronics, Electrical Drives, Automation and Motion (SPEEDAM)*, 2006, pp. 960-963.

[46] G. Yang, T. Chin, "Adaptive Speed Identification Scheme for Vector Controlled Speed Sensor-less Inverter-Induction Motor Drive," in *IEEE Industry Applications Society Annual Meeting*, 1991, pp. 404-408.

[47] Li Zhen, L. Xu, "Sensorless Field Orientation Control of Induction Machines Based on Mutual MRAS Scheme," *IEEE Trans. on Industrial Electronics*, vol. 45, no. 5, pp. 824-831, October 1998.

[48] C. Yang, J.W. Finch, "A Comparison of Induction Motor Speed Estimation using Conventional MRAS and AI-Based MRAS with a Dynamic Reference Model," in *Proceedings of the World Congress on Enginneering*, vol. I, London, 2008.

[49] K. Akatsu, A. Kawanura, "Sensorless Speed Estimation of Induction Motor Based on the Secondary and Primary Resistance On-line Identification Without Any Additional Signal Injection," in *IEEE Power Electronics Specialists Conference, PESC*, 1998, pp. 1575-1580.

[50] B. Hovingh, W.W.L Keerthipala, W.Y Yan, "Sensorless Speed Estimation of an Induction Motor in a Field Orientated Control System," School of Electrical and Computer Engineering, Curtin University of Technology,.

[51] M. Ishida, K. Iwata, "A New Slip Frequency Detector of an Induction Motor Utilizing Rotor Slot Harmonics," *IEEE Trans. on Industry Applications*, vol. IA-20, no. 3, pp. 575-582, May/June 1984.

[52] M. Ishida, K. Iwata, "Steady-State Characteristice of a Torque and Speed Control System of an Induction Motor Utilizing Rotor Slot Harmonics for Slip Frequency Sensing," *IEEE Trans. on Power Electronics*, vol. PE-2, no. 3, pp. 257-263, July 1987.

[53] A. Ferrah, K.J. Bradley, G.M Asher, "An FFT-Based Novel Approach to Noninvasive Speed Measurements in Induction Motor Drives," *IEEE Trans. on Instrumentation and Measurement*, vol. 41, no. 6, pp. 797-802, December 1992.

[54] A. Ferrah, K.J Bradley, G.M Asher, M.S Woolfson, "An Investigation into Speed Measurement of Induction Motor Drives Using Rotor Slot Harmonics and Spectral Estimation Techniques," in *International Conference on Electric Machines and Drives*, 1993, pp. 185-189.

[55] K.D Hurst, T.G Habetler, "A Comparision of Spectrum Estimation Techniques for Sensorless Speed Detection in Induction Machines," *IEEE Trans. on Industry Applications*, vol. 33, no. 4, pp. 898-905, July/August 1997.

[56] K.D Hurst, T.G Habetler, "Sensorless Speed Measurement Using Current Harmonic Spectral Estimation in Induction Machine Drives," *IEEE Trans. on Power Electronics*, vol. 11, no. 1, pp. 66-73, January 1996.

[57] A. Bandiabdellah, N. Benouzza, D. Toumi, "Cage Motor Faults Detection Algorithm Using Speed Estimation and Current Analysis," *Acta Electotechnica et Informatica*, vol. 7, no. 2, 2007.

[58] P.L Jansen, R.D Lorenz, "Transducerless Position and Velocity Estimation in Induction and Salient AC Machines," *IEEE Trans. on Industry Applications*, vol. 31, no. 2, pp. 240-247, March/April 1995.

[59] J.W Dixon, J.N Rivarola, "Induction Motor Speed Estimator and Synchronous Motor Speed Position Estimator Based on a Fixed Carrier Frequency Signal," *IEEE Trans. on Industrial Electronics*, vol. 43, no. 4, pp. 505-509, August 1996.

[60] G. Rata, M. Rata, I. Graur, D. Milici, "Induction Motor Speed Estimator Using Rotor Slot Harmonics," *Advances in Electrical and Computer Engineering*, vol. 9, no. 1, 2009.

[61] P. Mehrotra, J. Quaicoe, R. Venkatesan, "Induction Motor Speed Estimation Using Artificial Neural Networks," in *Conference on Electrical and Computer Engineering*, Canada, 1996, pp. 607-610.

[62] J. Yang, L.Wang, D. Xu, B. Xue, "Sensorless Speed Estimation for Line-connected Induction Motor Based on Recurrent Multilayer Neural Networks," in *Proceedings of the IEEE International Conference on Automation and Logistics*, 2007, pp. 2013-2018.

[63] K. L. Shi, T.F. Chan, Y.K. Wong, S.L Ho, "Speed Estimation of an Induction Motor Drive Using an Optimizer Extended Kalman Filter," *IEEE Trans. on Industrial Electronics*, vol. 49, no. 1, pp. 124-133, February 2002.

[64] R. Supangat, N. Ertugrul, W. Soong, D.A Gray, C. Hansen, J. Grieger, "Estimation of the Number of Rotor Slots and Rotor Speed in Induction Motors Using Current, Flux or Vibration Signature Analysis," in *Australasian Universities Power Engineering Conference (AUPEC'06)*, Melbourne, 2006.

[65] H. Zhang, K. Bradley, P. Zanchetta, "A None-intrusive Load and Efficiency Evaluation Method for In-Service Motors Using Vibratration Tests with an Accelerometer," in *IEEE Industrial Applications Society Annual Meeting*, 2008, pp. 1-6.

[66] D. Wu, S.D Pekarek, "Using Mechanical Vibration to Estimate Rotor Speed in Induction Motor Drives," in *IEEE Power Electronics Specialist Conference, PESC*, 2007, pp. 2412-2417.

[67] T. Phumiphak, C. Chat-uthai, "Effective Estimation of Induction Motor Field Efficiency Based on On-site Measurements," Electrical Power Department, Mahanakorn University of Technology, Bangkok,.

[68] T.M Thomas. (2008, December) Motor Condition Monitoring: Efficiency Does Matter. [Online]. www.controlengeurope.com/article.aspx?articleID=21440

[69] E.B. Agamloh, A.K. Wallace, A. von Jouanne, K. J. Anderson, J.A Rooks, "Assesment of Nonintrusive Motor Efficiency Estimators," *IEEE Trans. on Industry Applications*, vol. 41, no. 1, pp. 127-133, January/February 2005.

[70] J.S Hsu, H.H Woodson, W.F. Weldon, "Possible Errors in Measurement of Air-Gap Torque Pulsations of Induction Motors," *IEEE Trans. Energy Conversion*, vol. 7, no. 1, pp. 202-208, March 1992.

[71] H3 200kg H961700 Load Cell Datasheet. Load Cell Services. [Online]. http://www.loadcell.co.za

[72] LM311 Voltage Comparator Datasheet. [Online]. http://www.national.com/ds/LM/LM111.pdf

[73] SKHI 21A MOSFET Driver Datasheet. [Online].. http://www.scut-co.com/maindoc/techtrade/Pdevice/driver/documents/datasheets/semidriver/SKHI22A.pdf

[74] IRFP064N MOSFET Datasheet. MOSFET datasheet. [Online]. http://www.irf.com/product-info/datasheets/data/irfp064n.pdf

[75] ADLX202E Accelerometer Datasheet. [Online]. http://pdf1.alldatasheet.com/datasheet-pdf/view/48922/AD/ADXL202E.html

[76] Aligent/HP Multimeter 4401A Manual. [Online]. http://www.hirstbrook.com/eelab/hp%2034401A%20manual.pdf

[77] LEM LA 55-P Datasheet. [Online].

http://www.datasheetcatalog.org/datasheets2/70/70473_2.pdf

[78] S. B Rabinovich, *Measurement Errors and Uncertainties: Theory and Practice*, 3rd ed. New York, USA: NY: Springer Science and Media Inc, 2005.

[79] W. Cao, K. J Bradley, H.Zhang, I. French, "Experimental Uncertainty in Estimation of the Losses and Efficiency of Induction Motors," , 2006.

[80] B. Lu, W. Cao, T.G Habetler, "Error Analysis of Motor-Efficiency Estimation and Measurement ," , 2007.

[81] W. Coa, "Assesment of Induction Machine Efficiency with Comments on the New Standard IEC 60034-2-1," in *IEEE International Conference on Electrical Machines*, 2008.

APPENDIX

A.1 MATLAB Simulink model of DC signal injection circuit for R_s estimation

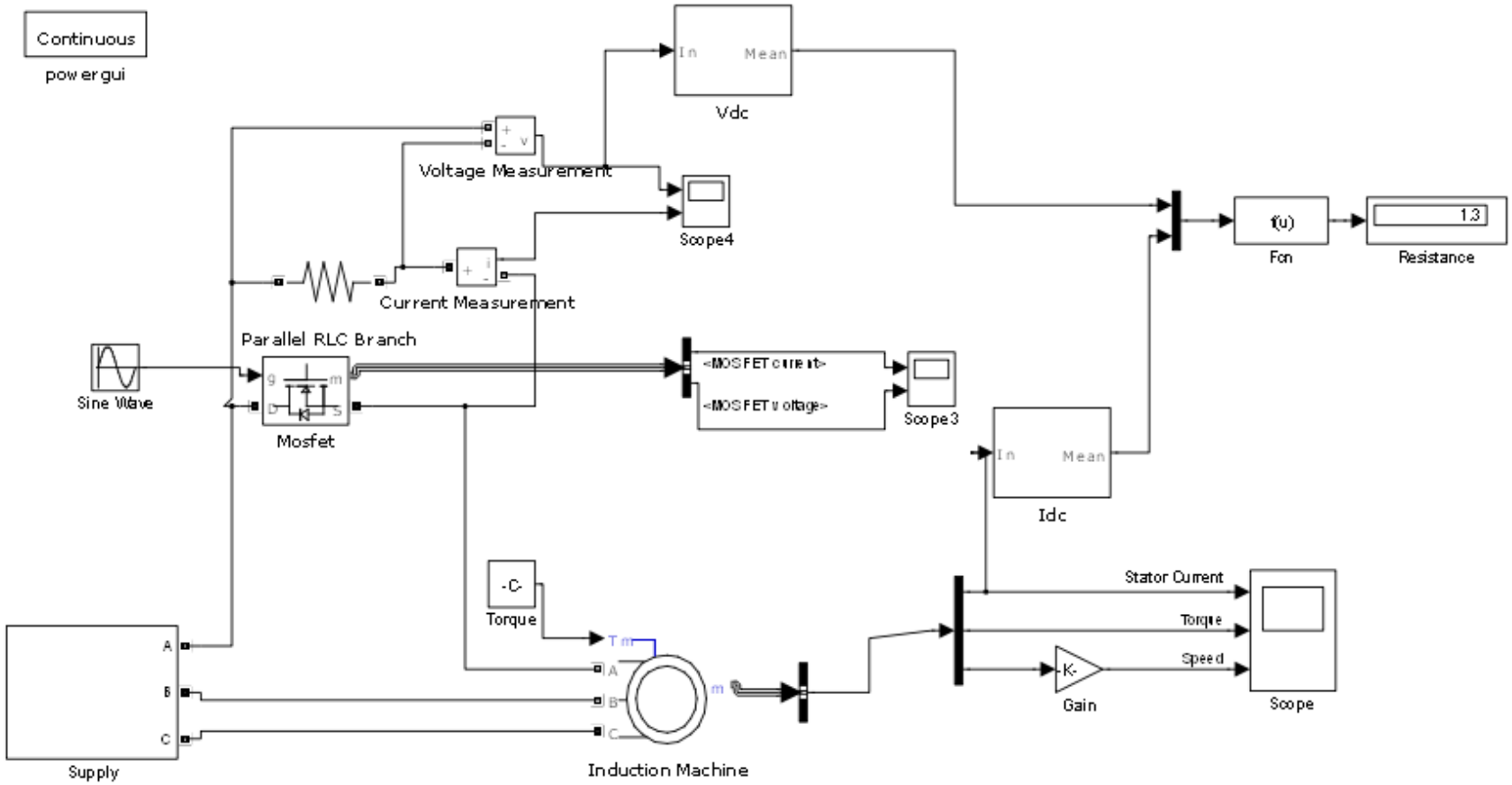

Figure A.1:Simulated model of the stator resistance estimation technique

A.2 Labview models used for the NAGT method

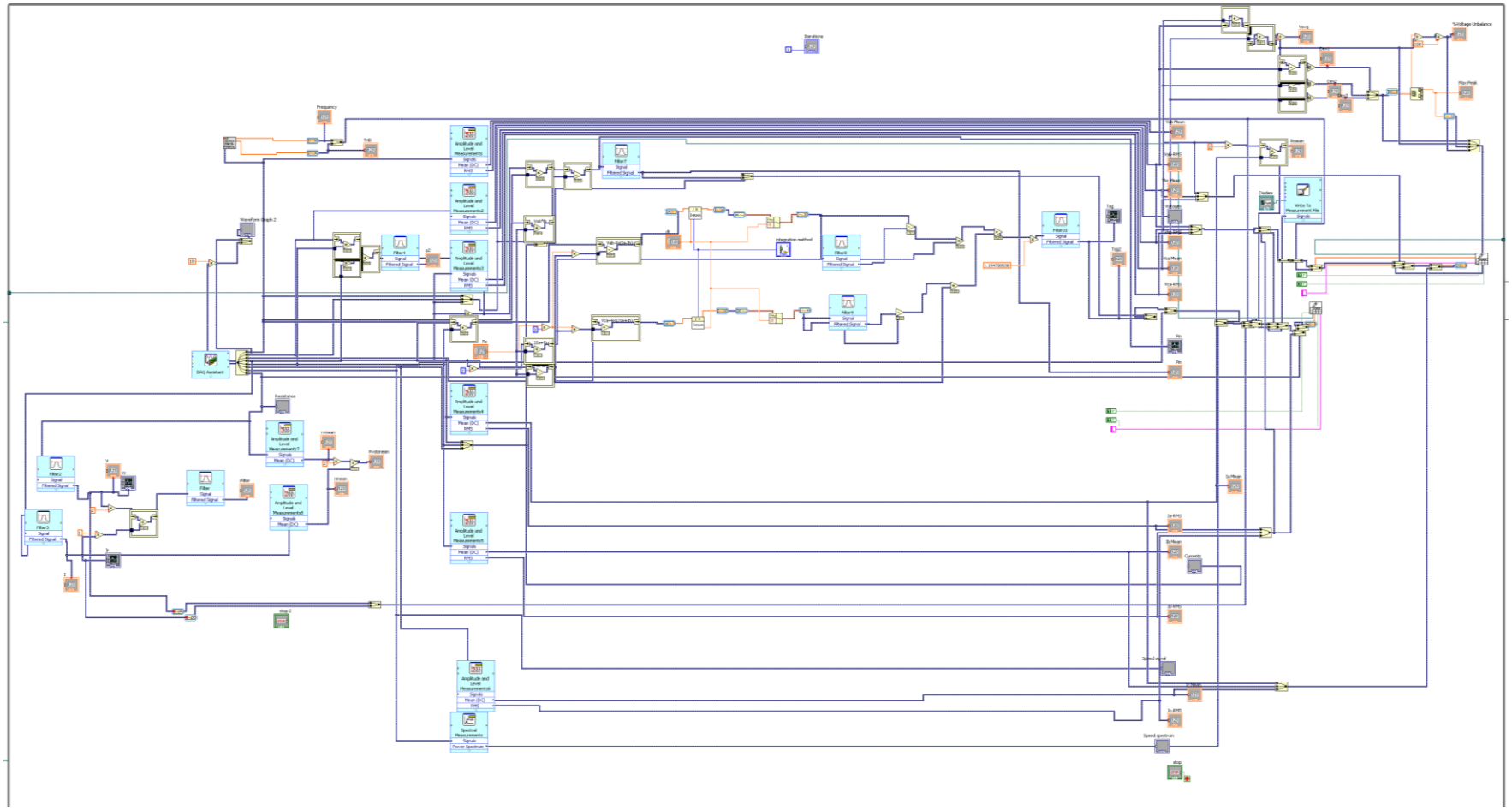

Figure A.2: Labview model

A.3 MATLAB Simulink models used for the NAGT method

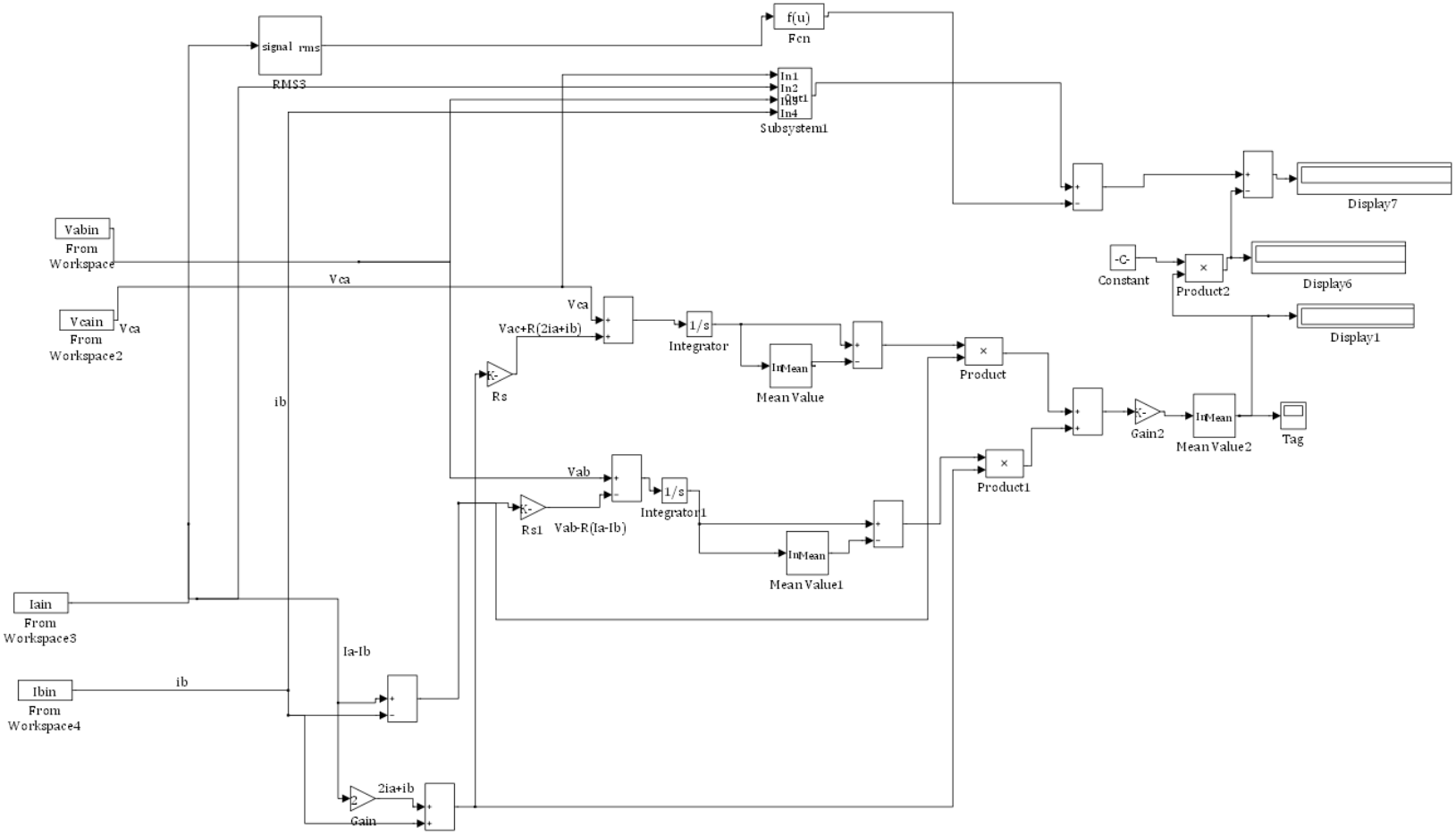

Figure A.3: MATLAB Simulink Model

A.4 Influence coefficients

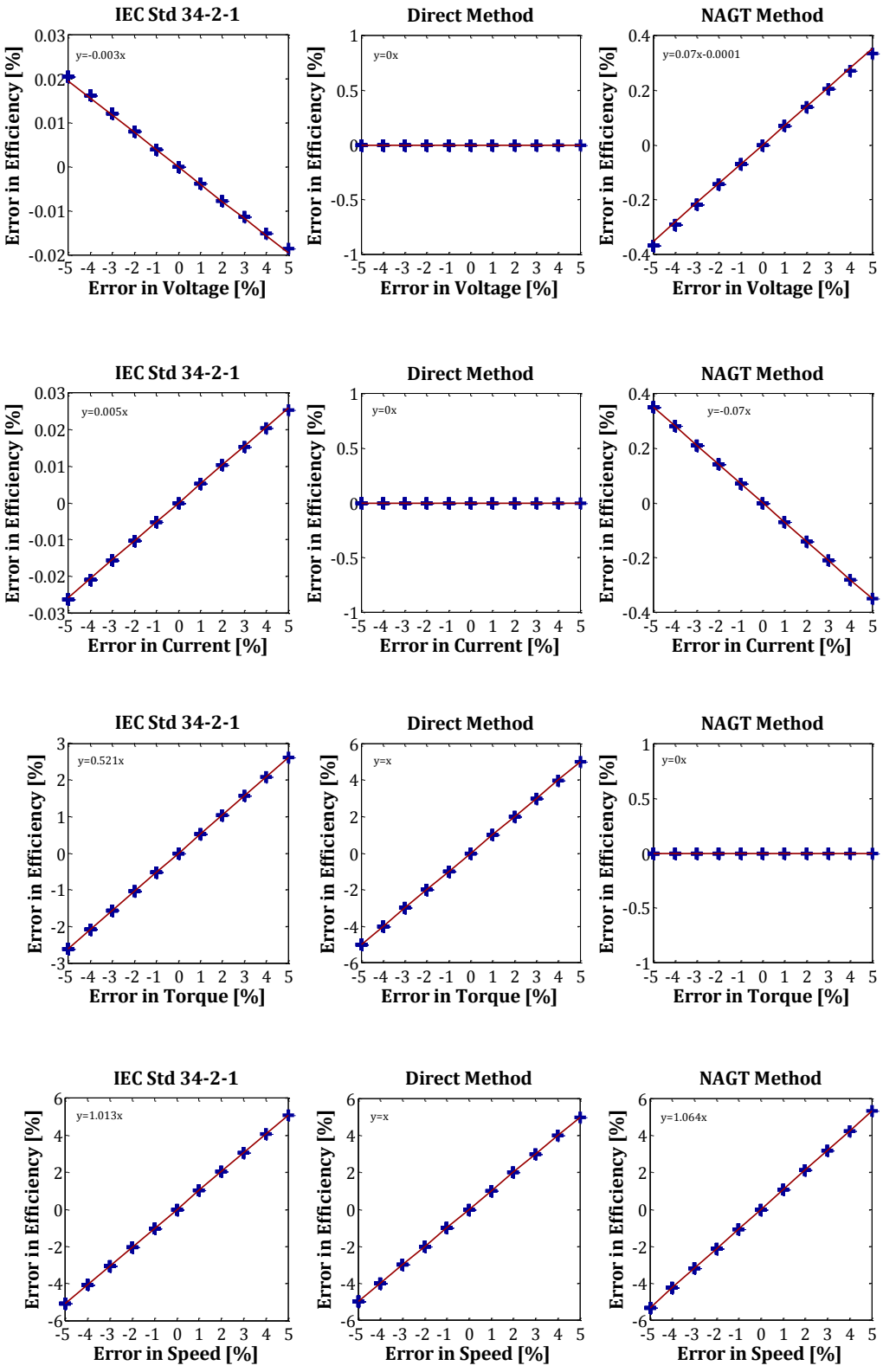

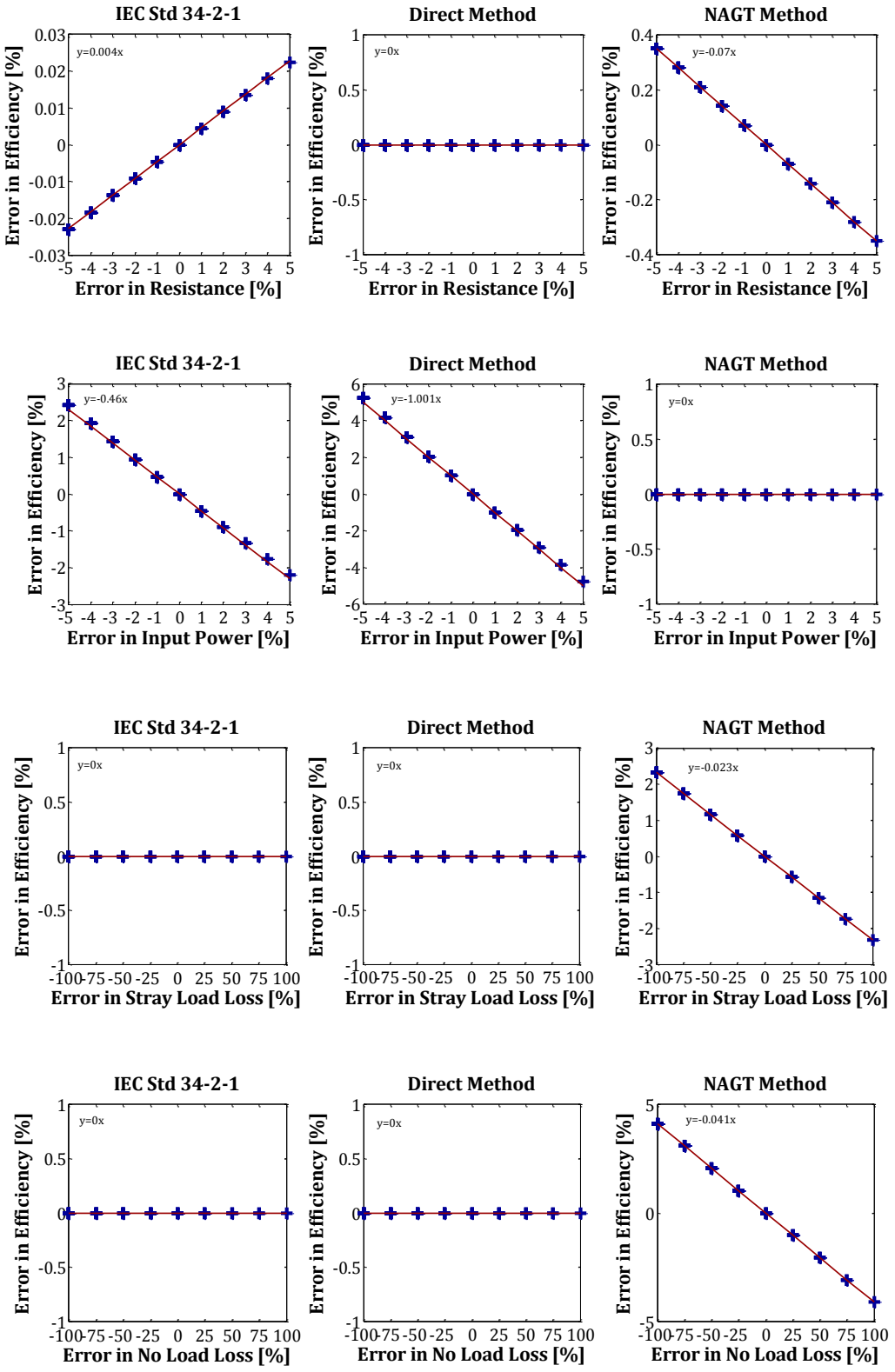

Figure A.4: Influecnce Coefficients for the 11kW motor at rated load

A.5 FFT code

```
%Sample fft code to calculate PSD
% Written by: Henry Liu 2010
%Adapted by: Barbara Herndler
clc


sampling_rate = 10000;%input('Sampling frequency (fs): ');
sample_time =60;%input('Sampling duration (s): ');
%This value acts as a multiplier to determine the number of datapoints been
ffted.
upper_frequency = 100;%input('Upper frequency limit (Hz): ');
lower_frequency = 0;%input('Lower frequency limit (Hz): ');
number_of_samples = sample_time*sampling_rate;


Speed
%Vibration data imported from file

y=Speed(1:100000)-mean(Speed(1:10000));
%Remove dc offset

fft_current = fft(y,number_of_samples)/number_of_samples;
PSD = 20*log10(fft_current.* conj(fft_current)./(2*pi));
%PSD = f(w)f*(w)/2pi. 20log10 is to put the fft in db scale.
Power_spectrum_normalised = (PSD);%./max(PSD);
%normalise the data by dividing everything by the highest value
Freq_axis = (sampling_rate).*(linspace(0,1,number_of_samples/2+1))./2;
%define the x-axis - /2 so only half of the spectrum shows
one_hz = 1/(sampling_rate/number_of_samples);
%sampling_rate/number_of_samples = freq resolution.
upper_limit = floor(one_hz*upper_frequency);

if lower_frequency == 0
    lower_limit = 1;
else
    lower_limit = floor(one_hz*lower_frequency);
end

%plot graph
figure(2)
plot(Freq_axis(lower_limit:upper_limit),Power_spectrum_normalised(lower_limit
:upper_limit),'r');
xlabel('frequency[Hz]')
ylabel('magnitude[dB]')
grid
```